Cracking in the concrete foundation for hydropower generators

Analyses of non-linear drying diffusion, thermal effects and mechanical loads

Elforsk rapport 13:63

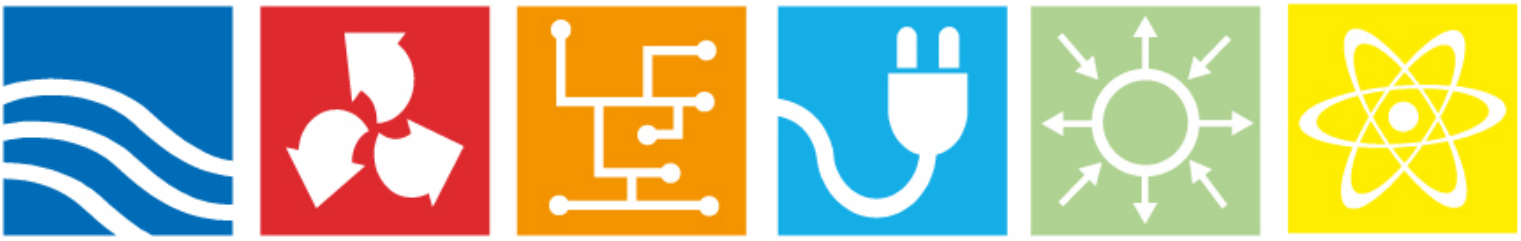

Richard Malm, Manouchehr Hassanzadeh
Tobias Gasch, Daniel Eriksson och
Erik Nordström

August 2012

ELFORSK

Cracking in the concrete foundation for hydropower generators

Analyses of non-linear drying diffusion, thermal effects and mechanical loads

Elforsk rapport 13:63

Richard Malm, Manouchehr Hassanzadeh
Tobias Gasch, Daniel Eriksson och
Erik Nordström

August 2012

Förord

Många stora konstruktioner inom vattenkraftindustrin består av betong. Att utveckla och effektivisera förvaltning av dessa är av största betydelse. Genom FoU-insatser ökar möjligheten att genomföra åtgärder vid rätt tid, till lägsta möjliga kostnad och till rätt kvalitet.

Vattenkraftföretagen*) har via Elforsk bedrivit forskning och utveckling inom det betongtekniska området sedan början av 90-talet.

Verksamheten syftar till att utveckla förvaltningen av vattenkraftens betongkonstruktioner för att minska produktionsbortfall orsakade av problem med betongkonstruktioner. Men det finns även en direkt koppling till dammsäkerhetstekniska krav på förvaltningen av betongkonstruktionerna.

Målet är att ta fram verktyg, riktlinjer, utförandebeskrivningar och teknik som fyller industrins behov. Målet är också att bygga kompetens. En uttalad ambition är att samarbeta med övrig industri och landets tekniska högskolor.

Under perioden 2010-2012 har tidigare inriktning mot kraftverkets yttre betongkonstruktioner kompletterats med aggregatnära betongkonstruktioner som utsätts för alltmer dynamisk belastning vid förändrade driftsätt och ökat reglerkraftbehov.

Programmet administreras med hjälp av en styrgrupp som under 2010-2012 bestått av följande ledamöter:

Mats Persson/Erik Nordström/Malte Cederström, Vattenfall Vattenkraft

Johanna Feldtman, E.ON Vattenkraft Sverige

Martin Hansson/Jan Liif, Statkraft Sverige AB

Robert Lundström/Markus Eriksson/Emma Sundelin, Skellefteå Kraft

Stefan Norberg/Karin Persson, Fortum

Marcus Hautakoski/Gunnar Sjödin, Vattenregleringsföretagen

Cristian Andersson/Marie Westberg Wilde, Elforsk AB

Stockholm november 2013

Cristian Andersson

Elforsk AB

*)Vattenfall Vattenkraft AB, Fortum Generation AB, E.ON Vattenkraft Sverige AB, Statkraft Sverige AB, Skellefteå Kraft AB, Jämtkraft AB, Sollefteåforsens AB, Karlstads Energi AB, Jönköping Energi AB deltar i Betongtekniskt program vattenkraft 2010-2012.

Sammanfattning

Ett kontinuerligt arbete med utvärdering och uppgradering av vattenkraften pågår i Sverige. Syftet är att säkerställa långvarig och säker drift av vattenkraftens konstruktioner ur ett byggnadstekniskt perspektiv.

Vid inspektioner av svenska vattenkraftsstationer har, i vissa fall, sprickor observerats i de betongfundament som utgör generatorns upplag och i synnerhet kring stator- och rotorupplagen. Möjliga förklaringar till sprickorna tros vara brister i statorfötternas rörelseförmåga samt den temperaturvariation som orsakas av nytt driftsmönster. Tidigare gick generatorerna kontinuerligt medan vattenkraften idag används för att balansera energitillförseln, vilket leder till många starter och stopp, ibland under ett och samma dygn. Syftet med föreliggande projekt är att förstå den komplicerade samverkan mellan generator (stator, rotor, turbin, etc.) och betongkonstruktionen som utgör generatorns upplag för att kunna bestämma orsaken till de sprickor som observerats i fält.

För att studera sprickinitiering och sprickpropagering i betongkonstruktionen har en tredimensionell icke-linjär modell utvecklats med finita element-metoden. I analyserna har flera olika typer av belastningar studerats utöver de mekaniska lasterna som orsakas av egentyngder och drift. Det nya driftmönstret med flera starter och stopp leder bland annat till att fundamentet utsätts för variation i temperaturer, och inverkan av detta har studerats i projektet. Utöver detta har även inverkan av ojämn uttorkningskrympning beaktats. Fundamentets strukturella beteende har därmed analyserats med beaktande av effekter som hur temperatur- och fuktgradienter varierar med tiden, i kombination med egentyngder och driftsbelastningar.

Analyserna visar att den armerade betongstrukturen som utgör generatorns upplag utsätts för uppsprickning på grund av de studerade belastningarna. Vid en kombination av mekaniska laster, uttorkningskrympning och temperaturvariation uppstår sprickor kring stator- och rotorupplagen. Analyserna visar även att det finns en stor variation i fukt i betong-fundamentet efter en så pass lång tid som 20 år, där centrum på det massiva betongtvärsnittet har en hög relativ luftfuktighet. Vid samma tidpunkt har däremot de slanka delarna av betongtvärsnittet och fundamentets fria ytor en relativ luftfuktighet som motsvarar omgivningens. Denna variation leder till att tvångsspänningar uppstår i fundamentet. Analyserna visade att ut-torkningskrympningen huvudsakligen orsakar uppsprickning på fundamentets insida och främst vid upplagen för stator- och rotorbalkar, vilket överens-stämmer med de sprickor som observerats i fält.

Resultatet från projektet visar att de sprickor som har observerats i fält kan simuleras och förklaras med hjälp av avancerade numeriska analysmetoder. Resultaten visar även att fortsatta studier krävs avseende den dynamiska effekten från lasterna som orsakas av generatorn. Detta eftersom upp-sprickningen orsakar en styvhetsreduktion som kan medföra att fundamentet utsätts för större belastning på grund av krafterna från magnetisk obalans och turbinimperfektioner, eller så kan dessa vibrationer leda till utmattning av t.ex. armeringen.

Summary

An extensive program for improvement of the hydropower plants in Sweden is currently on-going. The aims are to secure future production and to maintain and further develop an already high dam safety.

During inspection, cracks were discovered in the concrete foundation, near the stator and rotor spider supports, at some hydropower stations in Sweden. The cracks were believed to be related to the function of the stator supports and to new patterns of generator operation. In earlier times, the generators ran continuously, while nowadays there are many stops and starts, sometimes even several times during one day. The objective of this study is to understand the complex interaction between the power generating system (stator, rotor, turbine, etc.) and the supporting concrete structure to be able to determine the causes of the structural cracks that have been found in-situ.

A three dimensional non-linear finite element model has been developed in order to analyse formation and propagation of the cracks in the concrete foundation. Several different load effects have been studied in this project in addition to the mechanical loads during operation. The new pattern of generator operation with several starts and stops lead for instance to variations in temperature which have been studied. Besides this, the uneven drying shrinkage of concrete has also been studied in this project. Thereby, the structural behaviour of a concrete foundation for the power generating system has been analysed taking into account the time-dependent thermal and moisture gradients in combination with dead loads and some of the operational loads imposed to the foundation.

The analyses shows that reinforced concrete structure that constitute a support to the generator is subjected to cracking due to the loads considered in this study, where the cracks near the supports are caused by a combination of mechanical loads, long-term drying shrinkage and temperature variations. The analyses showed that even after 20 years, the moisture content in the centre of the thicker part in the concrete foundation still had a high relative humidity. At the same time the concrete close to the free surfaces and the slender parts of the concrete foundation had reached the same relative humidity as the environment. Thereby, a large difference in drying shrinkage is obtained between different parts of the concrete foundation and thereby large forces due to restrain. The analyses showed that the drying shrinkage induced cracking inside the concrete foundation and especially close to the supports of the stator and the rotor spider which coincides with location of the cracks found in-situ.

The results show that the cracks found in-situ can be simulated and explained with advanced numerical methods. The results also indicate that the dynamic effect from the loads caused by the power generating system have to be studied further. Its reduced structural stiffness, due to cracking, may result in larger loads imposed on the structure from the magnetic eccentricity and turbine imperfections or alternatively lead to a fatigue failure of for instance the reinforcement.

Contents

1 Introduction

1.1 Background

A rather extensive program for improvement of the Swedish hydropower plants is on-going. The aims are to secure future production and to maintain and further develop an already high dam safety.

In an earlier project which dealt with assessment of an existing buttress dam, a non-linear finite element model was applied to determine the cause of the observed cracks, Björnström et al. (2006), Ansell et al. (2007), Ansell et al. (2010). The results showed that the non-linear finite element method is a powerful tool to determine the structural behaviour of large concrete structures. The study in this report is a continuation of the previous project, aiming at applying the method to other parts of dam structure such as waterways.

The objective of this project is to understand the complex interaction between the power generating system (stator, rotor, turbine, etc) and the supporting concrete structure, which is needed for formulation of more realistic and accurate specifications regarding load, stiffness and displacement levels and tolerances. The achievement of the objective requires models that account for the behaviour of the mechanical systems, supporting structures and their interaction under various loading conditions. The various loading condition includes

- mechanical loads (static, dynamic, short-term, long-term, etc) such as weight of the structures and systems, and operating loads caused by the turbine, rotor, stator, etc
- environmental loads (physical, chemical, etc) such as strains and restraints caused by temperature, moisture variations, and chemical reactions.

The study that is presented in this report is a step in the direction of the target objective.

1.2 Project organisation

The project group consists of representatives from KTH Royal Institute of Technology, Vattenfall Research and Development and Vattenfall Hydro. The project is financially supported by Elforsk AB, the Swedish Power companies R&D association.

The project initiated from a M.Sc. project performed in 2008 by Mattis Larsson at Luleå University, under the supervision of Prof. Lennart Elfgren and assoc. Prof. Manouchehr Hassanzadeh.

This project is coordinated by assoc. Prof. Manouchehr Hassanzadeh from Vattenfall R&D, who also contributes with knowledge on material formulation

and fracture mechanics for concrete. From the department of Concrete Structures at KTH, Dr. Richard Malm contributed with defining the structural models and knowledge regarding advanced numerical simulations. He is also responsible for the formulation and evaluation of the numerical results presented in this report. From Vattenfall R&D, M.Sc. Daniel Eriksson and M.Sc. Tobias Gasch contributed with knowledge on advanced numerical simulations and they have also performed a majority of the numerical simulations presented. This project is a collaboration between different disciplines and therefore, several experts within Vattenfall have been involved. From Vattenfall R&D Dr. Mathias Näsellqvist and Dr. Rolf Gustavsson contributed with knowledge regarding the loads from generator and rotor, and Tech. Lic. Mats Rhen contributed with knowledge and data regarding monitoring and measurements of the structural behaviour of the concrete foundation. From Vattenfall Hydro, Dr. Erik Nordström contributes with knowledge regarding hydro power structures and also with data regarding operational stops of hydro power plants.

2 Generator foundation in hydropower stations

In Figure 1, a layout of a typical hydropower station is illustrated. From the intake (2), gravity will cause the water to fall through the penstock (1) inside the dam. At the end of the penstock there is a turbine runner, which is rotating by the moving water. The shaft from the turbine goes up into the generator, which produces the power. The generator is supported by a concrete foundation, illustrated as (5) in the figure.

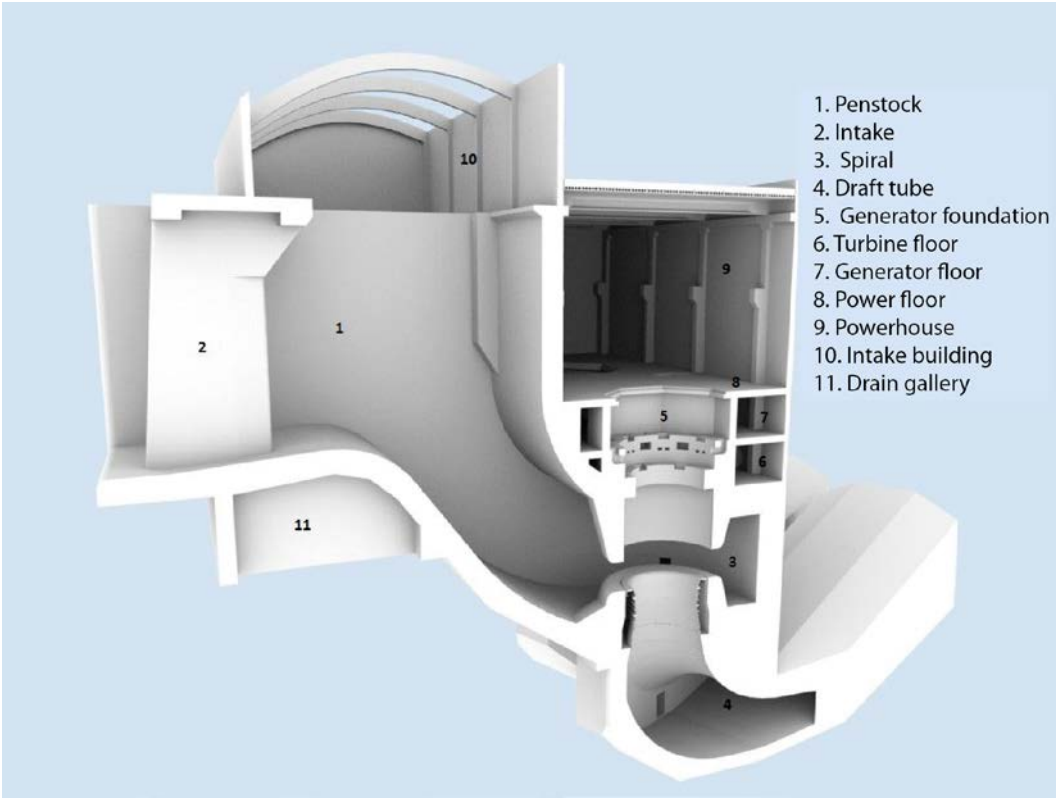

Figure 1 Layout of a hydropower station, from Paavola (2011).

The turbine converts the energy of flowing water into mechanical energy, while the hydroelectric generator converts this mechanical energy into electricity. The operation of a generator is based on the principles discovered by Faraday, where electricity is generated when a magnet is moved past a conductor. In a large generator, electromagnets are made by circulating direct current through loops of wire around stacks of magnetic steel laminations. These are called field poles, and are mounted on the perimeter of the rotor. The rotor is attached to the turbine shaft, and rotates at a fixed

speed. When the rotor revolves, it causes the field poles (the electromagnets) to move past the conductors mounted in the stator. This, in turn, causes electricity to flow and a voltage to develop at the generator output terminals. A typical layout of a hydropower unit is illustrated in Figure 2. (from http://ga.water.usgs.gov/edu/hyhowworks.html, available: 2012-04-05)

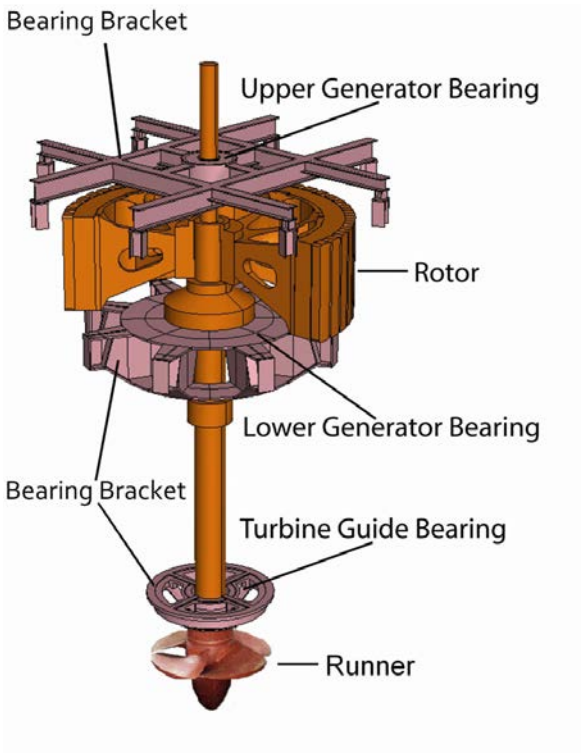

Figure 2 Schematic layout of a hydropower unit, from Nässelqvist (2011).

At some hydropower stations, structural damages (cracks) have been discovered around the stator and rotor spider supports, this is further described in Section 2.1. The cracks were believed to be related to the insufficient function of the stator supports and to new patterns of generator operation. In earlier times, the generators ran continuously, while nowadays there are many stops and starts, sometimes even several times during one day.

The variation of stresses in the concrete foundation and initiation and propagation of cracks influence both the static and the dynamic response of the foundation. Several generator manufacturers permit only negligible structural displacements. Therefore the analysis tools must be developed in order to determine the response of the foundations to the loads induced by the generators.

The purpose of this study is to highlight the complex stress conditions in the generator foundations of a hydropower plant and to reveal the causes of the stresses and to verify their role in formation of the cracks.

2.1 Hojum hydropower plant

A vertical cross-section of the power unit of the Hojum hydropower plant is shown in Figure 3. The figure shows the generator (stator and rotor), rotor spider, turbine shaft, spiral casing, turbine and draft tube. As it is shown the power unit is embraced by a concrete structure.

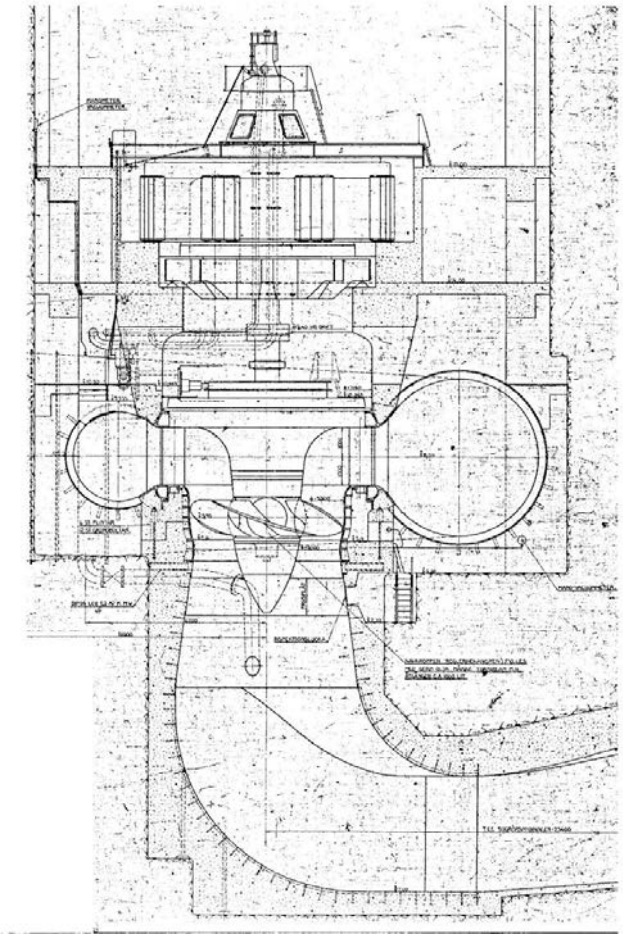

Figure 3 Vertical cross-section of the hydropower system, from Hassanzadeh et al. (2012).

The Hojum hydropower plant was constructed in the early forties. There is no conclusive data on the concrete's composition in terms of water binder ratio (W/B ratio), type and quantity of the binder, aggregate type and maximum particle size. The data that are available indicate that the binder is Portland cement with somewhat higher silicate quantity than usual to reduce the hydration rate and heat development of the binder. Moreover, according to the guidance which used to be applied when the power plant was constructed, the recommended W/B ratio and the binder quantity for the similar structures were 0.55 – 0.60, and 300 – 350 kg/m^3 respectively. According to the same guidance the W/B ratios 0.55 and 0.60 corresponded to 28 days compressive strength of 22 and 20 MPa. The corresponding values at 90 days were 35 and

30 MPa. Translated to the current conditions the concrete grade at the time of construction can be assumed to be C20/25.

The foundation is a massive reinforced concrete structure. The reinforcement drawings indicate that the average reinforcement diameter and the average distance between the bars are 25 and 250 mm respectively. According to the drawings the concrete cover should not be less than 30 mm or larger than 40 mm. By means of the casting instructions, it can be concluded that the target concrete cover was less than 30 mm and the maximum aggregate size was less than 25 mm. In Figure 4 an example of the reinforcement detailing is shown. The dimension of the foundation is later presented in Section 4.1. The foundation contains several entries and doors, which have been accounted for in a numerical model.

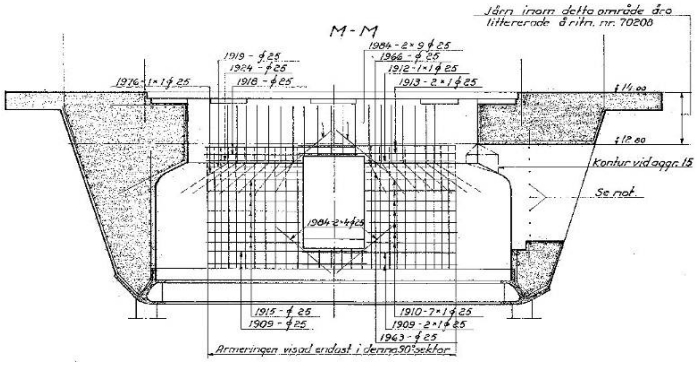

Figure 4 Vertical cross-section of the foundation and arrangement of the reinforcement, from Hassanzadeh et al. (2012).

The dead weight of the power generating system and the loads caused by the power generator is supported at the upper part of the concrete structure. The cylindrical upper part of the structure, which is here denoted as the foundation, has different wall thickness at the different sections, as seen in Figure 5. The loads from the power generating devices are transferred to the foundation through two sections, namely through the supports of the stator and through the supports of the rotor spider. A minor part of the loads are transferred through the supports of the turbine cover.

The weight of the rotor, rotor spider, turbine and turbine shaft are transferred to the foundation through the supports of the rotor spider. The vertical loads generated by the water at the turbine are also transferred through the supports of the rotor spider. The supports of the stator carry the weight of the stator and the cooling system. Horizontal loads, i.e. loads acting on the planes perpendicular to the rotor shaft, are transferred to the foundation through the supports of the stator and the rotor. For instance, the rotation of the rotor affects the stator in both tangential and radial direction. The resulted horizontal loads are transferred through the supports of the stator and the rotor.

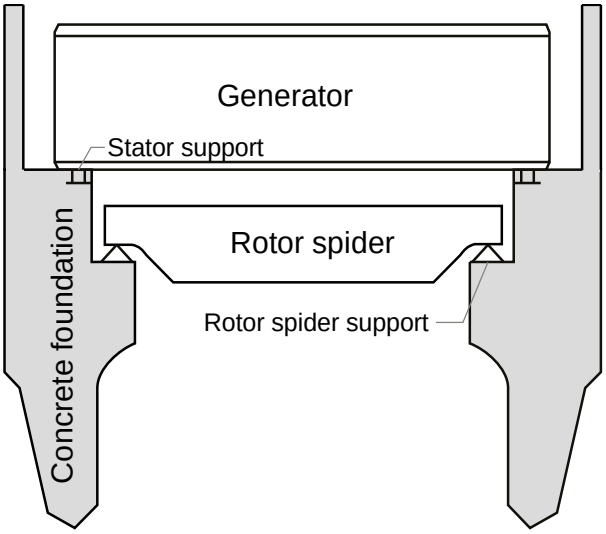

Figure 5 Vertical cross-section of the concrete foundation.

As shown in Figure 3 and Figure 5, the stator and the rotor are placed inside a concrete structure, which acts as a foundation for the stator and the rotor. The space inside the foundation is limited and the cooling system is not able to cool all the heat produced. Therefore, the temperature inside the foundation increases during the operation of the generator. Although, the air inside the foundation is cooled adequately for the operation of the power generating devices, the increased temperature may still have a structural impact. Increased temperature leads to extension of the rotor spider and the beams supporting the stator as well as displacement of the foundation. This causes a relative displacement between the beams supporting the stator and the foundation, which takes place on the supports. In order for the relative displacement to occur, the friction resistance must be overcome. This results in frictional forces in the radial direction, acting between the foundation and the beams that support the stator. The spider pushes the supports during heating and pulls the support during cooling. They thereby, impose compressive forces in the foundation during heating and tensile forces in the foundation during cooling.

Since the spiders are fixed at the supports their extension is restrained. The restraint will induce forces that act between the supports on the foundation and the end of the spiders. The magnitude of the forces depends on the stiffness/compliance of the spider and the foundation. As mentioned earlier, the spiders push the foundation during heating and pull the foundation during the cooling. However, it should be noted that the resulting displacement and the inertial of the heating and cooling processes might have large influence on the magnitude of the forces. As far as supports of the stator are concerned, the spider could extend without any restraint, if the bearings of the supports were frictionless. Since the bearings are not frictionless they restrain the supporting beams. Consequently, loads are imposed on the beams and on the supports as well. The beams respond to the temperature variations faster than the foundation structure. The inertia of the heating and cooling process

is important. In comparison with the “thin” steel structures such as supporting beams it takes long time for a massive concrete foundation to respond, to displace, and to adapt to a changed thermal condition. Therefore, a relative displacement is obtained and frictional forces occur during heating, during cooling or at any disruption of the thermal equilibrium.

Figure 6 shows a crack that has occurred between the support of the rotor spider and the wall of the foundation. The crack follows the foundation wall in the tangential direction. Similar cracks occur around the supports of the stator. Two photos of typical cracks around some of the stator and rotor spider supports are illustrated in Figure 7 and Figure 8.

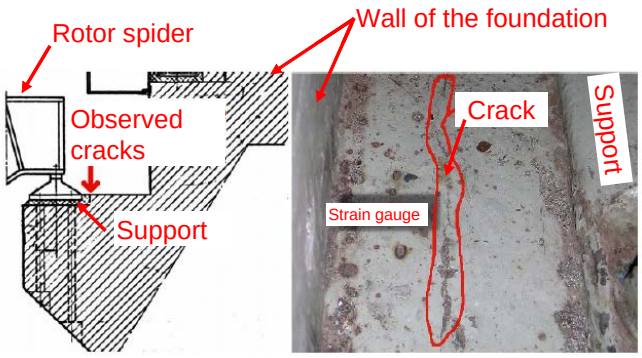

Figure 6 Observed cracks at the support of the rotor spider, from Rhen (2007).

Figure 7 Crack around a stator support, from Larsson (2008). The crack has been highlighted with a brighter background in the figure.

(a) (b)

Figure 8 (a) rotor spider support, (b) observed crack near the rotor spider support, from Larsson (2008).

The displacement between the support and the foundation wall includes the crack deformation (crack widening or closing) and the strains integrated over the mentioned distance, Rhen (2007). Crack deformation constitutes a considerable part of the total displacement and its contribution increases with increasing rate of temperature variation and increasing length and stiffness of the spider. In the case of the stator supports the frictional forces imposed by the bearings influence the crack deformations.

The structural consequences of the observed cracking are, stress concentrations on reinforcement within the cracked area, reduced structural stiffness and reduced fatigue resistance.

The temperature variations also cause thermal gradients through the foundation wall. Normally, the air temperature inside the foundation is higher than the air temperature outside the foundation. The thermal gradient causes stresses in tangential direction and in direction perpendicular to the horizontal plane. Although, high stresses may occur the stress levels are normally not high enough to cause cracks. However, the impact of stresses caused by the thermal gradients may be increased by the other factors such as mechanical loading and drying shrinkage.

The foundation is situated inside a plant and is protected against the outdoor weather. The foundation is protected against the precipitation and is mainly exposed to temperatures above what is considered indoor temperature. Since the outdoor air is used to cool the indoor air, it can be assumed that the indoor air has the same vapour content as the outdoor air. In this context, however, it should be mentioned that the vapour content of the indoor air normally follows the outdoor air's vapour content irrespective of the cooling system. It has been shown that the air's vapour content inside a nuclear

reactor building, i.e. the building that embraces a reactor containment, follows the outdoor air's vapour content, Johansson and Nilsson (2007).

The measurements show that the air temperature inside a generator chamber can be as high as 50 °C and the relative humidity (RH) can be as low as 14%. In Figure 9, the temperature variation during two month period is shown, from 2006-07-14 to 2006-09-04. The measurement shows the temperature of the rotor spider and the air inside the foundation as well as the surface temperature of the slab on both side of the foundation wall. As can be observed there is approximately 10 °C difference across the foundation wall. During the winter, the temperature outside the foundation can be as low as 15 °C while the daily average outdoor temperature in the area of the power plant can be as low as -5 °C.

The average temperature and humidity in the area of the power plant is -2 °C and 85% during winter, and +16 °C and 70% during summer respectively, corresponding to the average outdoor vapour content of $3.6 \cdot 10^{-3}$ kg/m^3 and $9.6 \cdot 10^{-3}$ kg/m^3. With the assumption that the air temperatures inside and outside of the foundation are 34 °C and 24 °C respectively, the RH on both sides of the foundation wall are 10% (winter) and 26% (summer), and 17% (winter) and 44% (summer). As it is noticed the foundation is exposed to relatively warm and dry environment.

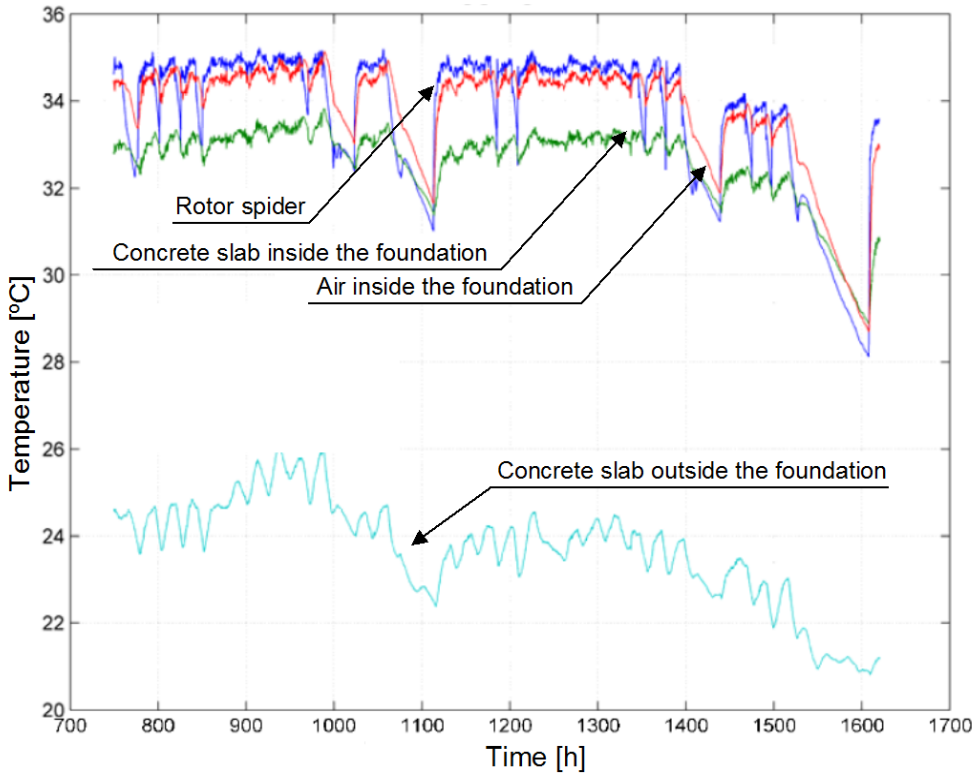

Figure 9 Temperature variation during the period 2006-07-14 – 2006-09-04, from Rhen (2007).

The exposure of the foundation to the described environment leads to drying shrinkage of the concrete. Given the size and design of the structure, and the dry environment, large stresses are expected to occur due to strain gradients and the restraints. The strain gradients are caused by the moisture gradients, which occur during the drying process before the final moisture equilibrium is reached within the sections of the structure, while restraints are caused when a part of the structure hinders another part to deform. Since the structure is more than 70 years old and it is exposed to a relatively warm and dry environment it is expected that the structure is not far from the moisture equilibrium condition, if it is not already dry.

The stresses caused by the drying shrinkage in most cases amplify the stresses caused by the thermal gradients and the mechanical loads.

Besides the above-mentioned thermal and moisture impacts there is another effect that should be considered and that is the restraint that occurs during the cooling process of the young concrete after hardening. It is however difficult to account for this effect. Disregarding the modelling difficulties there are other obstacles such as lack of data regarding material properties, heat development, concrete mix, casting phases, etc.

3 Benchmark examples of coupled temperature and diffusion

In order to analyse the non-linear behaviour of the concrete foundation, mechanical loads, thermal effects and drying shrinkage must be accounted for. In the numerical analyses, all these effects will be combined. Before doing so, two benchmark examples will be performed to verify that it is possible to perform diffusion analyses of the drying shrinkage and also that it is possible to couple all the effects into one analysis.

Two different benchmarks have been performed during this study; the first considers the modelling approach for moisture diffusion, i.e. drying shrinkage, in concrete while the second consider shrinkage and temperature induced stresses in the concrete. The analyses were performed in the commercial FE-program ABAQUS.

3.1 Diffusion

This benchmark example has the purpose to verify that the mass diffusion module in ABAQUS is able to simulate the drying of concrete. To describe the drying process in a more accurate manner, the model developed by Yunping et.al (1994a) has been used to define the material properties. This model does not treat moisture diffusivity and moisture capacity as two different parameters as some earlier diffusion models for concrete, see Bazant and Najjar (1972). These two parameters have also been shown to be dependent of several other parameters, for example the water/cement ratio, curing time, temperature and cement type Yunping et.al (1994b). In Yunping et al. (1994a), the proposed expression has been calibrated against test data from Molina (1990) and Molina (1992). To verify the mass diffusion module in ABAQUS, the results have been compared to the same test data. The test configuration, together with the applied boundary conditions, is shown in Figure 10.

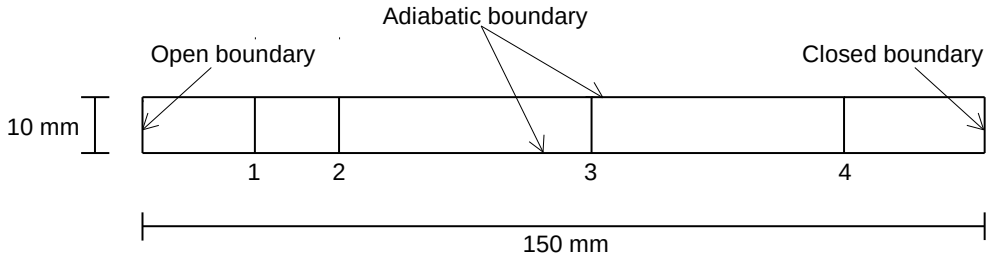

Figure 10 Test configuration. Section 1 is located 20 mm from the left side, section 2 35 mm, section 3 80 mm and section 4 125 mm.

In the test series, a number of saturated concrete specimens were exposed to a relative humidity of 50% in the ambient air. Single parameters were

changed between the different specimens in order to be able to determine their effect on the drying process.

Two analyses were performed, where the diffusivity and moisture capacity of the concrete were defined according to the expressions given by Yunping et al. (1994a) and with the given parameters from two of the tests from Molina (1990). The test parameters are shown in Table 1.

Table 1 Test specimen parameters

Parameter	Test 1	Test 2
w/c	0.63	0.75
Curing time (t_0)	3 days	3 days
Relative humidity (H_{en})	50%	50%

The moisture capacity is defined as the derivate of the adsorption isotherm while the diffusivity is calculated, as mentioned before, with the empirical formulae defined in Yunping et al (1994a). The adsorption isotherm, moisture capacity and the diffusivity used in the analyses of the two tests are presented in Figure 11 to Figure 13.

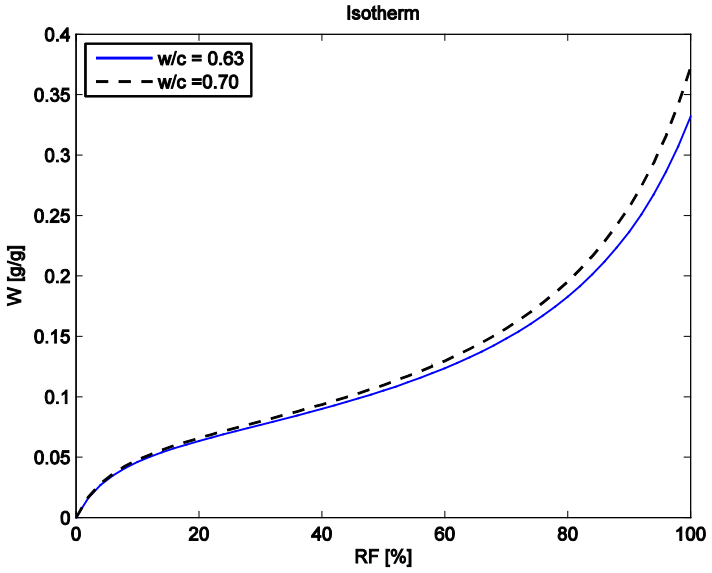

Figure 11 Adsorption isotherm for concrete in Test 1 (w/c 0.63) and Test 2 (w/c 0.75).

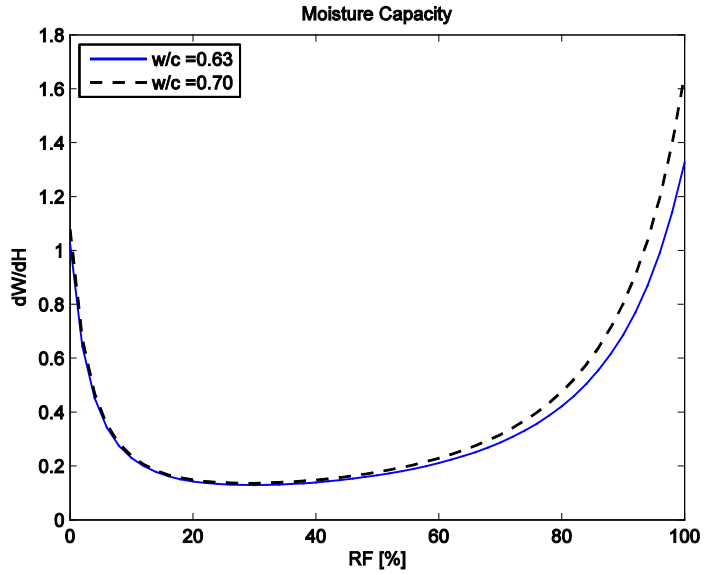

Figure 12 Moisture capacity for concrete in Test 1 (w/c 0.63) and Test 2 (w/c 0.75).

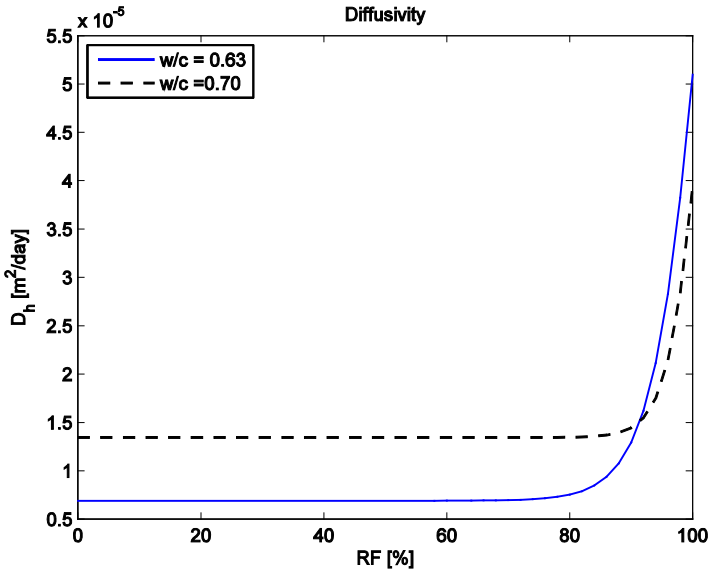

Figure 13 Diffusivity for concrete in Test 1 (w/c 0.63) and Test 2 (w/c 0.75).

To use the diffusion model in the mass diffusion module in ABAQUS, the governing equation in Yunping et al (1994a) has to be considered, see Eq. [1].

$$\frac{\partial H}{\partial t} = \frac{\partial H}{\partial W} div(D_h \, grad \, H) \qquad [1]$$

where

H	is the relative humidity
t	is the time in days
$\frac{\partial H}{\partial W}$	is the inverse of the moisture diffusion
D_h	is the diffusivity of the concrete

The mass diffusion module in ABAQUS is based on Fick's law. Eq. [1] is basically Fick's law, why the diffusivity in ABAQUS should be defined according to Eq. [2] in order to implement the dependency of the moisture capacity and the other parameters as proposed in Yunping et al (1994a).

$$D_{h,ABAQUS} = \frac{\partial H}{\partial W} D_h \qquad [2]$$

The results from the analyses and the experiments are shown in Figure 14 and Figure 15.

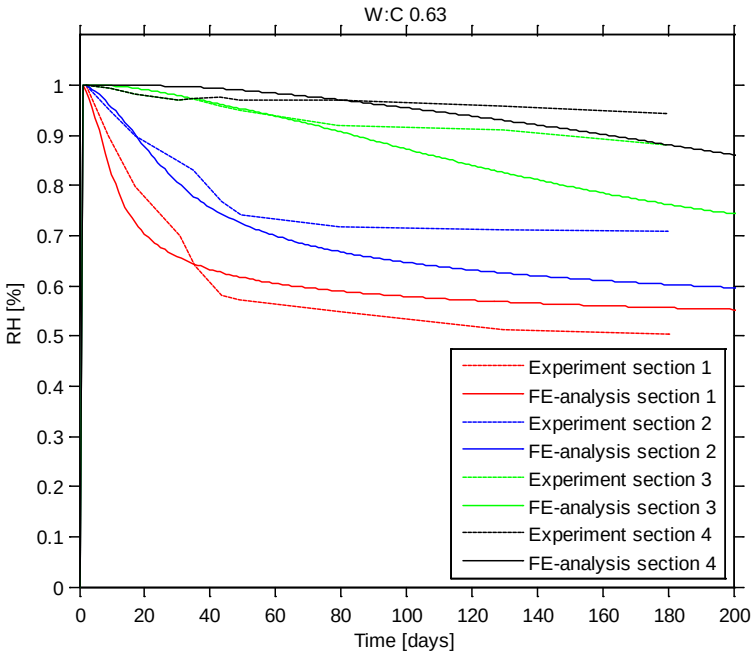

Figure 14 FE-analysis results compared to the experimental results in all 4 sections for w/c 0.63.

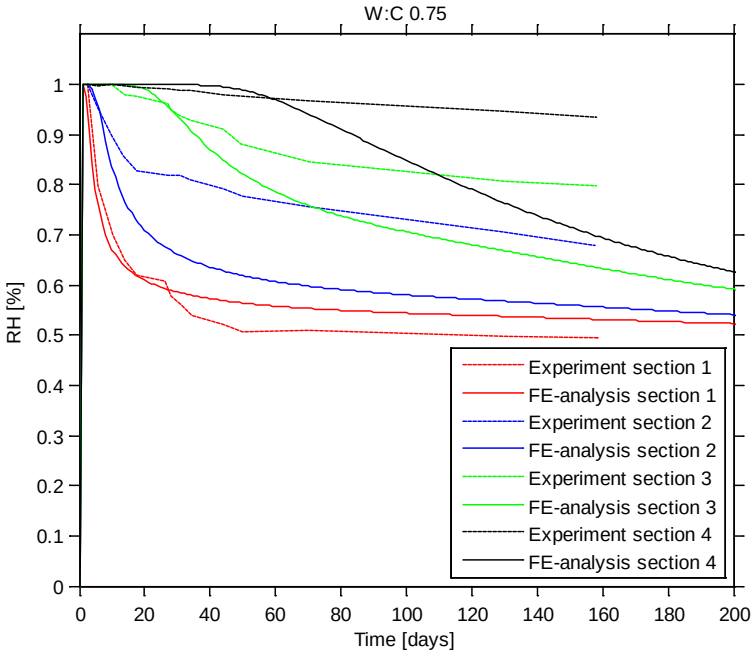

Figure 15 FE-analysis results compared to the experimental results in all 4 sections for w/c 0.75.

As can be seen, the FE-results differ a bit from the experimental results. Several aspects are most certainly causing the difference, where the empirical formulation of the diffusivity and moisture capacity in Yunping et al (1994a) probably is one of the main sources. As shown in Figure 13, there is a rapid change of the diffusivity for high values of relative humidity (typical above 90%), and therefore a small error in the relative humidity has a large impact on the early drying of the concrete.

During this project, an error was found in one of the presented equations (eq. (8)) in Yunping et al (1994a), which resulted in a negative diffusivity for a concrete with w/c 0.75. The error was probably caused by the curve fitting procedure and was solved through some adjustments to the empirical formulae for the factor β. The original expression for the factor β according to Yunping et al (1994a) is presented in Eq. [3].

$$\beta = -14.4 + 50.4\frac{w}{c} - 41.8\left(\frac{w}{c}\right)^2 \quad [3]$$

The modified version of the equation which gives a better curve fitting and was used in this project is presented in Eq.[4].

$$\beta = -14.28 + 50.4\frac{w}{c} - 41.8\left(\frac{w}{c}\right)^2 \quad [4]$$

3.2 Coupled diffusion, temperature and stress

The purpose with this benchmark example is to verify that ABAQUS is able to account for stresses induced by both shrinkage and temperature, i.e. different environmental loads. There will be a difference in shrinkage between the inside of the foundation and the outside because of the difference in humidity. This variation in shrinkage will induce stresses in the concrete while the constraints of the foundation will contribute to increase these stresses. Furthermore, the temperature differs between the inside and the outside of the foundation which causes the same phenomenon which increase the stresses.

To be able to study if ABAQUS is able to account for both these aspects in an analysis, a simple geometry is studied; the geometry and the defined boundary conditions are shown in Figure 16. The purpose of this study is only to verify that it is possible to combine the two effects, and therefore only fictitious values of the shrinkage has been used.

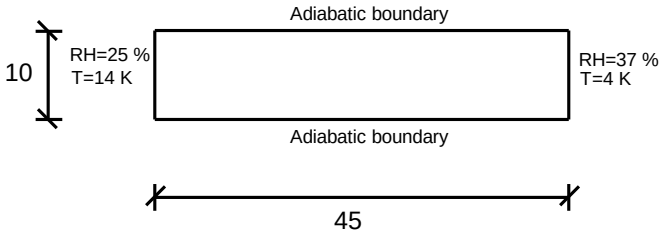

Figure 16 Geometry and boundary conditions.

The material properties used in the benchmark are given in Table 2 and Table 3.

Table 2 Material properties.

Concrete	
Young's modulus	25 GPa
Poisson's ratio	0.2
Thermal conductivity	2.5 W/(mK)
Coefficient of thermal expansion	$1.2*10^{-5}$ m/K
Specific heat capacity	1000 J/(kgK)
Diffusivity	$3.76*10^{-10}$ m^2/s
Solubility	1

Table 3 Defined shrinkage; note that the shrinkage values are fictitious.

Shrinkage	Relative Humidity [%]
-0.16	0
-0.08	25
-0.027	37
0	100

The complete analysis is performed in three steps where each step includes one type of analysis (sequential analysis). The first step is a steady state moisture diffusion analysis which results in a moisture distribution in the analysed geometry. The mass diffusion module in ABAQUS is used for the analysis, which is based on Fick's Law. The second step consists of a steady state temperature analysis, which is performed with the temperature-module in ABAQUS. In the third and last step, the results from the two previous analyses are imported to a static analysis, where the moisture and temperature distribution results in a stress field based on the defined material properties. To be able to determine whether ABAQUS accounts for both the shrinkage and the temperature expansion in the stress field, the strains obtained from the two separate analyses are compared to the strains in the combined analysis. The results are shown in Figure 17.

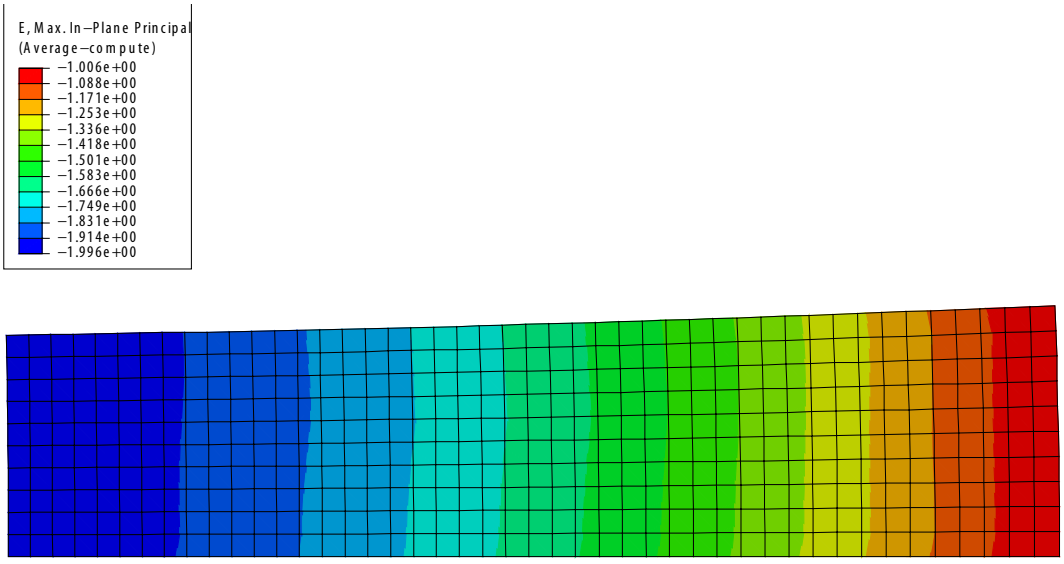

a)

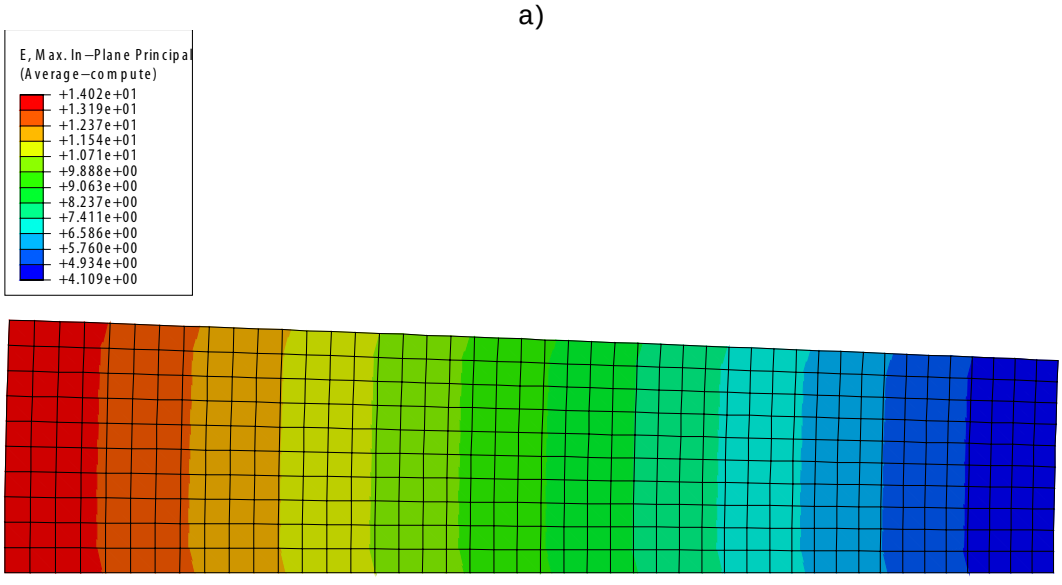

b)

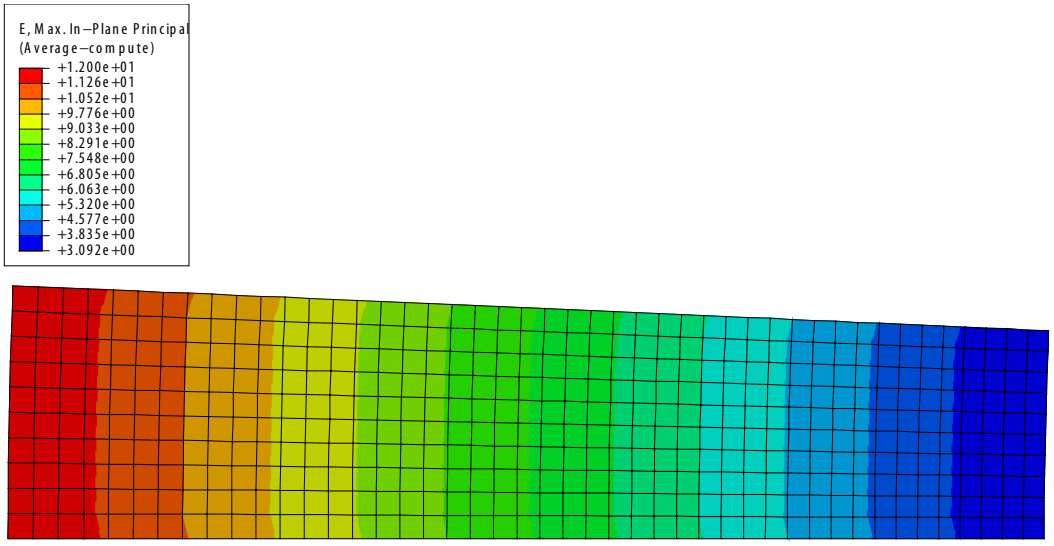

c)

Figure 17 Obtained strains for analysis considering a) Shrinkage, b) Temperature and c) Shrinkage and temperature.

As can be seen in Figure 17 c), the total strain is the sum of the strains obtained in the moisture and temperature analysis, see Figure 17 a) and b) respectively. These results imply that it is possible to account for stresses induced by both shrinkage and temperature expansion. However, it is only possible to use the implicit solver in ABAQUS if result from a mass diffusion analysis is imported to another analysis. This is quite a drawback since it sometimes is easier to get a converged solution with an explicit solver, for example when using a non-linear material model to describe cracking in concrete.

4 Non-linear finite element model

A 3D solid FE model has been developed in Abaqus version 6.11 of the reinforced concrete foundation presented in section 2.1. The purpose of the FE model is to simulate the response of the foundation subjected to the mechanical and environmental loads and to study the possible causes for cracking. The structural behaviour the foundation has been analysed taking into account the time-dependent thermal and moisture gradients in combination with dead loads and some of the operational loads imposed to the foundation. The finite element model has been defined with a non-linear material model in order to simulate the formation and propagation of the cracks.

4.1 Geometry

The geometry of the generator foundation is partly axisymmetric; however, there are some penetrations, i.e. entries and doors, in the wall of the foundation why the rotational symmetry not can be utilized in the analyses. In Figure 18 the general geometry of the foundation without the penetrations is shown, where the *x*-axis is the radius and the *y*-axis the height of the foundation.

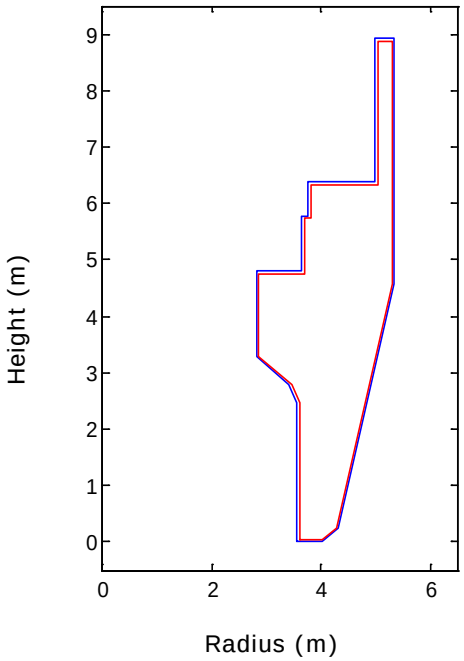

Figure 18 The general geometry of the foundation.

There are a number of penetrations in the wall of the generator foundation. In the upper part of the foundation, above the supports for the stator, four

evenly distributed penetrations are located, see Figure 19. The dimension of these penetrations is 800x1200 mm^2 (hxw) and are approximately placed at 0°, 90°, 180° and 270° relative to a conventional Cartesian coordinate system placed in the middle of the foundation, see Figure 19. In the lower part of the generator foundation, a total of three more penetrations can be found, as seen in Figure 19. One large penetration with a dimension of 2300x2000 mm^2 located at 180° and 2650 mm from the bottom of the foundation to the centre of the penetration. The other two penetrations can be found at 90° and 270°, where the height is equal to the aforementioned penetration while the width is 1200 mm. The geometry of the generator foundations is shown from two different views in Figure 19.

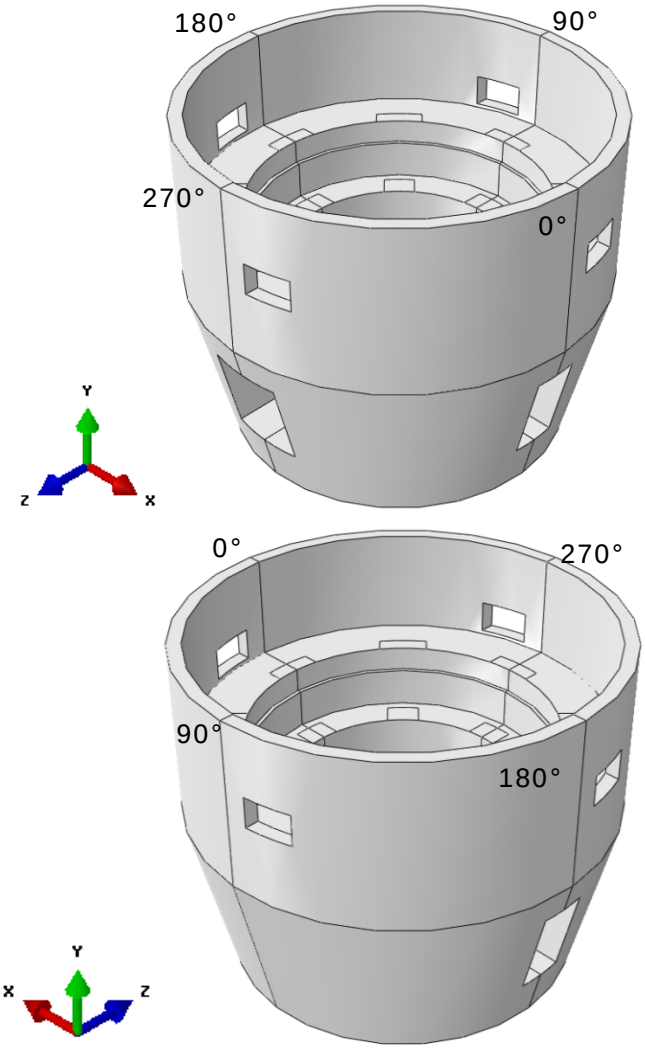

Figure 19 The geometry of the generator foundation from two views showing the different penetrations.

The reinforcement has been modelled with a simplified method which assumes an evenly distributed reinforcement in two perpendicular directions. The average reinforcement diameter is 25 mm with an average distance between the reinforcement bars of 250 mm. In the FE-model, the centre of

the reinforcement is assumed to be placed 50 mm from the surface of the foundation; which yields a 37.5 mm concrete cover. According to the blueprints, the distance from the centre of the reinforcement to the surface should not exceed 40 mm or be less than 30 mm. With the assumptions made above, these requirements are fulfilled. In Figure 20, the surface of the foundation is illustrated in blue and the reinforcement in red.

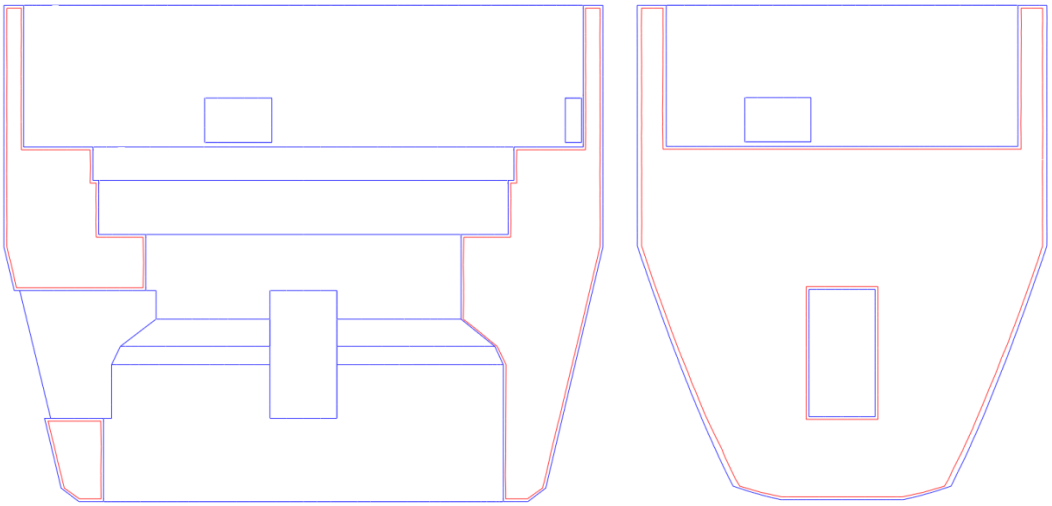

Figure 20 The surface of the foundation is illustrated in blue and the reinforcement in red.

4.2 Mesh

A high mesh density is required to be able to analyse the crack propagation in the foundation. The elements used for the concrete foundation in the FE-model are called C3D8R, which is an 8-node hexahedron with reduced integration and has a characteristic length of 0.2 m. The reinforcement has been modelled using rebar layers defined in shell elements S4R. The shell elements have a characteristic length of 0.2 m and are defined as embedded in the concrete. Perfect bond, i.e. no slip is allowed, between the reinforcement and the concrete have thereby been assumed. The model consists of a total of approximately 50 000 elements and 200 000 degrees of freedom. The used mesh density is high enough to be able to describe the crack propagation, which has been verified previously in for instance Hassanzadeh et al. (2012).

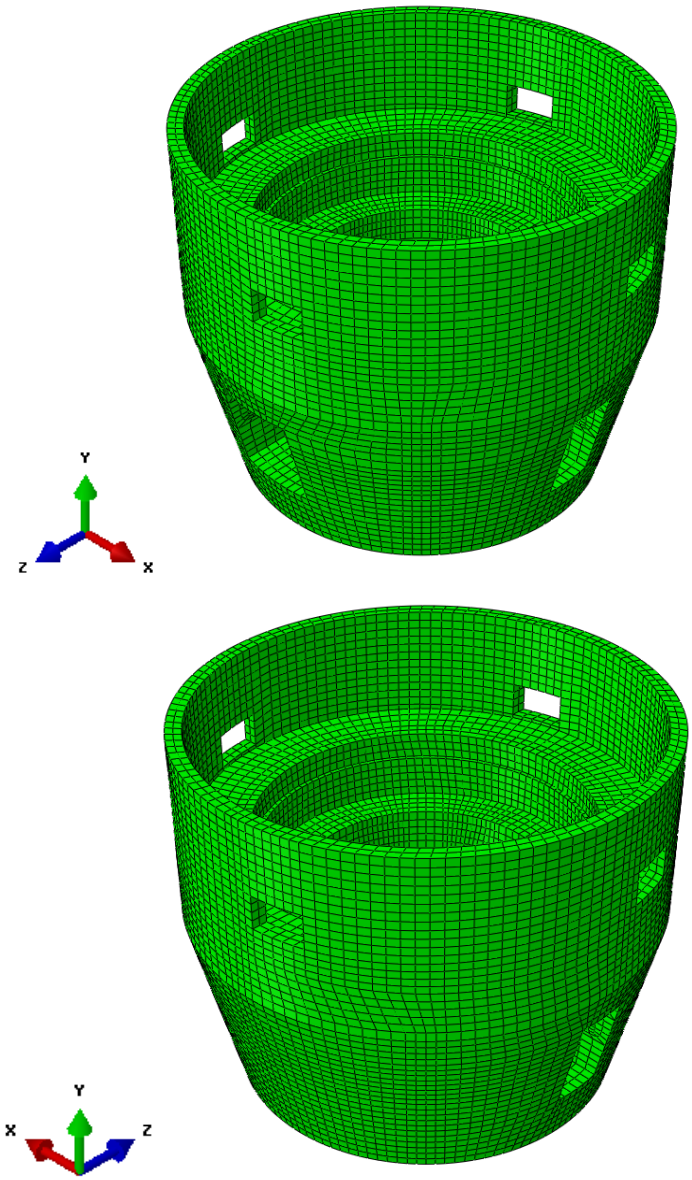

Figure 21 Geometric mesh of the concrete foundation.

4.3 Material properties

4.3.1 Elastic properties

The concrete and steel material properties used in the analyses are based on the properties presented by Larsson (2008). Since the analyses presented herein also will include stresses induced by shrinkage of the concrete, some additional moisture material properties are given in Table 4.

Table 4 Concrete material properties.

Concrete	
Density	2300 kg/m^3
Young's modulus	25 GPa
Poisson's ratio	0.2
Thermal conductivity	2.5 W/(mK)
Coefficient of thermal expansion	1.2*10^{-5} m/K
Specific heat capacity	1000 J/(kgK)
Diffusivity	3.76*10^{-10} m^2/s
Solubility	1

The reinforcement is of quality B500, all steel material properties used in the analyses are given in Table 5.

Table 5 Reinforcement material properties

Reinforcement	
Density	7800 kg/m^3
Young's modulus	200 GPa
Poisson's ratio	0.3
Thermal conductivity	2.5 W/(mK)
Coefficient of thermal expansion	1.2*10^{-5} m/K

4.3.2 Non-linear behaviour

The concrete damaged plasticity model in Abaqus has been used to simulate concrete crushing and cracking. A description of the material model can be found in Malm (2009).

According to Larsson (2008), the concrete quality in the foundation is K25 which corresponds to a C20/25 concrete in Eurocode 2. Therefore, the non-linear material properties are defined in accordance with the mean values given in Eurocode 2.

In Figure 22 the mean material properties given in Eurocode 2 for a concrete quality of C20/25 are shown together with the defined stress-strain curve in compression. Note that this curve is used to define the compressive material behaviour in the FE-analyses.

Compression
f_{cm} = 28 MPa
E_{cm} = 30 GPa
ε_{c1} = 2.0 ‰
ε_{cu1} = 3.5 ‰

Tension
f_{ctm} = 2.2 MPa

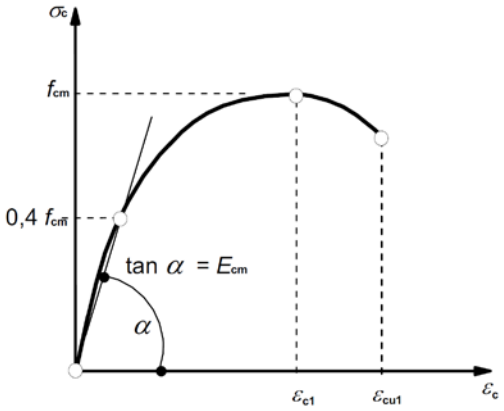

Figure 22 Non-linear material properties according to Eurocode 2.

The stress-strain curve used to describe the compressive material behaviour of the concrete in the analyses is shown in Figure 23.

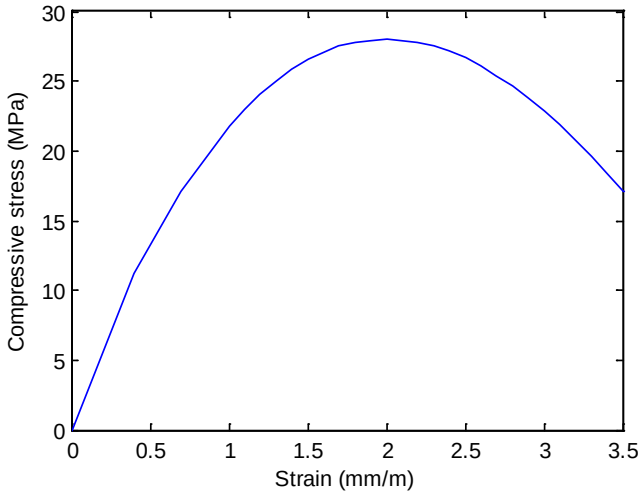

Figure 23 Compressive stress-displacement curve.

The fracture energy is not given in Eurocode 2, why the values defined in Model Code 90 (1993) are used in the analyses, see Table 6. In Model Code 90, the fracture energy was dependent on the size of the aggregates. However, in the most recent version, Model Code (2010), this dependence is not included. Instead, only a dependence on the concrete compressive strength is included, as shown in Eq. [5].

$$G_f = 180 - \frac{1385}{f_{cm}} \qquad [5]$$

Table 6 Fracture energy for different concrete qualities and aggregate sizes, from Model Code 90 (1993)

	Fracture energy G_f (Nm/m^2)							
D_{max}	C12	C20	C30	C40	C50	C60	C70	C80
8	40	50	65	70	85	95	105	115
16	50	60	75	90	105	115	125	135
32	60	80	95	115	130	145	160	175

If the aggregate size is assumed to be 16 mm, the fracture energy according to Model Code 90 is 60 Nm/m^2. Based on the compressive strength of the concrete, Model Code 2010 gives a fracture energy of 130 Nm/m^2. Since this is an old concrete structure with uncertainties regarding its material properties, the lower value of fracture energy has been defined according to Model Code 90 as a conservative measure in the analyses, i.e. 60 Nm/m^2.

In tension, the stress-displacement curve is assumed to be bilinear according to Petersson (1981) and is depicted in Figure 24.

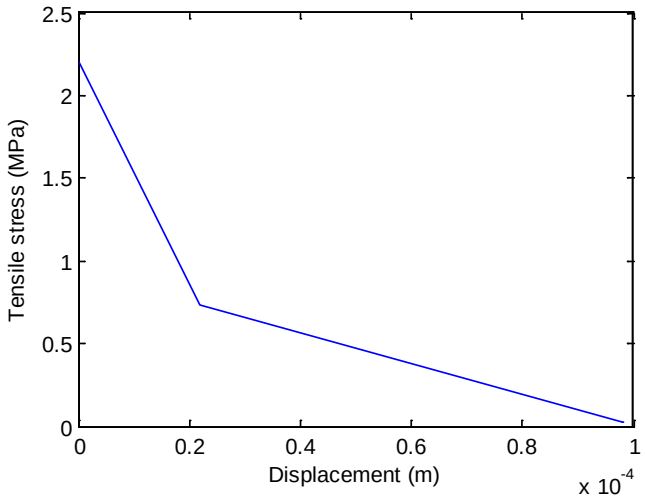

Figure 24 Tensile stress-displacement curve.

The concrete damaged plasticity model also requires that the dilation angle is defined and in these analyses it has been defined as 30°. This angle describes the volume change due to shear displacement so that a low value results in smooth cracks and a small volume strain occurs when two crack surfaces slide against each other. This parameter has almost no influence on the results in these studies since the crack propagation is governed by a tensile opening behaviour, i.e. Mode I failure (Malm, 2009).

In the analyses, perfect bond, i.e. no slip is allowed, between reinforcement and concrete has been defined. The non-linear behaviour of reinforcement has been accounted for by assuming perfect elasto-plastic behaviour with a yield

strength of 500 MPa. The analyses will however show that the maximum stress in the reinforcement is less than the yield strength in all calculations and therefore the reinforcement will behave as linear elastic.

4.3.3 Drying shrinkage

The shrinkage of the concrete has been calculated according to Betonghandboken (Ljungkrantz et al. 1994) with an assumed water content of 160 kg/m^3. The water content assumption is based on the experimental results presented in Hedenblad (1996) and Hedenblad (1995). The shrinkage definition used in the analyses is shown in Figure 25.

Shrinkage [-]	RH
2.032E-04	0
2.030E-04	10
2.015E-04	20
1.977E-04	30
1.902E-04	40
1.778E-04	50
1.593E-04	60
1.335E-04	70
9.914E-05	80
5.506E-05	90
0.000E+00	100

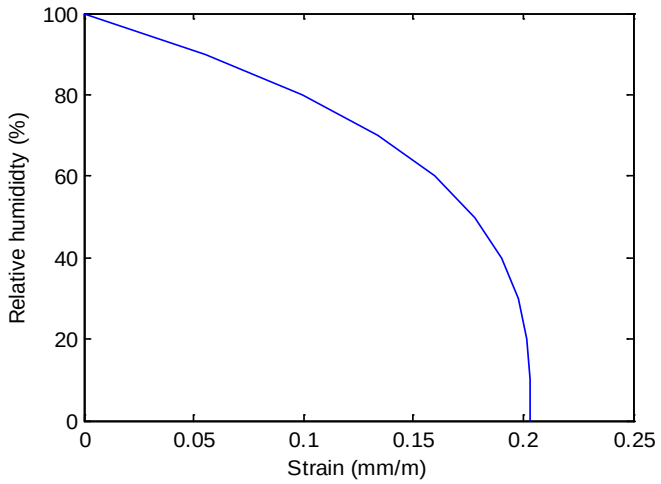

Figure 25 Concrete shrinkage.

4.4 Loads and boundary conditions

The objective of this study is to understand the complex interaction between the power generating system (stator, rotor, turbine, etc) and the supporting concrete structure, which is needed for formulation of more realistic and accurate specifications regarding load, stiffness and displacement levels and tolerances. The achievement of the objective requires models that account for the behaviour of the mechanical systems, supporting structures and their interaction under various loading conditions. The various loading conditions include

- mechanical loads (static, dynamic, short-term, long-term, etc) such as weight of the structures and systems, and operating loads caused by the turbine, rotor, stator, etc
- environmental loads (physical, chemical, etc) such as strains and restraints caused by temperature and moisture variations, and chemical reactions.

The work presented here is limited to the modelling of the behaviour of the foundation under the influence of the dead weight, loads from the stator and rotor spider, temperature effects and moisture variations. Although the other effects are disregarded in this report the study will continue to include the factors, which were described above.

As shown in Section 4.1, the concrete foundation is massive and its thickness and radius varies along with the axis of the revolution, which can lead to high tensile stresses caused by both temperature and moisture gradients. The temperature and moisture gradients exist in three directions, the radial, tangential and vertical directions of the foundation. Mechanical loads caused by the oscillation of the generator, friction at the supports and the weight of the structure and machines are the additional factors, which must be taken into account.

4.4.1 Mechanical loads

The mechanical loads that are considered in this study are summarized in Table 6. These loads are based on the loads presented by Larsson (2008).

Table 7 Loads caused by the power generating system.

Device	Duration	Load level	
Vertical loads on stator support			
Stator	Permanent	1200	kN
Cooling system	Permanent	100	kN
	Sum	**1300**	**kN**

Vertical loads on the rotor spider			
Rotor	Permanent	2890	kN
Turbine	Permanent	1200	kN
Spider and bearings	Permanent	250	kN
Turbine cover	Permanent	530	kN
Water	Variable (normal)	5720	kN
Water	Variable (exceptional)	8140	kN
	Sum (normal)	**10590**	**kN**
	Sum (exceptional)	**13010**	**kN**
Tangential loads acting on the stator support			
Moment acting on stator	During operation	4,974	kNm
The moment is opposed by 4 couples (lever arm 4 m)	During operation	157	kN
Radial loads acting on the stator support			
Sinusoidal load caused by magnetic eccentricity.	During operation (in the opposite direction of the load acting on the rotor spider)	180	kN
Frictional load acting on the each support	(A parametric study of influence have been performed, from frictionless to the case of a fixed boundary when the full thermal load of the stator beam expansion is subjected to the supports)	F_{max}= 1254 (assuming a fixed support)	kN
Radial loads acting on the rotor spider support			
Sinusoidal load caused by magnetic eccentricity.	During operation	180	kN
Thermal force acting on the each support (assuming $\Delta T = 20\ ^{\circ}C$)		627	kN

The thermal force has been calculated based on the thermal expansion of the steel beams for a maximum temperature difference of $\Delta T=20^{\circ}C$ from cooling.

The loads presented in Table 7 are applied to the supports for the stator and rotor spider, as illustrated in Figure 26. The support locations are located with 45-degree placement and have a size of 1200x400 mm^2 and 600x800 mm^2 for the stator and rotor spider respectively. The vertical loads are applied as uniform surface pressure on each support. The tangential and radial loads were applied as surface tractions, i.e. distributed load acting in the plane of each surface in radial or tangential direction respectively.

All loads in Table 7 are treated as static loads in most of the simulations. However, the load caused by magnetic eccentricity that acts in radial direction on both stator and rotor spider supports have in addition also been studied as a dynamic load. This load and its dynamic effect on the structure is further described in section 5.5.

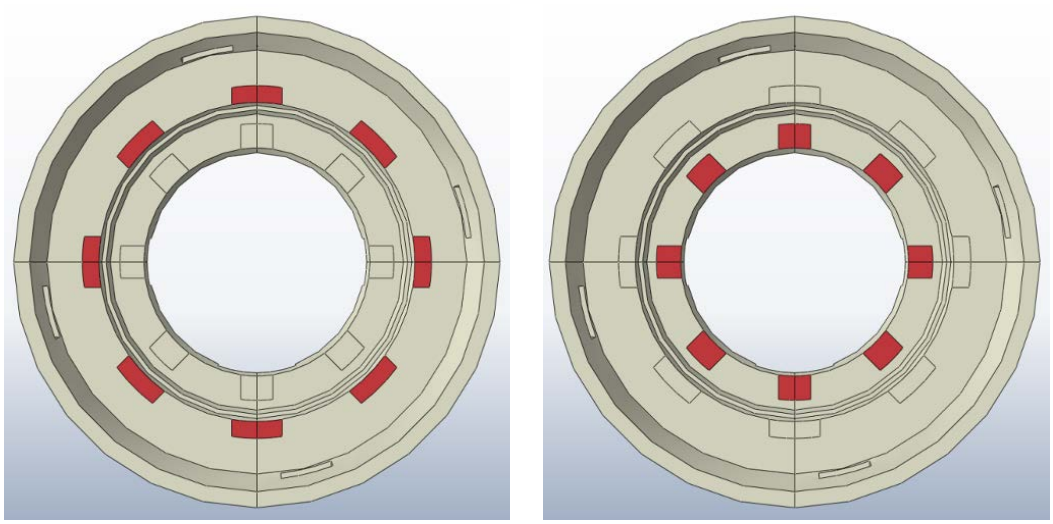

a) b)

Figure 26 Areas for the support from stator (a) and rotor spider (b) respectively.

4.4.2 Boundary conditions

According to the drawings shown in Figure 3 the concrete foundation is connected to the turbine floor and the generator floor. This is also illustrated in the 3D sketch in Figure 1. To include the constraints and the stiffness from the floors, each floor has been modelled with springs.

The FE model of the foundation is constrained to translations in vertical and radial direction in the bottom. At the top and middle part, the foundation is only partly constrained in the radial direction since the connecting floor structures do not fully prevent the motions of the foundation. To simulate this in the FE model, all springs have been defined with a relatively low stiffness in order to allow for a relative displacement of the foundation in relation to the turbine and generator floors. Connector elements are used to model the

elastic boundary, one connector element is introduced at each node in three rows in the circumference at both the top and middle part of the foundation. Each connector are assigned with a stiffness of 500 or 1000 N/m in radial direction, where the higher stiffness is assigned to the connectors belonging to a middle row and the lower stiffness to the remaining rows. The boundary conditions used in the structural analyses are illustrated in Figure 27.

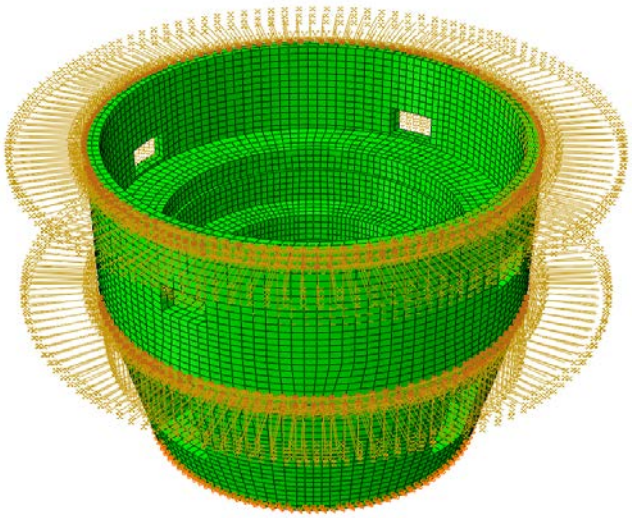

Figure 27 Structural boundary conditions.

The boundary conditions shown in Figure 27 differ from the boundary conditions used in Larsson (2008) and Hassanzadeh et al (2012) in regards of how the turbine and generator floors are modelled. In those studies, only two points were constrained at 0° and 180° respectively. That was a simplification of the actual boundary conditions and the boundary conditions used in the present report is assumed to give a more accurate description.

4.4.3 Temperature and moisture conditions

Both the ambient temperature and humidity have been considered in the analyses. During operation it is assumed that there is a temperature difference of 10 °C between the inside and the outside of the foundation. The inside temperature is approximately 34 °C during summer and 25 °C during winter; the corresponding outside temperatures are 24 °C and 15 °C. However, to describe the real variation of the ambient temperature, a transient analysis has to be performed. Temperature induced stresses due to a steady state thermal distribution based on the assumed temperature difference, as well as stresses induced by the time-dependent thermal distribution have been presented in Hassanzadeh et al. (2012).

The shrinkage of the concrete is of course dependent on the relative humidity in the ambient air. To calculate the boundary conditions to be used in the mass diffusion analysis, climate data from Trollhättan produced by SMHI have been used, see Figure 28.

a)

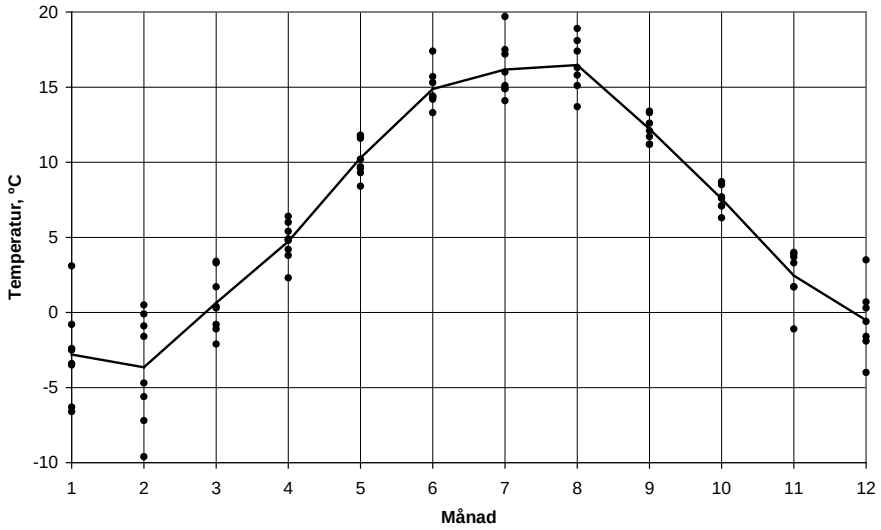

b)

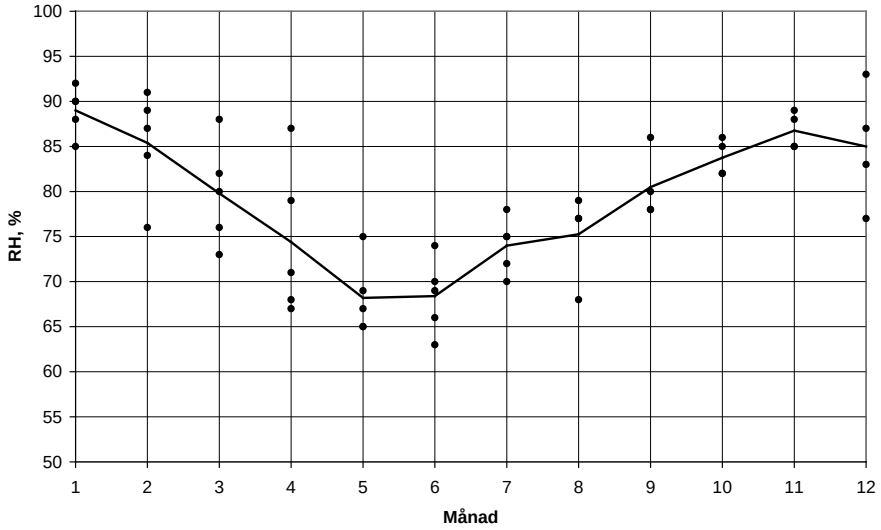

Figure 28 Measured monthly variation in Trollhättan, a) temperature and b) relative humidity.

The vapour content in the air inside the generator building can be assumed to be the same as in the outside air; this assumption together with the aforementioned boundary temperatures result in the boundary conditions, for January and June, presented in Table 8.

Table 8 Boundary conditions for the mass diffusion analysis.

Boundary	RH [%]
$RH_{outside,january}$	26.5
$RH_{inside,january}$	14.8
$RH_{outside,june}$	40
$RH_{inside,june}$	23.2

5 Numerical results

5.1 Mechanical loads

All loads specified in Table 7 are considered in the analyses, and are applied in the following steps in the analyses:

1. Gravity load of the foundation
2. Loads on rotor spider supports
    - Vertical (from the water load and additional masses of structural components, see Table 7)
    - Radial (from magnetic eccentricity and thermal expansion of the steel beams in the rotor spider, see Table 7)
3. Loads on stator supports
    - Vertical (from the of stator and the cooling system, see Table 7)
    - Tangential (from the reaction moment during operation, see Table 7)
    - Radial (from magnetic eccentricity and thermal expansion of the steel beams in the rotor spider, see Table 7)

In general, when applying all the loads mentioned above the behaviour of the concrete foundation is linear elastic. However, depending on the size of the assumed radial force due to thermal expansion of the stator beams there is a risk that micro cracking is introduced into the model. Small plastic strains occur near the stator supports, when assuming a 20 °C temperature increase of the stator beam and fixed boundary, i.e. where the full thermal load of the stator beam expansion is subjected to the stator supports. The behaviour due to the mechanical loads is presented in section 5.1.1 and section 5.1.2, below.

5.1.1 Gravity load and loads on the rotor spider supports

In the first two steps only linear elastic behaviour was obtained with low stresses induced in the concrete foundation. The induced stresses in the concrete foundation are approximately between 3 MPa in compression and 1 MPa in tension. The principal tensile stresses are shown in Figure 29.

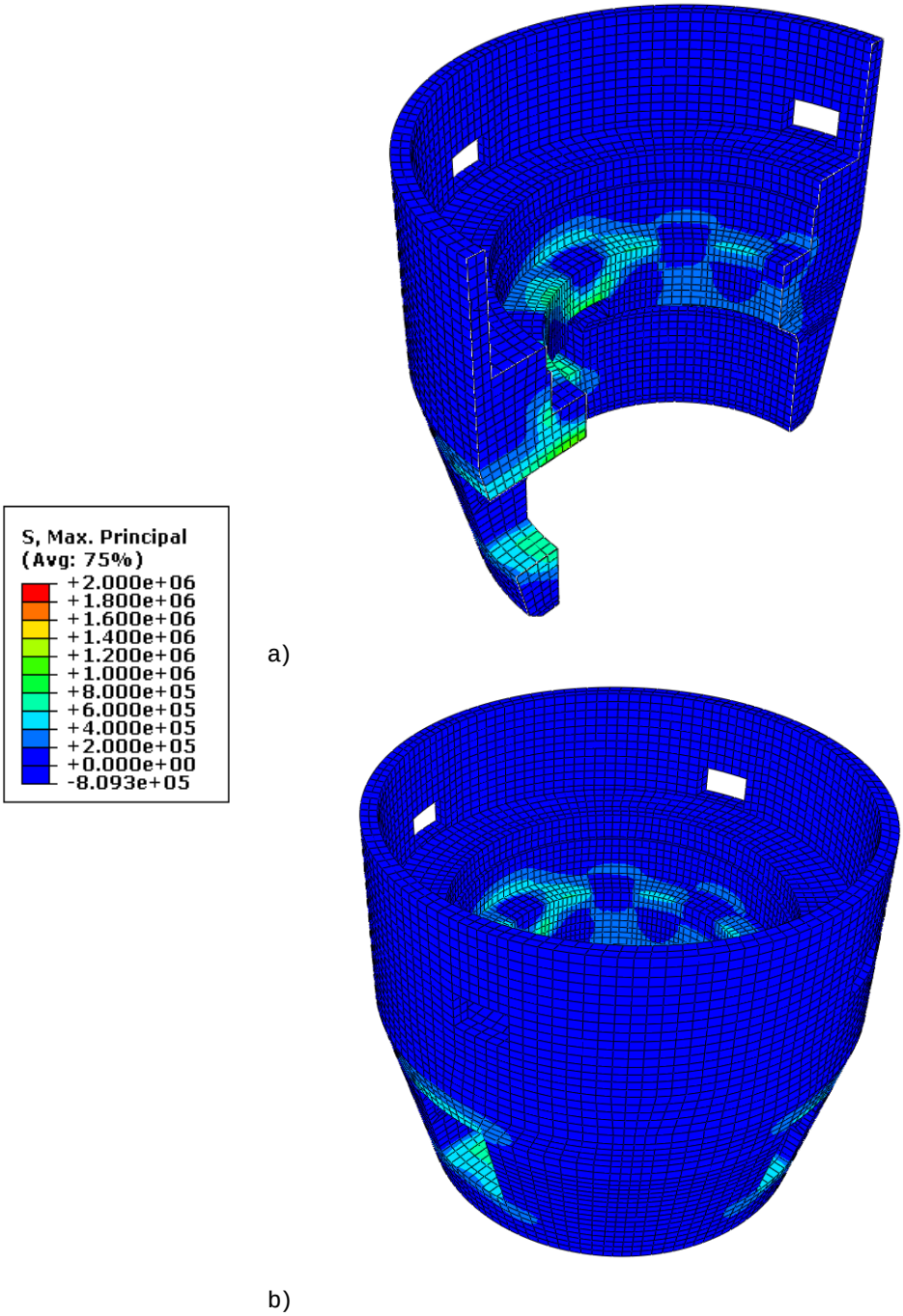

Figure 29 Principal tensile stresses from gravity and the loads acting on the rotor spider support

The loads acting on the rotor spider supports are mainly in the vertical direction as previously shown in Table 7 and also illustrated in Figure 30 below.

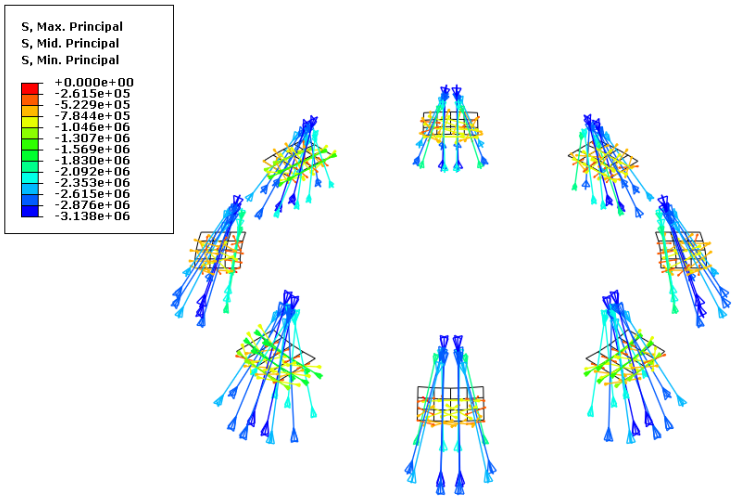

Figure 30 Direction of principal stresses in the rotor spider supports.

5.1.2 Loads acting on the stator support

In the third analysis step, large stresses are introduced in the concrete foundation as the loads acting on the stator support are taken into account. It is especially the radial forces, from for instance the thermal expansion of the stator beam that cause initiation of high stresses. The direction of the principal stresses at the stator supports are illustrated in Figure 31 and the induced tensile stresses in the concrete foundation are shown in Figure 32.

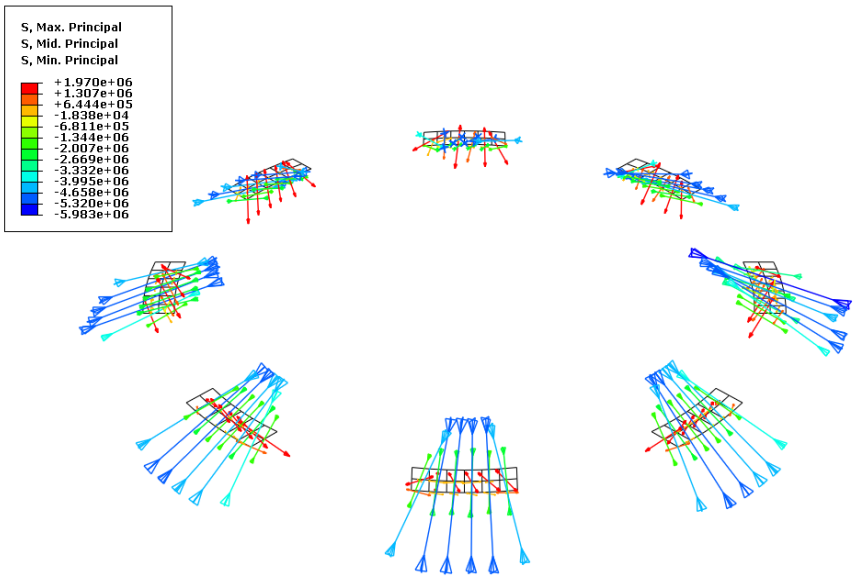

Figure 31 Direction of principal stresses in the stator supports.

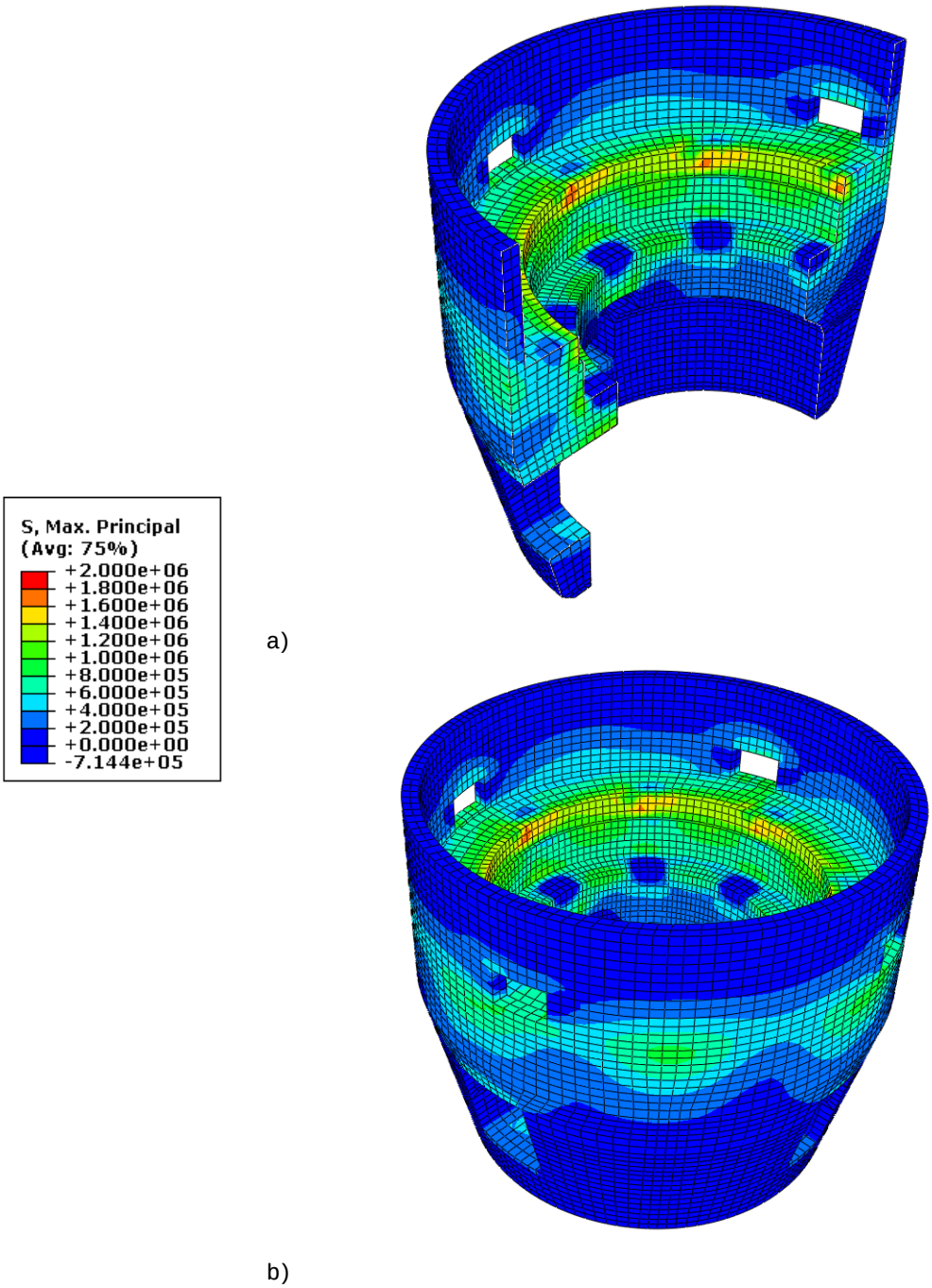

Figure 32 Principal tensile stresses from gravity and the loads acting on the rotor spider and stator support.

Due to the loads acting on the stator supports, large tensile stresses are introduced in the radial direction. This is primarily caused by the thermal expansion of the stator beams. With a thermal expansion equal to 20 °C, see Table 7, the numerical model indicates that some minor cracking occurs in a

few elements of the foundation near the stator supports. The induced plastic strains that occur near the stator supports are illustrated in Figure 33 .

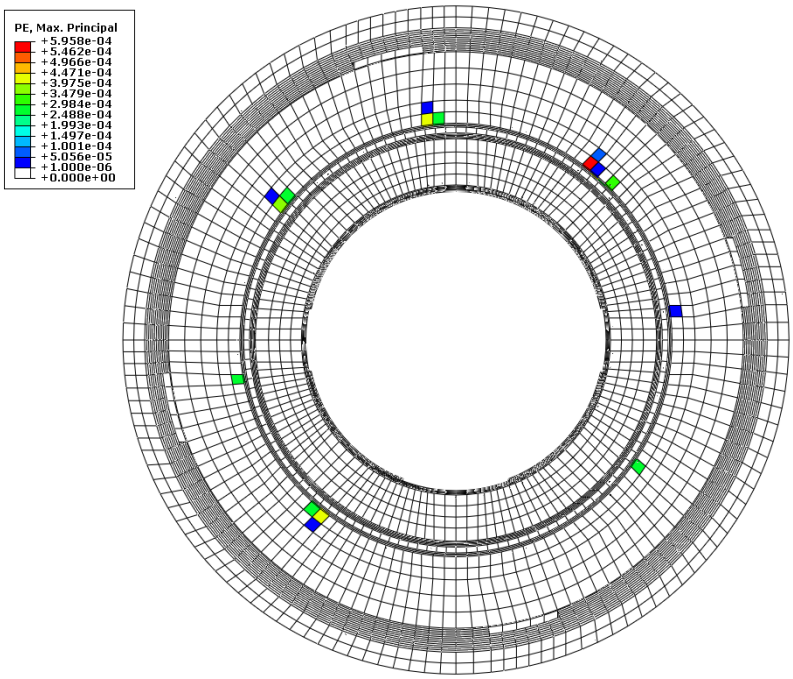

Figure 33 Plastic strains, i.e. cracks, near the stator supports.

The frictional forces at the stator and rotor spider supports due to the thermal expansion of the steel beams have a large effect and could, as shown in Figure 33, induce cracking near the supports. The influence of friction has been studied in the analyses through a parametric study, where different values of the frictional forces at the stator support were studied. The worst-case scenario is if the frictional supports lose their ability to slide, i.e. becomes a fixed boundary. In the following analyses it has been assumed that the full load from the thermal expansion of the stator is applied to the stator supports, i.e. a fixed support of the stator and rotor spider beams.

5.2 Climatic conditions

In the analyses temperature effects and moisture content will be taken into account. First the distribution of temperature and relative humidity will be calculated in two separate analyses. These distributions will then be introduced as predefined fields into the numerical models with the principle described earlier in Section 3.2, i.e. where the temperature and moisture is calculated into strain.

5.2.1 Steady state temperature

The temperature gradients obtained from the steady state temperature analyses for summer and winter are presented in Figure 34 and Figure 35, respectively. The temperature distributions are later used as a predefined filed for the analyses of thermal induced stresses, see Section 5.3.2 and 5.3.3.

Note that the reference temperature is 20 °C and not 0 °C, why the boundary temperatures in the figures only shows the difference compared to the reference temperature and not the total temperature.

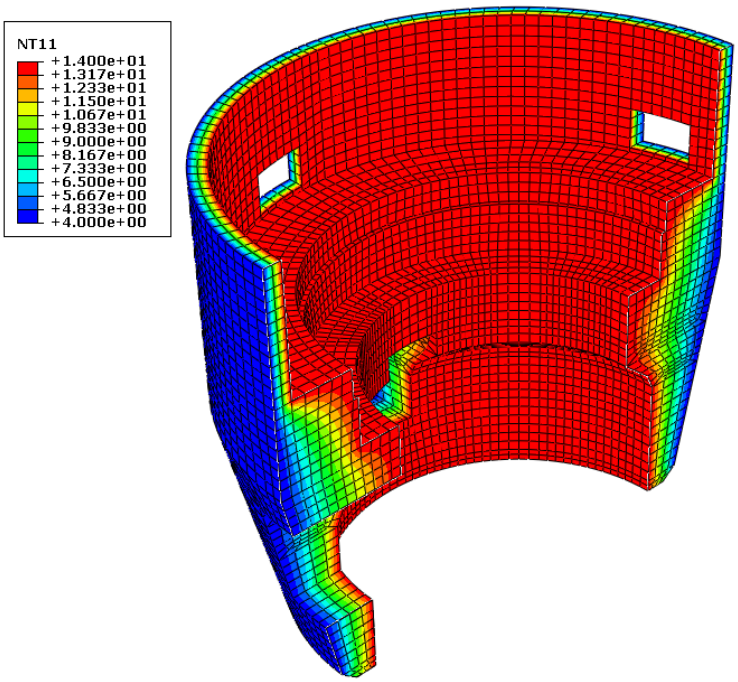

Figure 34 Temperature distribution for summer, compared to the reference temperature 20 °C.

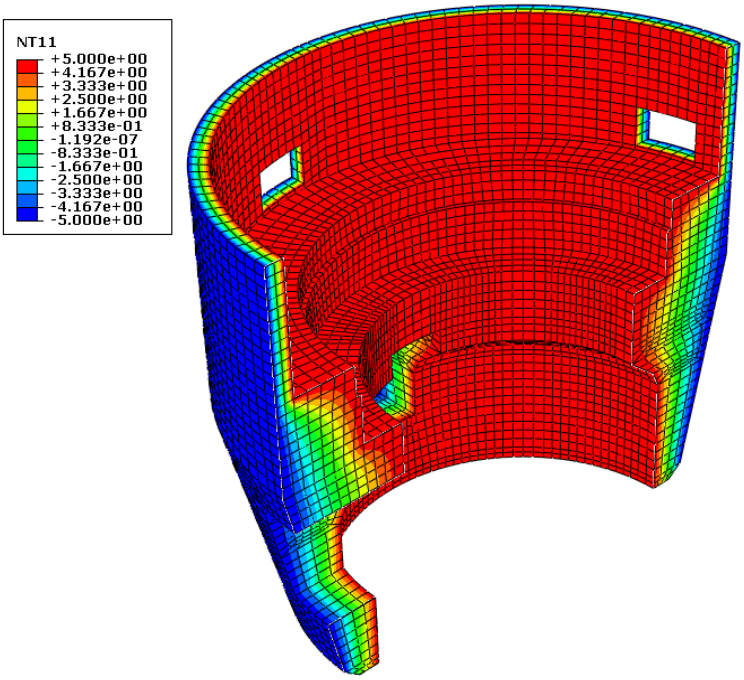

Figure 35 Temperature distribution during winter, compared to the reference temperature 20 °C.

5.2.2 Relative humidity

The mass diffusion analysis has been performed as a transient analysis where the foundation is assumed to have 80% relative humidity as an initial condition. The inside and outside boundaries of the foundation are then subjected to the January conditions for 6 months and then to the June conditions for 6 months; the procedure is repeated for 20 years. The relative humidity for the winter and summer condition was previously shown in Section 4.4.3.

The transient calculation of mass diffusion, i.e. drying of concrete, was performed for a time period equal to 20 years. The obtained distribution in relative humidity can be seen in Figure 36 and Figure 37 and with a relative humidity at the surface equal to summer and winter conditions respectively.

The calculated distribution of relative humidity, i.e. moisture, is later used as a predefined filed for the analyses of shrinkage induced stresses, see section 5.3.1.

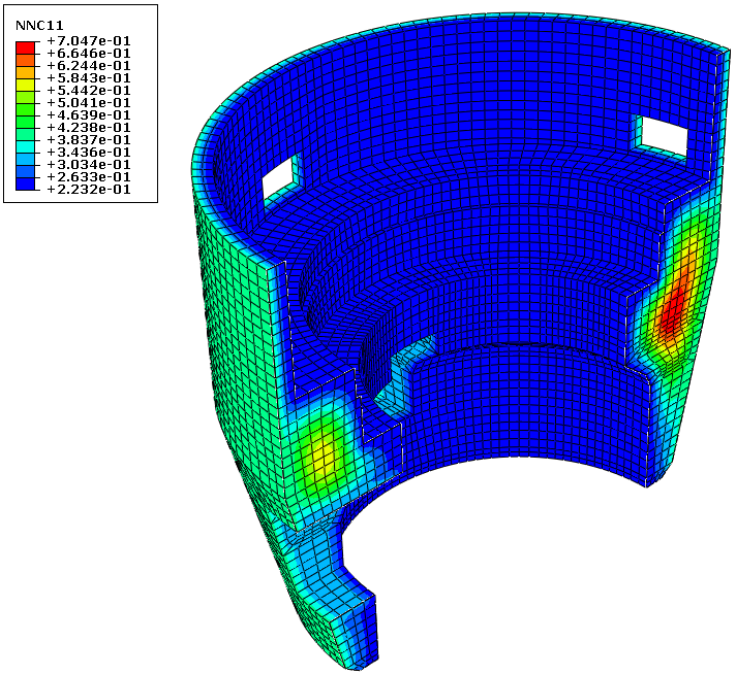

Figure 36 Relative humidity inside the foundation after 19.5 years, summer conditions.

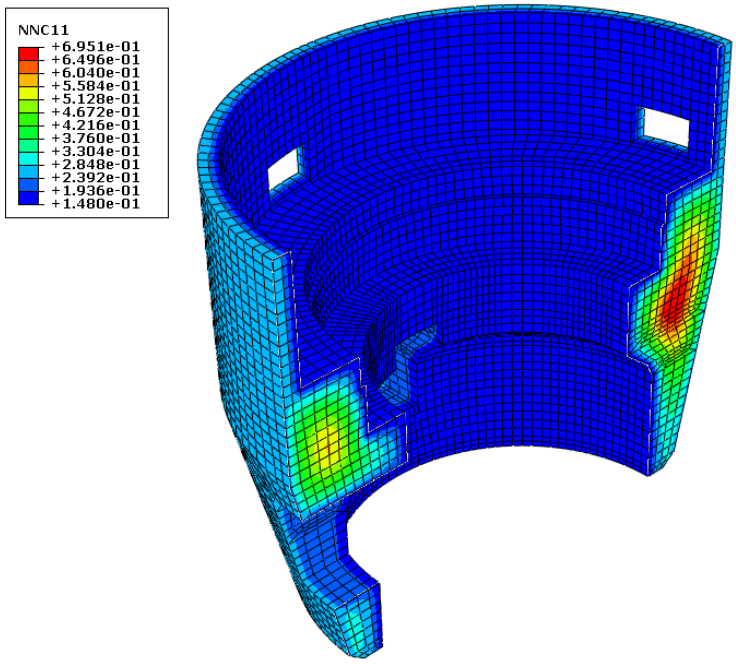

Figure 37 Relative humidity inside the foundation after 20 years, winter conditions.

5.3 Coupled diffusion, temperature and stress analysis

This analysis is performed to study the combined effect of drying shrinkage and variation in temperature. The results are used to predict the time dependent degradation of the concrete foundation and especially to study whether the long-term effects may be the reason behind the cracks close to the stator and rotor spider supports that have been found in-situ, see Section 2.1.

In this analysis loads were applied in six different steps

1. Gravity
2. Loads on rotor spider support (incl. thermal expansion of beams)
3. Loads on stator supports (incl. thermal expansion of beams)
4. Drying shrinkage
5. Summer temperature state
6. Winter temperature state

The first three steps of the analysis have already been presented in Section 5.1 and therefore only step 4 – 6 are shown here.

5.3.1 Drying shrinkage

In this step the drying shrinkage that has occurred for a time period of 20 years is estimated. From the mass diffusion calculation presented in Figure 36 and Figure 37 it could be seen that even after 20 years, there are significant differences in relative humidity within the structure. The centre of the thickest part of the concrete foundation has a relative humidity of 70% after 20 years while the surfaces are assumed to have a relative humidity equal to the ambient air, i.e. between approximately 15% and 40%. Due to the time it takes for the drying shrinkage to occur, the effect of the non-uniform shrinkage, over the thickness of the concrete foundation, is significant. The more slender parts of the concrete foundation have reached their full drying shrinkage after a much shorter time period. Due to the large variation in thickness of the concrete foundation, there is a differential shrinkage between the thinner and the thicker parts of the foundation, which results in restraint forces within the structure. Similar results have been found in for instance box-girder bridges, where the bottom flange usually is much thicker than the webs and the top flange. According to Kristek et al. (2006), the deflection of some cast-in-place box-girder bridges has continued to increase over very long periods due to the differential shrinkage, and the deflection curves do not level of even after 30 years

It can be seen in Figure 38 that cracking has occurred inside of the concrete foundation. The cracks that occurred in the analysis are located around the stator supports. The cracks that were obtained in the analysis correspond with the cracks found near the stator supports in situ, as seen in Figure 7. There are also some cracks near the rotor spider supports just above one of the large penetrations. This crack is thereby located in the same position as the crack that was found in situ, previously shown in Figure 6.

One important effect that however is not included in this analysis is the differential shrinkage due to casting sequences, where new concrete is casted next to older concrete. The supports for the stator beams are cast in concrete, and therefore additional cracking would occur around the stator supports if differential shrinkage due to the casting sequences would be considered.

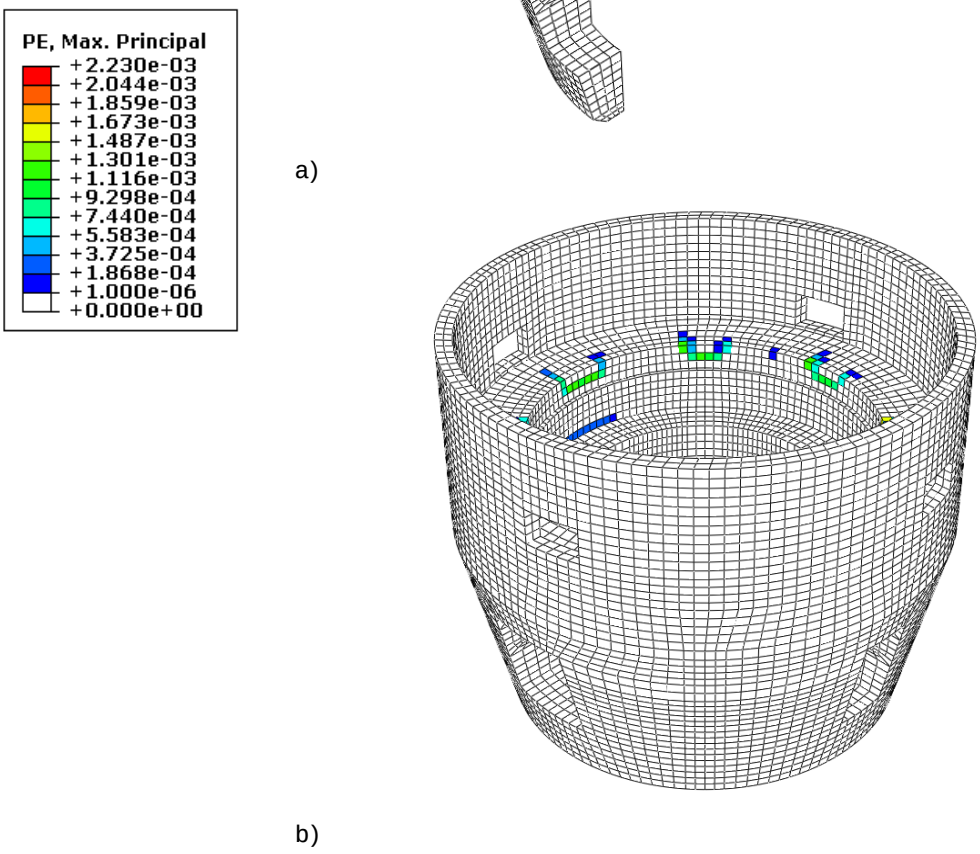

Figure 38 Plastic strains near the stator supports due to drying shrinkage.

5.3.2 Summer temperature state

In this step the temperature conditions corresponding to a summer case, see Figure 34, is taken into account. The calculated extent of cracking is illustrated in Figure 39.

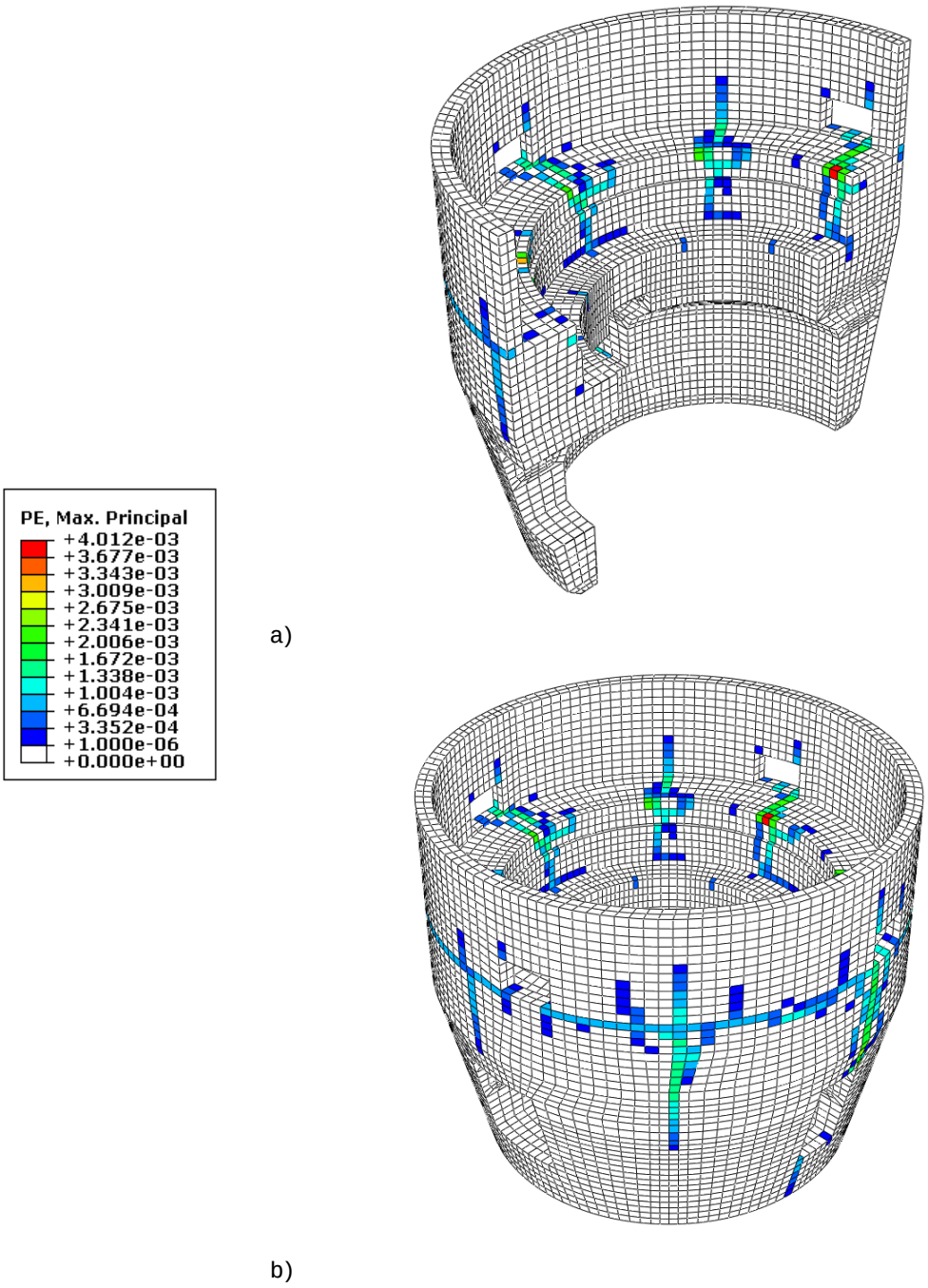

Figure 39 Plastic strains after the summer temperature state.

The results show that the cracks near the supports for the stator that initiated due to the drying shrinkage propagates further and several new cracks are found inside the concrete foundation. Several of the cracks have propagated downwards in the structure to the supports for the rotor spider. In the previous step, the cracks were found around the stator supports, in the same way as have been observed in situ, as seen in Figure 7. In Figure 39 it can be seen that these cracks has propagated in a vertical direction both downwards and upwards. The cracks that propagated downwards have reached the supports for the rotor spider, where cracks are found in the tangential direction behind the supports.

The summer temperature case has also introduced several cracks, both in tangential direction and vertical direction on the outside of the concrete foundation. These cracks initiated mainly at the corners of the penetrations and then propagated in a tangential direction as shown in Figure 40 b).

5.3.3 Winter temperature state

The temperature distribution corresponding to winter conditions, as shown in Figure 35, is taken into account in this step. The calculated extent of cracking is illustrated in Figure 40. As seen in Figure 40 the extent of cracking on the outside of the concrete foundation has only increased marginally, where some vertical cracks have propagate a bit further. During the winter condition the temperature difference between inside and outside is approximately the same as in the summer case, i.e. 10 °C. However, the temperature on both sides has been reduced approximately 9 °C to 15 °C and 25 °C on the outside and inside respectively.

During the winter temperature state, new cracks have initiated in the radial direction next to the rotor spider supports. The extent of cracking obtained from the calculations corresponds well with the cracks found near the rotor spider support which was presented earlier in Figure 8. It seems thereby that the cracks that have been found near both stator and rotor spider supports could have been initiated by the drying shrinkage and temperature effects during operation.

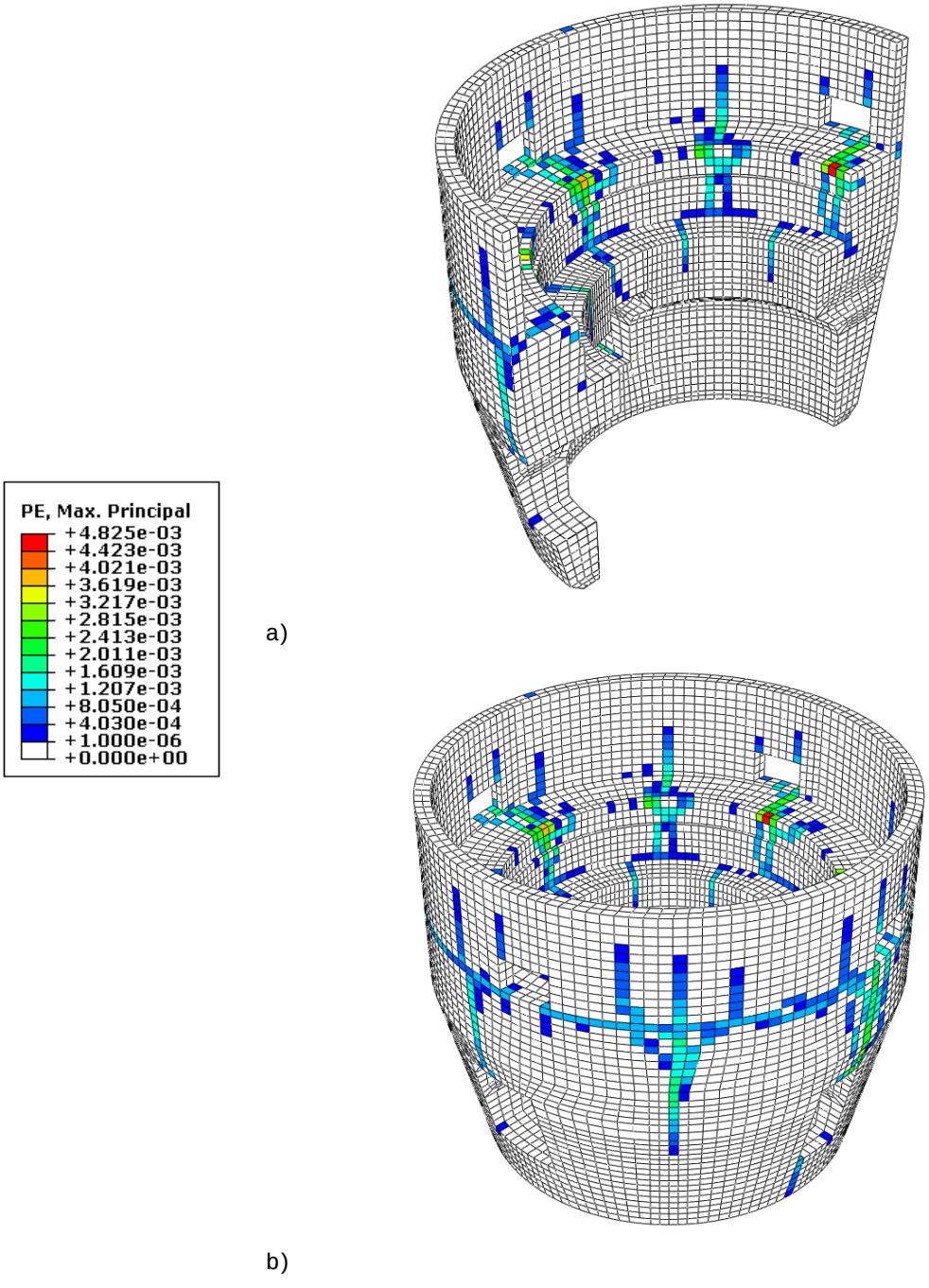

Figure 40 Plastic strains after the winter temperature state.

Even though a quite significant amount of cracking has occurred, the stress in the reinforcement is never close to yielding. The maximum stress obtained in the reinforcement is approximately 300 MPa and it therefore acts linear elastic during the whole analysis.

5.4 Temperature variations due to starts and stops

In this analysis loads were applied in five different steps

1. Gravity
2. Loads on rotor spider support (incl. thermal expansion of beams)
3. Loads on stator supports (incl. thermal expansion of beams)
4. Steady state temperature distribution
5. Time-dependent temperature variation

The difference between step 2 and 3 in this analysis and the previous in section 5.3 is that the thermal expansion is not included in the analysis presented here. The reason for this is that the temperature in the steel beams of the stator and rotor spider is based on the measured values presented by Rhen (2007) and is instead applied in step 4 and 5, i.e. together with the thermal loads.

5.4.1 Measured temperature variation

During operation, the temperature on the inner surface of the foundation increases due to the heat developed by the generator. Simulations have been performed based on measurements by Rhen (2007), previously presented in Section 2.1 and shown in Figure 41 below. The temperature difference between the inner and outer surfaces of the foundation is normally about 10°C.

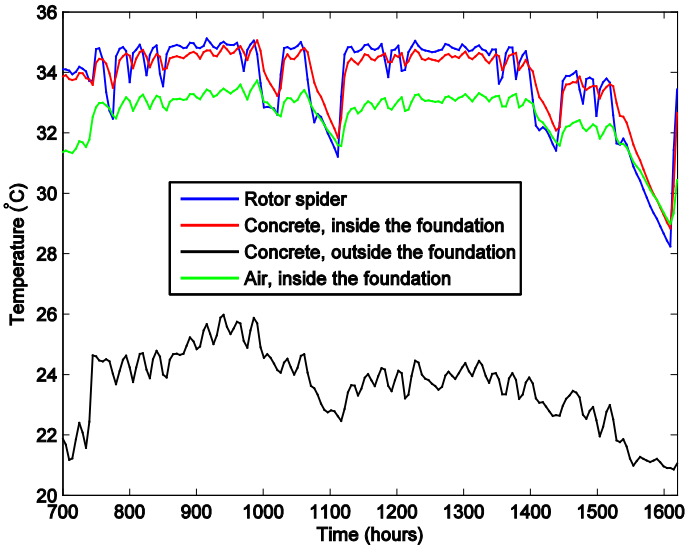

Figure 41 Measured temperature variation used as input in the FE analyses, from Rhen (2007).

5.4.2 Temperature distribution

In calculation step 4, the initial temperatures, i.e. at 700 hours, in Figure 41 were assumed to be in a steady state condition. Based on these values the temperature distribution shown in Figure 42 was calculated for the concrete foundation.

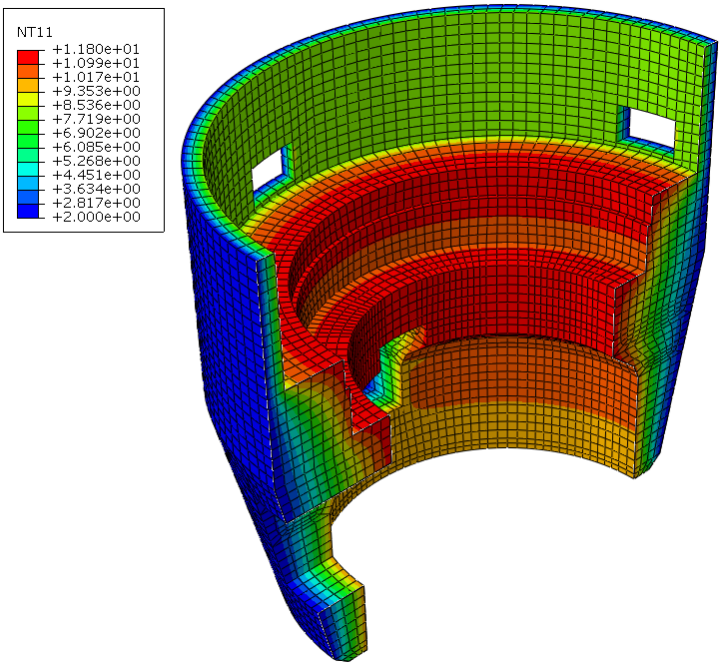

Figure 42 Initial steady state temperatures, compared to the reference temperature 20 °C.

In the following step, i.e. step 5, a transient temperature analysis was performed where the surface temperatures were varied according to Figure 41. A temperature calculation was performed for every fifth hour, resulting in about 180 transient temperature calculations.

In the measurements in Figure 41 it can be seen that at approximately 920 hours the highest temperatures on the outside of the foundation is obtained. At this point the lowest temperature gradient between the inside and outside of the foundation is obtained during the measuring period, as shown in Figure 43. The maximum temperature difference between the inner and outer surfaces is between approximately 7.5 °C and 10 °C. The corresponding temperature distribution at this time is shown in Figure 44.

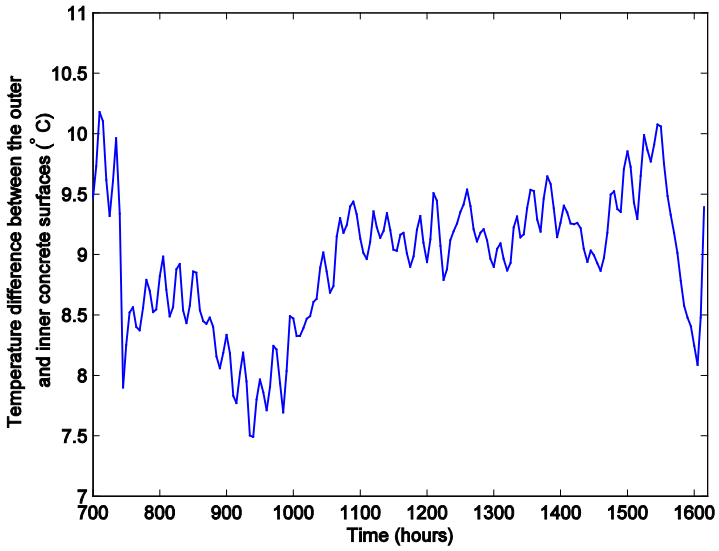

Figure 43 Temperature difference between outer and inner concrete surface.

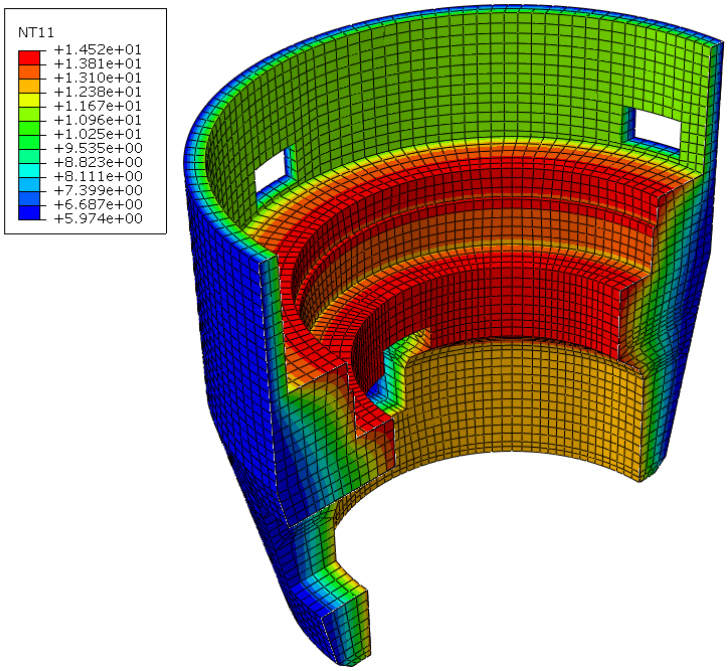

Figure 44 Temperature distribution (reference temperature 20 °C) at the time with the lowest thermal gradient, i.e. 920 hours.

According to the measurements there is a long operational stop between approximately 1520 – 1600 hours. During this period the temperature decreases about 5 °C and the temperature distribution at this time is shown in Figure 45.

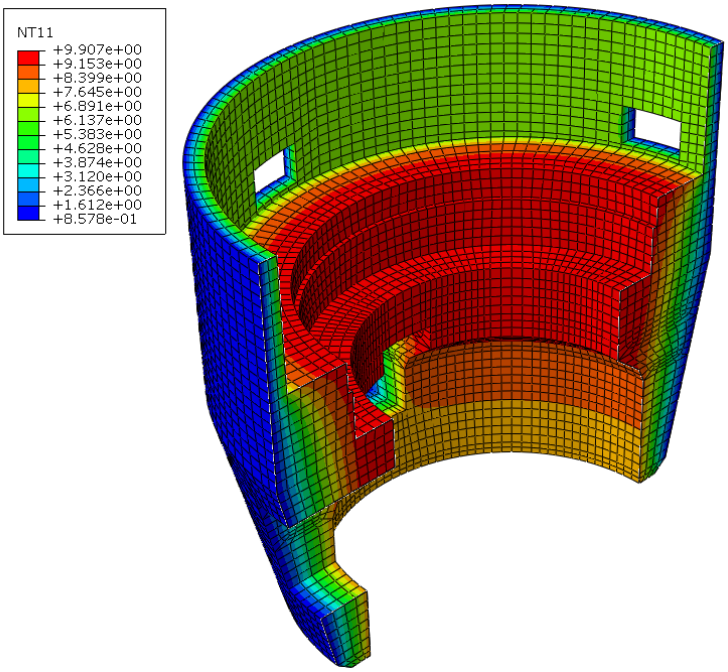

Figure 45 Temperature distribution (reference temperature 20 °C) after an 80 hours long operational stop, i.e. at 1600 hours.

5.4.3 Temperature induced cracking due to start and stops

After the analysis of the mechanical loads from gravity and loads on rotor spider and stator supports, the temperature distributions presented in Section 5.4.2 were analysed.

A finite element simulation was therefore performed to calculate the structural effect of the steady state thermal distribution shown in Figure 42. In this analysis, the frictional forces at the stator and rotor spider supports due to the thermal expansion of the steel beams were applied. The thermal expansion according to the measurements is however lower than in the previous analyses presented in Section 5.1.2. There it was assumed to be equal to 20 °C, while the measurements in Figure 41 the thermal expansion corresponds to approximately 14 °C.

Based on the steady state temperature condition, it can be seen that the concrete foundation is subjected to cracking, as shown in Figure 46. The concrete foundation cracked mainly on its outside, i.e. on the cold side, and the cracking initiated from the corners of each opening and at the transition to the thin section above the stator supports.

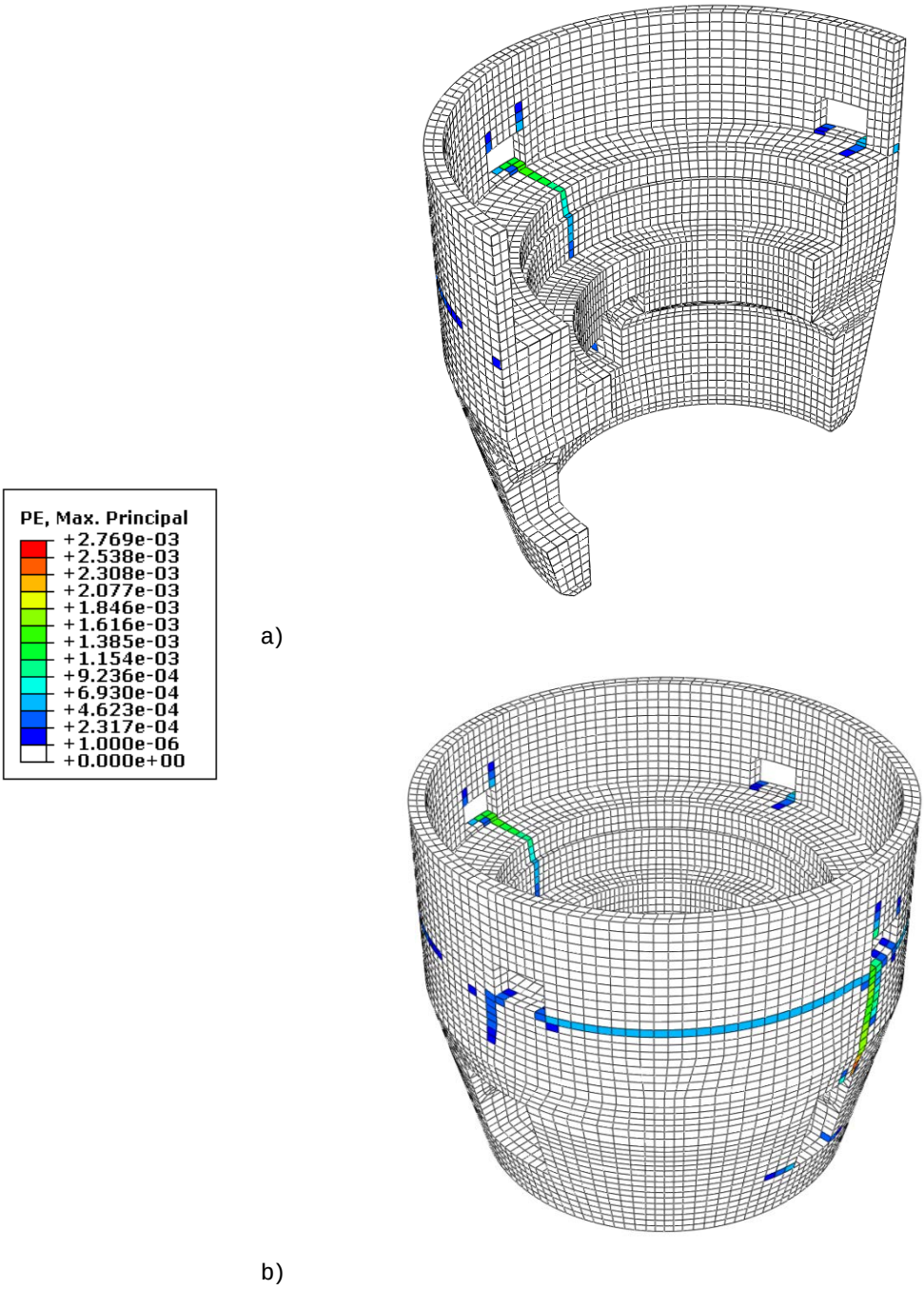

Figure 46 Areas subjected to cracking due to the measured temperature gradient.

The estimated cracking due to a steady state temperature distribution is almost identical to the result that was obtained in Hassanzadeh et al (2012), where the same type of cracks was found even though a slightly different interpretation of the boundary conditions was used in that study.

To further study the effect of the temperature, the measuring period shown in Figure 41 was simulated as a transient thermal calculation. The simulation started with the initial temperature difference between inner and outer surface of 10 °C and continued to simulate the two-month period that the measurements were performed, previously shown in Figure 41. The measured temperature of the rotor spider was introduced as an amplitude function and the forces were applied to the concrete foundation at the stator and rotor spider supports. The forces were calculated based on the thermal expansion of the steel beams, i.e. assuming that the stator supports are fixed supports just as the rotor spider supports. In Figure 47 the crack propagation due to the time-dependent temperature variation is shown. It can be seen that cracking in the foundation is initiated as a result when the temperature decrease due to an operational stop.

It is mainly the outside of the concrete foundation that is subjected to cracking due to the time-dependent temperature variation and the variation of the forces from the thermal expansion of the stator and rotor spider beams. In Figure 47 it can be seen that there are some cracks that has occurred near the stator supports that are similar to the cracks found in-situ. However, the analysis shows no indication of cracking at the supports of the rotor spider. The time-dependent temperature variation due to operational stops is according to this, not likely the main reason for the cracks that have been found near the supports of the rotor spider. However, it can be seen that the starts and stops of the generator causes crack initiation in the foundation mainly on the outside of the foundation but also at the stator supports.

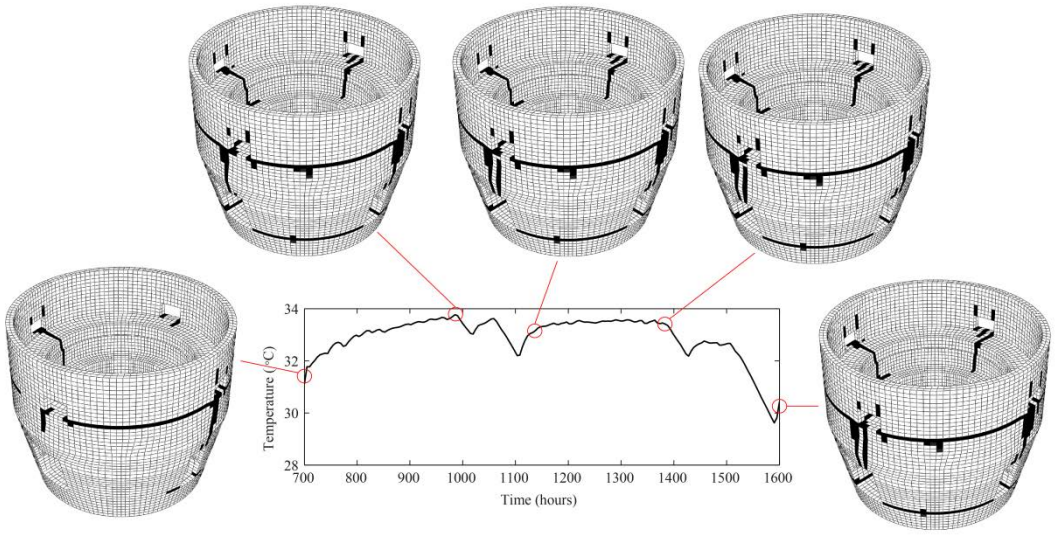

Figure 47 Crack propagation from to time-dependent temperature variations due to operational stops.

In Figure 48, the variation in tensile plastic strain, i.e. indicating when the crack width starts to propagate, at one of the elements near one of the large openings is shown. It can be seen in the figure that crack initiation starts quite rapidly at the time when the temperature has decreased. This stop that

initiated the propagation in crack width is about 50 hours long and results in a decreasing ambient air temperature of approximately 3ºC. It can also be seen that after this, the subsequent stops that cause a decreasing temperature will cause the crack width to increase further. In the simulation, the reinforcement stresses are at maximum 200 MPa and thereby never reach the yield strength and can therefore be considered as elastic. The stop that occurred before the initiation of this crack was about 30 hours long and resulted in an ambient temperature decrease of approximately 2ºC. As it seems, this decrease in temperature was too small to cause an initiation of the crack.

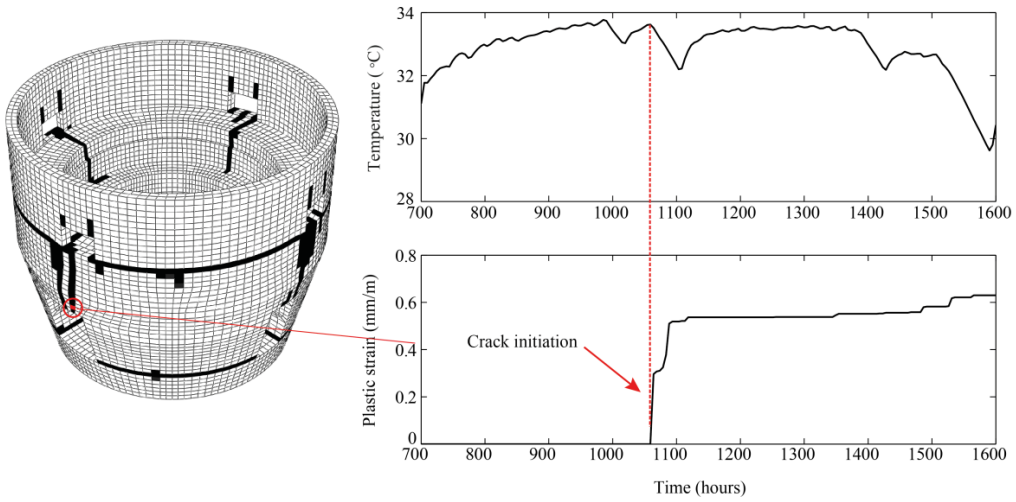

Figure 48 Development of plastic strain due to time-dependent temperature variation caused by operational stops.

The measured difference between the ambient air temperature inside the concrete foundation and the temperature measured at the rotor spider is shown in Figure 49. It can be seen, that the time when the crack was initiated corresponds to the time when there is a significant drop in the relative temperature between the measured temperature in the ambient air and the rotor spider.

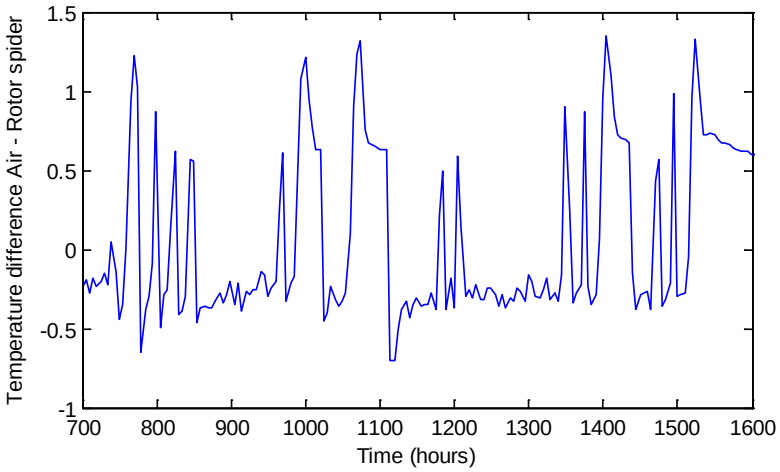

Figure 49 Difference between temperatures measured in the ambient air and at the rotor spider

5.5 Dynamic loads from the generator

In the previous analyses, the dynamic loads due to magnetic eccentricity from the generator have been treated as static. In this section, the purpose is to study the dynamic effect of this load.

The actual loads are caused when the rotor and stator are not perfectly cylindrical and centred to each other, Näsellqvist (2011). These forces are applied in the radial direction to the supports of both the stator and the rotor spider. The direction of the forces applied to the stator and rotor spider supports must be in the opposite direction in order to satisfy equilibrium. Below three different cases of magnetic eccentricity is presented, where the third case is the worst case and is a combination of the two previous.

- The rotor is placed eccentric to the turbine axle which causes the turbine axle to swing back and forth and cause a periodical load. The load is assumed to be sinusoidal originating from a rotation of 150-200 rpm, with an amplitude of 180 kN.

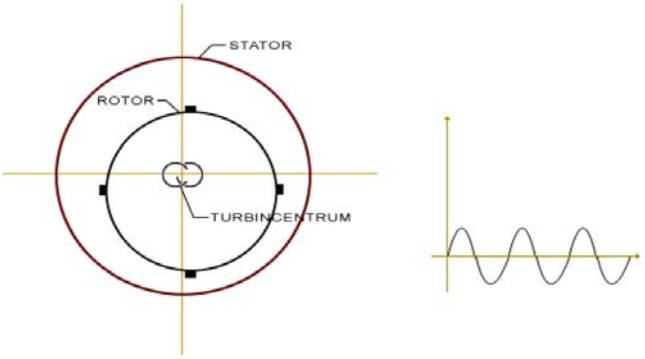

Figure 50 Magnetic eccentricity case 1, from Larsson (2008).

- The stator is placed eccentric to the supporting structure which causes a constant applied load. The load is assumed to be constant and equal to 180 kN.

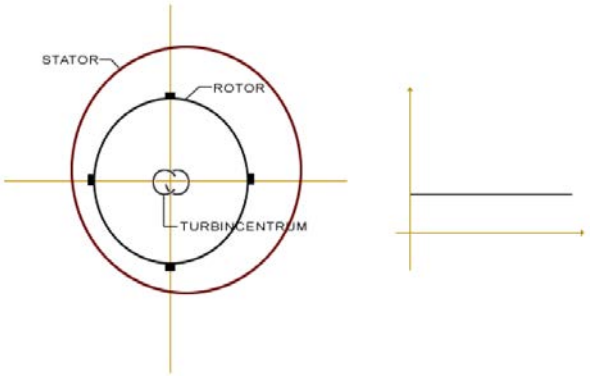

Figure 51 Magnetic eccentricity case 2, from Larsson (2008).

- The combination of these two effects, i.e. when both the rotor is eccentric in relation to the turbine axle and also where the stator is assembled eccentric to the concrete foundation. The load is assumed to be sinusoidal originating from a rotation of 150-200 rpm, with an amplitude of 180 kN and a constant load of 180 kN.

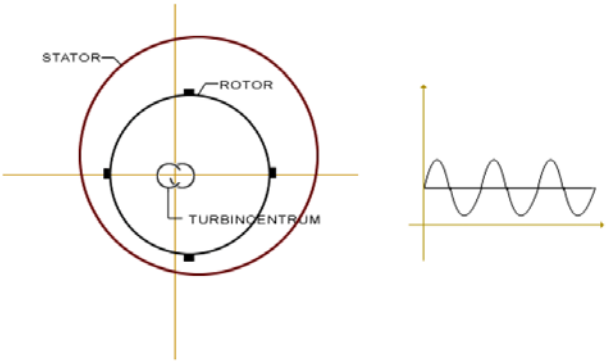

Figure 52 Magnetic eccentricity case 3, from Larsson (2008).

To simulate this in the numerical model, the loads were applied to the supports of the stator and rotor spider respectively. The load on each support was defined with an amplitude according to Figure 52 and a frequency corresponding to 150 rpm. The loads were applied with a delay to each of the supports, starting with the supports numbered as 1 in Figure 53. After this, the remaining supports were activated in the counter clockwise direction, i.e. in the same order as they are numbered in the figure. The delay in time for applying the load at the supports was calculated based on the rpm of the generator. This was performed to introduce a phase difference between each of the sinusoidal loads. Besides this, the loads on the stator supports was

applied in a radial direction outwards while the loads on the rotor supports was applied in a radial direction inwards.

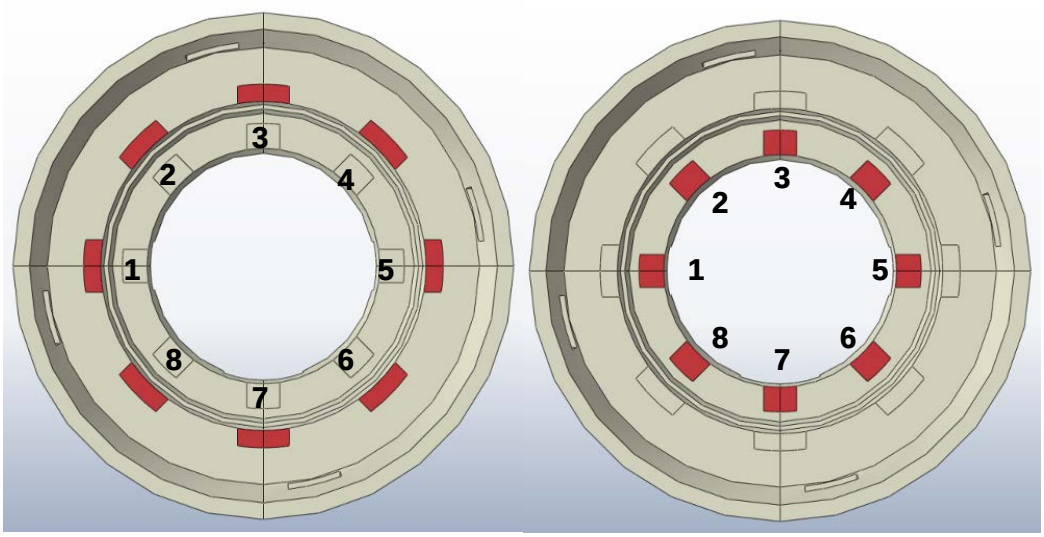

Figure 53 Areas for the support from stator and rotor spider respectively.

5.5.1 Linear elastic structure

In this case the concrete foundation is assumed to be linear elastic without any cracks and only the static gravity load and the dynamic effect due to magnetic eccentricity are considered. In this analysis Abaqus explicit was used. The total time studied in this analysis was defined as two seconds.

In Figure 54, the maximum tensile stresses in the whole model during all time steps are shown. In several regions the tensile stress has exceeded the tensile strength of concrete, as shown with red color in the figure.

The dynamic effect of the unbalanced forces due to magnetic eccentricity appears to give higher stresses in the structure than the corresponding assumed static load. It is especially in the regions close to the supports for stator, rotor spiders and the openings that are affected by high tensile stresses. The high stresses due to the dynamic effect should be studied further to determine if they could be harmful for the concrete foundation.

It is also important to study the influence of the dynamic loads if the concrete foundation is already cracked. A cracked structure is weaker and may therefore exhibit larger displacements.

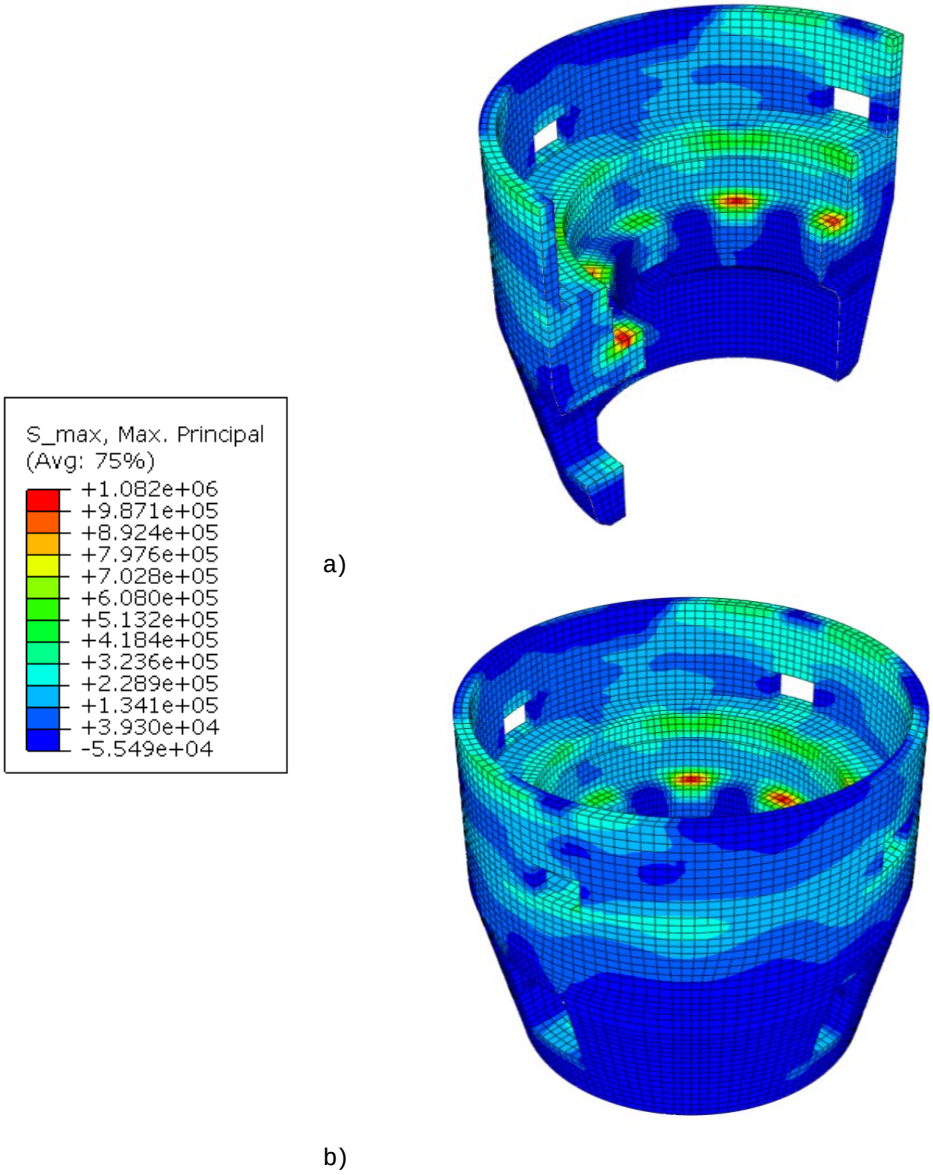

Figure 54 Envelop of maximum tensile stresses during all time steps in the dynamic analysis.

6 Discussion

The analyses performed in this report shows that reinforced concrete structure that constitute a support to the generator is subjected to cracking due to the combination of mechanical loads, temperature and drying shrinkage.

The analyses showed that the static mechanical loads alone did not cause cracking found in the concrete foundation. However, the thermal expansion of the steel beams in the stator and rotor spider during operation may initiate cracking to a small extent. This occurred for the case where a thermal expansion corresponding to 20 °C was assumed in combination with assuming that the beams were constrained at their supports, i.e. the frictional supports has lost their ability to slide, as shown in section 5.1.2. The function of the supports and the loads transferred from the stator and rotor spider should be studied further. In these analyses these have been considered as mechanical loads, but in order to include them in a more realistic manner these steel beams should also be included in the numerical analyses. In addition, the relative displacement that can occur between the steel beams and their supports, and thereby calculating the resulting frictional forces automatically, should be included in future analyses.

In conventional design considerations, uneven shrinkage over the cross-section is normally not considered. Instead, a constant drying shrinkage is assumed for the whole structure. The analyses in section 5.2.2 showed that even after 20 years, the moisture content in the centre of the thickest part of the concrete foundation was still high, with a relative humidity of approximately 70%. At the same time the concrete close to the free surfaces and the slender parts of the concrete foundation had reached the same relative humidity as the environment. Thereby, a large difference in drying shrinkage is obtained between different parts of the concrete foundation. The analyses showed that the drying shrinkage induced cracking inside the concrete foundation and especially close to the supports of the stator and the rotor spider. These cracks have also been found in situ and they were the main reason why this research project was initiated.

Due to the thermal gradient of the concrete foundation during operation, additional cracks were initiated. The temperature gradients primarily introduced cracking on the outside of the concrete foundation, i.e. on the cold side. The analyses also showed that the cracks that had occurred on the inside of the concrete foundation increased significantly due to the temperature effects, as seen in section 5.3. At the end of the analysis a large part of the concrete foundation was subjected to cracking both on its inside and on its outside.

Nowadays, there are many starts and stops of the generator and these stops results in cooling of the inside of the concrete foundation. It was shown in the in section 5.4.3 that these stops result in initiation and propagation of cracks in the concrete foundation. In the analyses presented in section 5.4.3 it could be seen that the temperature decrease that occurred during longer

operational stops initiated cracks, primarily on outside surface of the concrete foundation. The longest operational stop that was considered in this analysis was about 80 hours and resulted in a temperature decrease of about 5 °C. The influence of operational stops will be furthered discussed in section 6.1.

In all previously mentioned analyses the loads acting on the stator and rotor spider support have been considered as static. In order to study the effect of dynamic loads an analysis was performed where the loads due to magnetic eccentricity was applied to the structure. This analysis is to be considered as a feasibility study and was only performed based on the assumption that the concrete foundation is linear elastic. The analyses showed however, that large stresses were induced in the structure due to the dynamic effect of the loads from magnetic eccentricity. The results in section 5.5.1 showed that these dynamic loads resulted in high stresses that exceeded the tensile strength of concrete in several regions of the structure. Thereby, this load is likely to induce cracks in the concrete foundation. Besides this, these loads could be exaggerated if applied to a cracked concrete foundation. Several generator manufacturers permit only negligible structural displacements. It is likely that cracks which decrease the structural stiffness of the foundation would result in increased displacements and thereby increasing the eccentricity of the dynamic loads.

6.1 Operational stops

During this project, statistics have been studied regarding operation of several different hydropower units. The number of starts and stops for the different hydropower units varies, where some are running more or less continuously while others are subjected to starts and stops on almost a daily basis. Several different factors influence the number of starts and stops for the different aggregates, time of year, i.e. the water supply, the number of aggregates in the facility, type of runner etc.

The massive concrete structure that constitutes the foundation has a high heat storage capacity and thereby due to relatively short stops, the temperature only decreases slightly. Based on the measurements presented in section 2.1 and section 5.4.1, the longest stop during that period was about 80 hours and during that time the temperature decreased from about 33.5ºC to 28.5ºC, which corresponds to an average temperature decrease of 0.06ºC/hour.

Initially in the project different extremes were studied, i.e. one type that had a large amount of starts and stops and one that rarely are subjected to stops. For one of the studied generators that had a large amount of stops, the average time when power production was off was about 13 hours based on all the stops during one year, as seen in Figure 55. One of the power units that have a high availability had only 13 stops in total during one year, with the average stop time being about 28 hours.

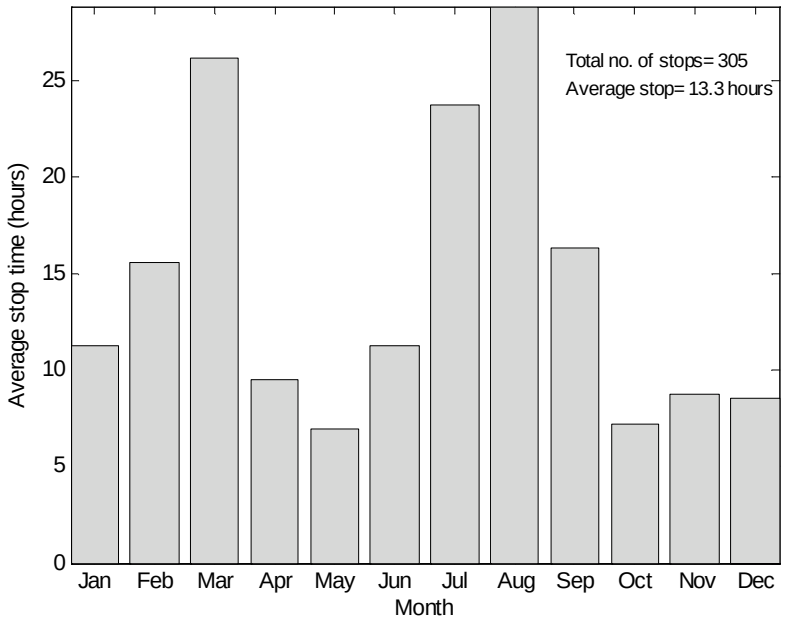

Figure 55 Average stop time for one of the studied hydropower units.

The simulations based on the measurements presented in Section 5.4 showed that cracking is mainly initiated in the structure as a result of the cooling of the concrete foundation. It also showed that relatively short stops of a few hours only result in a small decrease in temperature. Due to this effect, the cases with stops that last for longer time periods are more important to study in case of thermal cracking. The hydropower plants are generally subjected to several starts and stops nowadays and based on this study there is a high risk of thermal cracking due to operational stops if they occur for longer time periods. On the other hand, the results also show that shorter stops leads to small decrease in temperature and a short operational stop has therefore a small risk of cracking due to thermal gradients. However, when the hydropower plant is subjected to stops other loads occur, such as dynamic loads from the generator, change in vertical loads on the rotor spider supports from the water, runner vibrations due to passage through non-optimal parts of the efficiency curve etc. and it is possible that these loads also may cause cracking in the concrete foundation and possibly also fatigue of reinforcement.

6.2 Further research

It is important to determine the causes of the structural cracks that have been found in-situ and also to evaluate the effect of the reduced stiffness due to cracking. A reduced structural stiffness can result in larger loads imposed on the structure from the magnetic eccentricity and turbine imperfections or alternatively lead to a fatigue failure of for instance the reinforcement.

The cracking of the concrete foundation reduces its stiffness and it is therefore of importance to take it into consideration, since a reduced stiffness

of the structure may result in larger loads acting on the structure and vibrations on the unit exceeding the limits. It is also important to create input to the evaluation of existing structures with cracks, to define suitable limits when a structural repair is needed or not.

In the next step of this project, the focus will be on calculating the uneven drying shrinkage of the concrete structure and evaluate its structural effect. Furthermore, this project will also continue to study the oscillating forces that can occur due to magnetic eccentricity caused if the rotor is not centred in relation to the turbine axle. In the next phase the dynamic effect of this load will be evaluated as well as its influence on a cracked foundation.

7 References

Ansell A., Björnström J., Ekström T., Hassanzadeh M. and Unosson M. (2007) *Spricktillväxt i lamelldamm – Tillämpning av icke-linjära modeller – Del I*. (in Swedish). Elforsk Report 08:21. Elforsk. Stockholm.

Ansell A., Ekström T., Hassanzadeh M. and Malm R. (2010) *Crack propagatin in buttress dams: Application of non-linear models – Part II.* Elforsk Report 10:69. Elforsk. Stockholm.

Bazant, Z.P. and Najjar L.J. (**1972).** *Nonlinear water diffusion in nonsaturated concrete.* Matériaux et constructions. 1972, Vol. 5, 25.

Björnström J., Ekström T. and Hassanzadeh M. (2006) *Spricktillväxt i lamelldamm – Tillämpning av icke-linjära modeller – Del I*. (in Swedish). Elforsk Report 08:21. Elforsk. Stockholm.

Eurocode 2 (2004). *EN 1992-1-1: Design of concrete structures - Part 1-1: General rules and rules for buildings.* Brussels : European Committee for Standardization.

Hassanzadeh M., Malm R., Nordström E. (2012). *Analysis of displacement and crack formations in foundations for hydropower generators.* In: 24th ICOLD Congress, 24 EME Congres De La CIGB, Kyoto. Q95-2.

Hedenblad G. (1995). *Uttorkning av Byggfukt i betong - Torktider och fuktmätning. Fuktsäkerhet i byggnader.* Byggforskningsrådet & SBUF. Stockholm.

Hedenblad G. (1996). *Materialdata för fukttransportberäkningar. Fuktsäkerhet i byggnader.* Byggforskningsrådet. Stockholm.

Johansson P., Nilsson L-O. (2007). Climatic conditions at the surfaces of concrete containments – examples for two BWR and PWR reactors, Proceedings of SMiRt 19, Toronto, August 2007, Paper # DH01/2.

Kristek V., Bazant Z., Zich M., Kohoutkova A. (2006). Box girder bridge deflections_Why is the initial trend deceptive? Concrete International; 28(1):55_63.

Larsson, M. (2008). *Fundament för vattenkraftgeneratorer - analys av krafter och deformationer.* Luleå : LTU, 2008.

Ljungkrantz C., Möller G. and Petersons N. (1994). Betonghandbok – Material. 2nd Edition. Svensk Byggtjänst. Stockholm.

Malm R. (2009). *Predicting shear type crack initiation and growth in concrete with non-linear finite element method.* PhD Thesis. KTH Royal Institute of Technology, Civil and Architectural Engineering. Stockholm.

Model Code 90. (1993). *CEB-FIP Model Code 1990.* Thomas Telford. London.

Model Code 2010, CEB-FIP. (2010). *CEB-FIP Model Code 2010.* Thomas Telford. London.

Molina L. (1990). *Measurement of high humidity in cementitious material at an early age.* CBI Report 3:90. Swedish Cement and Concrete Institute (CBI). Stockholm.

Molina L. (1992). *On predicting the influence of curing conditions on the degree of hydration.* CBI Report 5:92. Swedish Cement and Concrete Institute (CBI). Stockholm.

Nässelqvist M. (2011). *Simulation and Characterization of Rotordynamic Properties for Vertical Machines.* PhD Thesis. Luleå University of Technology, Division of Mechanics of Solid Materials. Luleå.

Paavola J. (2011). *FEM-Modellering av en vattenkraftstation – Utvärdering av beräkningar i 3D*. M.Sc Thesis Luleå University of Technology, pp79. Luleå.

Petersson P-E. (1981). *Crack growth and development of fracture zones in plain concrete and similar materials.* Lund Institute of Technology, Division of Building Materials. Report TVBM-1006. Lund.

Rhen M. (2007). *Förslag till dimensionerande lastfall för generator- och bärlagerarmkorsupplag. Rotor- och temperaturdynamiska laster.* Elforsk Report 07:54. Elforsk. Stockholm.

Yunping X., Bazant Z.P., Molina L. and Jennings H.M. (1994a) *Moisture Diffusion in Cementitious Materials - Moisture Capacity and Diffusivity.* Advanced Cement Based Materials. 258-266.

Yunping X., Bazant Z.P. and Jennings H.M. (1994b) *Moisture Diffusion in Cementitious Materials - Adsortion Isotherms.* Advanced Cement Based Materials. 248-257.

Appendix A

Paper 1

Hassanzadeh, M., Malm, R., Nordström, E. (2012). *Analysis of displacement and crack formations in foundations for hydropower generators.* In: 24th ICOLD Congress, 24 EME Congres De La CIGB, Kyoto. Q95-2.

COMMISSION INTERNATIONALE
DES GRANDES BARRAGES
---
24 EME CONGRES DE LA CIGB
Kyoto, Juin 2011

ANALYSIS OF DISPLACEMENTS AND CRACK FORMATIONS IN FOUNDATIONS FOR HYDROPOWER GENERATORS

Manouchehr HASSANZADEH
Ph.D. (Civ. Eng.), Senior Technical Specialist
Vattenfall Research and Development AB / Lund University

Richard MALM
Ph.D (Civ. Eng.), Technical Specialist
Vattenfall Research and Development AB / Royal Institute of Technology (KTH)

Erik NORDSTRÖM
Ph.D. (Civ. Eng.), Dam Engineering Specialist
Vattenfall AB, Hydropower

SWEDEN

1. INTRODUCTION

A rather extensive program for improvement of the Swedish hydropower plants is ongoing. The aims are to secure future production and to maintain and further develop an already high dam safety. In connection with earlier work, which dealt with assessment of an existing buttress dam where a non-linear finite element model was applied to determine the cause of the observed cracks. The results showed that the non-linear finite element method is a powerful tool to determine the structural behaviour of large concrete structures. The study in this paper is a continuation of the previous project, aiming at applying the method to other parts of dam structure such as waterways.

During the program, structural damages (cracks) were discovered around some of the stator and rotor spider supports. The cracks were believed to be related to the function of the stator supports and to new patterns of generator operation. In earlier times, the generators ran continuously, while nowadays there are many stops and starts, some times even several times during one day. The purpose of this study is to illuminate the complex stress conditions in the genera-

tor foundations of a hydropower plant and to reveal the causes of the stresses and to verify their role in formation of the cracks.

The variation of stresses in the structure and formation of cracks influence both the static and the dynamic response of the structure. Several generator manufacturers permit only negligible structural displacements. Therefore the analysis tools must be developed in order to determine the response of the foundations to the loads induced by the generators. As shown in this paper, the structure is massive and it's thickness and radius varies along with the axis of the revolution, which can lead to high tensile stresses caused by the temperature and moisture gradients. The temperature and moisture gradients exist both in the radial and the tangential directions of the foundation. Mechanical loads caused by the oscillation of the generator, friction at the supports and the weight of the structure and machines are the additional factors, which must be taken into account.

The structural behaviour of a foundation has been analysed taking into account the transient thermal gradients in combination with dead loads and some of the operational loads imposed to the foundation. A three dimensional non-linear finite element model has been applied in order to analyse formation and propagation of the cracks.

2. DESCRIPTION OF THE STRUCTURE

2.1. DESCRIPTION OF THE STRUCTURE

Fig. 1 shows a vertical cross-section of the power unit of the hydropower plant, which this study deals with. The figure shows the generator (stator and rotor), rotor spider, turbine shaft, spiral casing, turbine and draft tube. As it is shown the power unit is embraced by a concrete structure.

The hydropower plant was constructed in the early forties. There is no conclusive data on the concrete's composition in terms of water binder ratio (W/B ratio), type and quantity of the binder, aggregate type and maximum particle size. The data that are available indicate that the binder is Portland cement with somewhat higher silicate quantity than usual to reduce the hydration rate and heat development of the binder. Moreover, according to the guidance which used to be applied when the power plant was being constructed, the recommended W/B ratio and the binder quantity for the similar structures were 0,55 - 0,60, and 300 – 350 kg/m^3 respectively. According to the same guidance the W/B ratios 0,55 and 0,60 corresponded to 28 days compressive strength of 22 and 20 MPa. The corresponding values at 90 days were 35 and 30 MPa. Translated to the current conditions the concrete grade at the time of construction can be assumed to be C20/25.

The foundation is a massive reinforced concrete structure. The reinforcement drawings, which are available, indicate that the average reinforcement di-

ameter and the average distance between the bars are 25 and 250 mm respectively. According to the drawings the concrete cover should not be less than 30 mm or larger than 40 mm. By means of the casting instructions can be concluded that the target concrete cover was less than 30 mm and the maximum particle size was less than 25 mm.

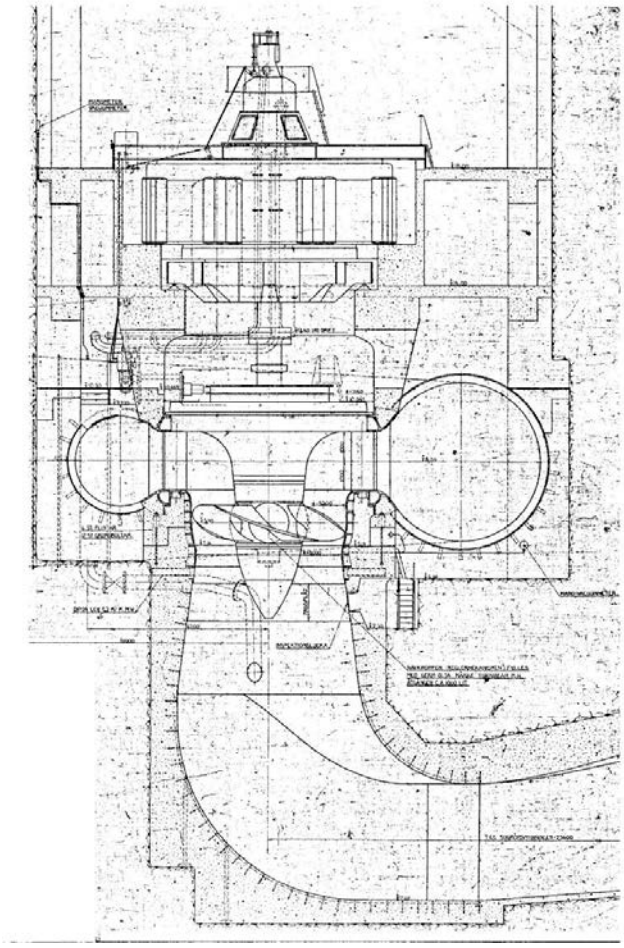

Fig. 1
Vertical cross-section of the hydropower system.
Coupe verticale du système hydroélectrique

The dead weight of the power generating system and the loads caused by the power generator is supported at the upper part of the concrete structure. The cylindrical upper part of the structure, which is here denoted as the *foundation*, has different wall thickness at the different sections, as seen in Fig. 1. The loads from the power generating devices are transferred to the foundation through two sections, namely through the supports of the stator and through the supports of the rotor spider. A minor part of the loads are transferred through the supports of the turbine cover.

The weight of the rotor, rotor spider, turbine and turbine shaft are transferred to the foundation through the supports of the rotor spider. The vertical loads generated by the water at the turbine are also transferred through the sup-

ports of the rotor spider. The supports of the stator support the weight of the stator and the cooling system. Horizontal loads, i.e. loads acting on the planes perpendicular to the rotor shaft, are transferred to the foundation through the supports of the stator and the rotor. For instance, the rotation of the rotor affects the stator in both tangential and radial direction. The resulted horizontal loads are transferred through the supports of the stator and the rotor.

Another example of a horizontal loads are those caused by the friction in the bearings supporting the stator and the loads imposed by the restrained thermal displacement of the rotor spider. The heat produced by the generator causes a relative displacement between the beams supporting the stator and the foundation. The displacement takes place on the supports. In order for the relative displacement to occur, the friction resistance must be overcome. This results in frictional forces that act between the beams supporting the stator and the foundation in the radial direction. Furthermore, the rotor spider will expand due to the increased temperature. Since, the spider is fixed at the supports it will be restrained. The spider pushes the supports during heating and pulls the support during cooling. Since this investigation deals with the mechanical behaviour of the foundation, only the foundation is treated henceforth. Fig. 2 shows an example of the reinforcement detailing, and later in Fig. 5 the dimension of the foundation is shown. As it can be observed in Fig. 2 the foundation contains several entries and doors, which have been accounted for in Finite Element Model, FEM.

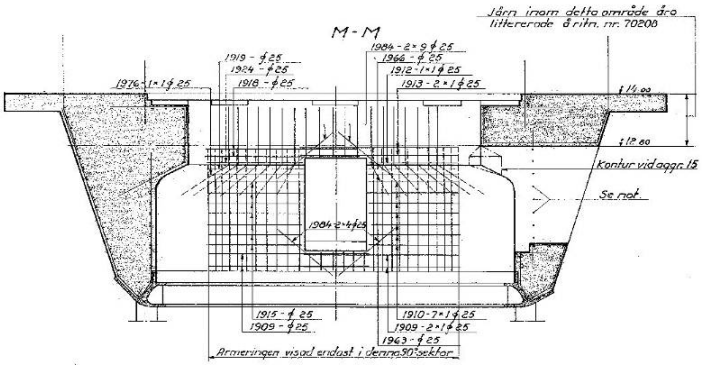

Fig. 2
Vertical cross-section of the foundation and arrangement of the reinforcement.
Coupe verticale de la fondation et exemple d'arrangement de l'armature

2.2. THERMAL AND MOISTURE EFFECTS ON THE FOUNDATION

As shown in Fig. 1, the stator and the rotor are placed inside a concrete structure, which acts also as a foundation for the stator and the rotor. Since the space inside the foundation is limited and the cooling system is not able to cool all the heat produced and therefore, the temperature inside the foundation increases during the operation of the generator. Although, the air inside the foundation is cooled adequately for the operation of the power generating devices the increased temperature may have a structural impact. Increased temperature

leads to extension of the rotor spider and the beams supporting the stator as well as displacement of the supports, which result in a netted displacement between the spiders, beams supporting the stator and the foundation at the supports.

Since the spiders are fixed at the supports their extension is restrained. The restraint will induce forces that act between the supports on the foundation and the end of the spiders. The magnitude of the forces depends on the stiffness/compliance of the spider and the foundation. As mentioned earlier, the spiders push the foundation during heating and pull the foundation during the cooling. However, it should be noted that netted displacement and the inertial of the heating and cooling processes might have big influence on the magnitude of the forces.

As far as supports of the stator are concerned, the spider could extend without any restraint, if the bearings of the supports were frictionless. Since the bearings are not frictionless they restrain the supporting beams. Consequently, loads are imposed on the beams and on the supports as well. The beams respond to the temperature variations faster than the foundation structure. The inertia of the heating and cooling process is important. In comparison with the “thin” steel structures such as supporting beams it takes long time for a massive concrete foundation to respond, to displace, and to adapt to a changed thermal condition. Therefore, frictional forces occur during heating, during cooling or at any disruption of the thermal equilibrium.

The supporting beams extend due to the increased temperature. They impose compressive forces on the foundation in the radial direction. During cooling the beams impose tensile forces on the foundation. The tensile forces induce cracks perpendicular to the direction of the forces.

Fig. 3 shows a crack between the support of the rotor spider and the wall of the foundation. The crack follows the foundation wall in the tangential direction. Similar cracks occur around the supports of stator. The preliminary analysis indicates that it is not exactly the same processes and mechanisms that cause the cracks close to the supports on in the foundation, as later described in section 4.2.

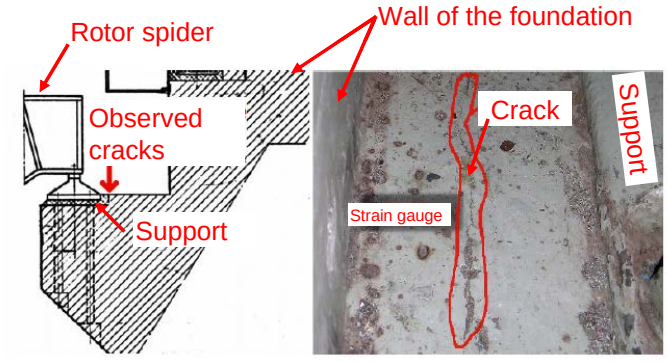

Fig. 3
Cracks at the support of the rotor spider [2].
Fissures au niveau du support de la commande de rotor [2]

The displacement between the support and the foundation wall includes the crack deformation (crack widening or closing) and the strains integrated over the mentioned distance, [2]. Crack deformation constitutes a considerable part of the total displacement and its contribution increases with increasing rate of temperature variation [2] and increasing length and stiffness of the spider. In the case of the stator supports the frictional forces imposed by the bearings influence the crack deformations.

The structural consequences of the observed cracking are, stress concentrations on reinforcement within the cracked area, reduced structural stiffness and reduced fatigue resistance.

The temperature variations also cause thermal gradients through the foundation wall. Normally, the air temperature inside the foundation is higher than the air temperature outside the foundation. The thermal gradient causes stresses in tangential direction and in direction perpendicular to the horizontal plane. Although, high stresses may occur the stress levels are normally not high enough to cause cracks. However, the impact of stresses caused by the thermal gradients may be increased by the other factors such as mechanical loading and drying shrinkage.

The foundation is situated inside a plant and is protected against the outdoor weather. The foundation is protected against the precipitation and is mainly exposed to the temperatures above what is considered indoor temperature. Since the outdoor air is used to cool the indoor air it can be assumed that the indoor air has the same vapour content as the outdoor air. In this context, however, it should be mentioned that the indoor air's vapour content normally follows the outdoor air's vapour content irrespective of the cooling system. It has been shown that the air's vapour content inside a nuclear reactor building, i.e. the building that embraces a reactor containment, follows the outdoor air's vapour content, [3].

The measurements show that the air temperature inside a generator chamber can be as high as 50 ºC and the relative humidity (RH) can be as low as 14%. Fig. 4 shows the temperature variation during the period 2006-07-14 – 2006-09-04. The measurement shows the temperature of the rotor spider and the air inside the foundation as well as the surface temperature of the slab on both side of the foundation wall. As can be observed there is approximately 10 ºC difference across the foundation wall. During the winter, the temperature outside the foundation can be as low as 15 ºC while the daily average outdoor temperature in the area of the power plant can be as low as -5 ºC.

The average temperature and humidity in the area of the power plant is -2 ºC and 85% during winter, and +16 ºC and 70% during summer respectively, corresponding to the average outdoor vapour content of $3{,}6 \cdot 10^{-3}$ kg/m^3 and $9{,}6 \cdot 10^{-3}$ kg/m^3. With the assumption that the air temperatures inside and outside of the foundation are 34 ºC and 24 ºC respectively, the RH on both sides of the foundation wall are 10% (winter) and 26% (summer), and 17% (winter) and 44% (summer). As it is noticed the foundation is exposed to relatively warm and dry environment.

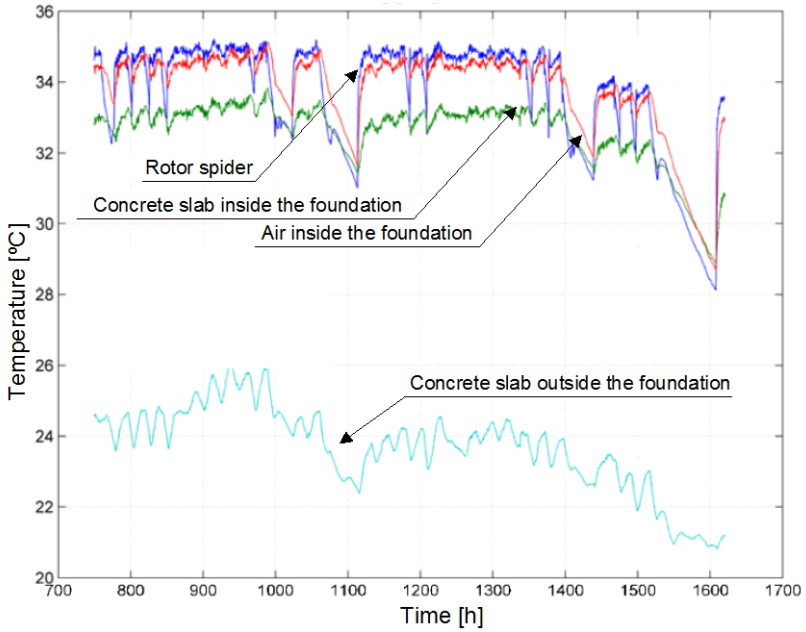

Fig. 4

Temperature variation during the period 2006-07-14 – 2006-09-04, [2].

Variations de la température au cours de la période du 14-07-2006 au 04-09-2006 [2].

The exposure of the foundation to the described environment leads to drying shrinkage of the concrete. Given the structure's size and design, and the dry environment, large stresses are expected to occur due to strain gradients and the restraints. The strain gradients are caused by the moisture gradients, which occur during the drying process before the final moisture equilibrium is reached within the sections of the structure, while restraints are caused when a part of the structure hinders another part to deform. Since the structure is more than 70 years old and it is exposed to a relatively warm and dry environment it is expected that the structure is not far from the moisture equilibrium condition, if it is not already dry.

The stresses caused by the drying shrinkage in most cases amplify the stresses caused by the thermal gradients and the mechanical loads.

Besides the above-mentioned thermal and moisture impacts there is another effect that should be considered and that is the restraint that occurs during the cooling process of the young concrete after hardening. It is however difficult to account for this effect. Disregarding the modeling difficulties there are other obstacles such as lack of data regarding material properties, heat development, concrete mix, casting phases, etc.

2.3. LOADS ACTING ON THE CONCRETE FOUNDATION

The objective of this study is to understand the complex interaction between the power generating system (stator, rotor, turbine, etc) and the supporting

concrete structure, which is needed for formulation of more realistic and accurate specifications regarding load, stiffness and displacement levels and tolerances. The achievement of the objective requires models that account for the behaviour of the mechanical systems, supporting structures and their interaction under various loading conditions. The various loading condition includes

- mechanical loads (static, dynamic, short-term, long-term, etc) such as weight of the structures and systems, and operating loads caused by the turbine, rotor, stator, etc
- environmental loads (physical, chemical, etc) such as strains and restraints caused by temperature and moisture variations, and chemical reactions.

The study that is presented in this paper is a step in the direction of the target objective. The work that is presented here is limited to the modelling of the behaviour of the foundation under the influence of the dead weight, loads from the stator, rotor spider and temperature gradient across the foundation wall. Although the other effects are disregarded in this paper the study will continue to include the factors, which were described above. The loads that are considered in this part are presented in Table 1.

Table 1
Loads caused by the power generating system.

Device	Duration	Level [kN]
Vertical loads on stator support		
Stator	Permanent	1200 kN
Cooling system	Permanent	100 kN
	Sum	**1300 kN**
Vertical loads on the rotor spider		
Rotor	Permanent	2890 kN
Turbine	Permanent	1200 kN
Spider and bearings	Permanent	250 kN
Turbine cover	Permanent	530 kN
Water	Variable (normal)	5720 kN
Water	Variable (exceptional)	8140 kN
	Sum (normal)	**10590 kN**
	Sum (exceptional)	**13010 kN**
Tangential loads acting on the stator support		
Moment acting on stator	During operation	4,974 kNm
The moment is opposed by 4 couples (lever arm 4 m)	During operation	157 kN
Radial loads acting on the stator support		
Sinusoidal load with 150-200 Hz frequency caused by mag-	During operation (in the opposite direction of the load	180 kN

netic eccentricity.	acting on the rotor spider)	
Frictional load acting on the each support	(A parametric study of influence have been performed, from frictionless to the case of a fixed boundary when the full thermal load of the stator beam expansion is subjected to the supports)	F_{max} = 1254 kN (assuming a fixed support)
Radial loads acting on the rotor spider support		
Sinusoidal load with 150-200 Hz frequency caused by magnetic eccentricity.	During operation	180 kN
Thermal force acting on the each support (assuming ΔT= 20 ˚C)		627 kN

The thermal force has been calculated based on the thermal expansion of the steel beams for a maximum temperature difference of ΔT=20˚C from cooling.

3. FINITE ELEMENT MODEL

3.1. FINITE ELEMENT MODEL

A 3D solid FE model has been developed in Abaqus/Standard version 6.10 of the reinforced concrete foundation. The purpose of the FE model is to simulate the response of the foundation subjected to the loads described in section 2.3 and study the possible causes for cracking. The foundation is basically rotational symmetric except for three large openings in the lower half and four smaller openings in the upper part. In Fig. 5 the geometrical model of the foundation is shown.

The reinforcement has been modeled as rebar layers in shell elements that have been placed within the 3D solid concrete volume. The shell elements are generally placed 50 mm from the concrete surfaces resulting in a typical concrete cover of 37.5 mm. In Fig. 6, the placements of the rebar layers are illustrated for two vertical cuts of the 3D model. The concrete surfaces are shown with blue color and the rebar layers are shown with red color.

Full bond between reinforcement bars and concrete has been assumed in the model, where the constraint has been modeled as an embedded region with the Abaqus option Embedded element.

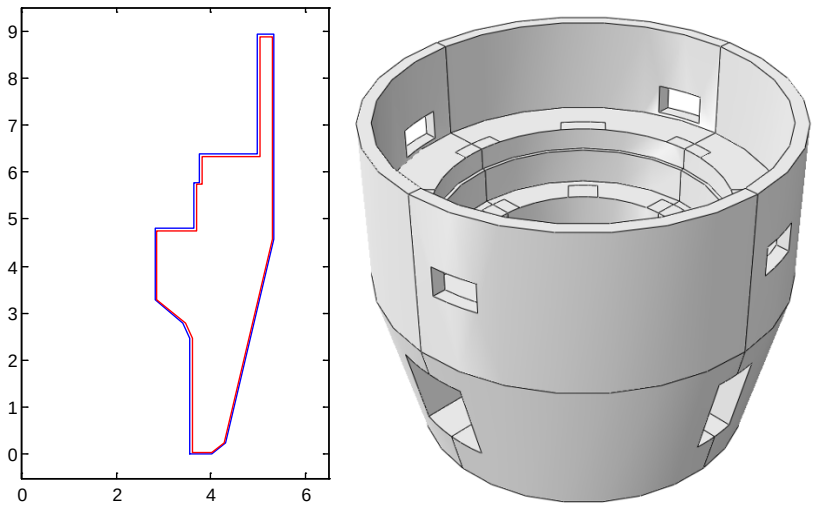

Fig. 5
Sketch of the concrete foundation and the 3D model used in the simulations.
Schéma de la fondation en béton et modèle 3D utilisé lors des simulations

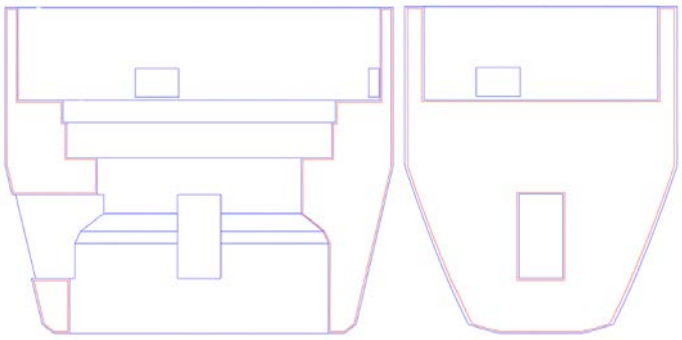

Fig. 6
Sketch of the concrete foundation and the placement of rebar layers.
Schéma de la fondation en béton et emplacement des couches de barres d'armature

The model was defined with 4-node linear tetrahedral elements, called C3D4, for the concrete foundation. The model had typically an element length of 0.25 m and consisted of a total of approximately 150 000 elements. The shell elements, representing the reinforcement, were modeled with linear triangular elements called S3R with reduced integration and hourglass control. Mesh sensitivity analyses have been verify that the element types and mesh size used in the model are sufficient to describe the structural response.

A vertical boundary condition has been applied to the horizontal bottom surface of the foundation, while radial and tangential boundary conditions were applied on the outside of the concrete foundation as shown in Fig. 1, at two positions; at the vertical level of the rotor spider and at the top of the structure. The loads on the concrete foundation are applied at the position of the supports of the rotor spider and the stator, as shown in Fig.7. Besides the loads from the stator and rotor spider, gravity load and temperature effects are studied. The support

locations are located with 45-degree placement and have a size of 1200x400 mm^2 and 600x800 mm^2 for the stator and rotor spider respectively.

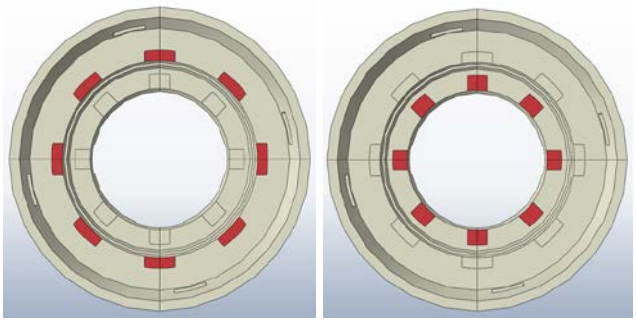

Fig.7
Areas for the support from stator and rotor spider respectively.
Zones du support du stator et de la commande de rotor

The vertical loads from the stator and the rotor spider have been modeled as pressure loads to the surfaces showed in Fig.7. The forces in radial and tangential direction were modeled as surface distributed loads with the Abaqus load type called surface traction with a local cylindrical coordinate system. The surface traction loads were defined with a constant resultant, i.e. so that deformations of the surface area do not affect the size of the applied load.

3.2. MATERIAL PROPERTIES

The concrete material properties have been assumed to correspond to the old Swedish concrete grade K25 that corresponds to C20/25 according to Eurocode 2. The reinforcement has been assumed to correspond to grade B500. The material properties of the concrete and reinforcement in the foundation are presented in Table 2.

Table 2
Material properties

Concrete			**Reinforcement steel**		
Strength grade	C20/25		Strength grade	B500	
Compressive strength	28	MPa			
Tensile strength	2,2	MPa	Yield strength	500	MPa
Modulus of elasticity	25	GPa	Modulus of elasticity	200	GPa
Poisson's ratio	0,2		Poisson's ratio	0,3	
Density	2300	Kg/m^3	Density	7800	Kg/m^3
Coefficient of thermal expansion	$1,2 \cdot 10^{-5}$	1/K	Coefficient of thermal expansion	$1,2 \cdot 10^{-5}$	1/K
Heat conductivity	2,5	W/(mK)			
Specific heat capacity	1000	J/(kgK)			

The concrete compressive curve has been calculated according to Eurocode 2 where it is defined linear elastic up to 40 % of the compressive strength, as illustrated in Fig. 8. The concrete tensile stress-displacement curve has been defined according to Petersson 1981, [4], with a tensile strength equal to 2.2 MPa, as shown in Fig. 8. The fracture energy has been assumed equal to of 60 Nm/m^2 based on Model Code 90 for a maximum gravel size of 16 mm.

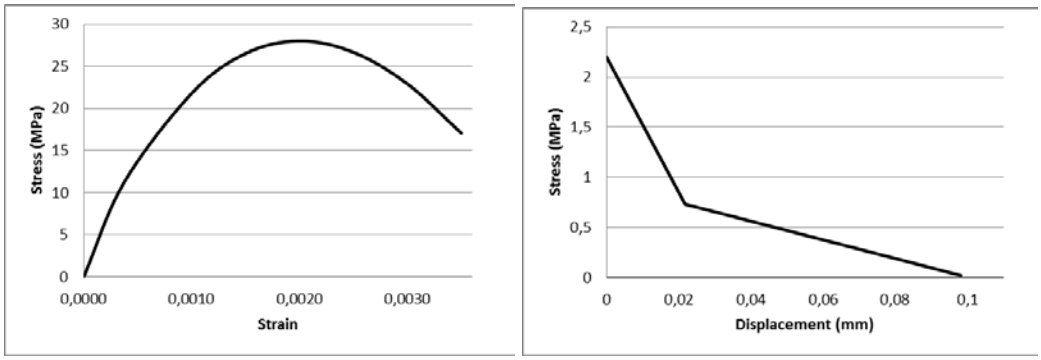

Fig. 8
Compressive stress-strain curve and tensile stress-displacement curve.
Courbe contrainte-déformation de compression du béton un courbe effort-déplacement de tension du béton

The non-linear concrete material behavior was simulated with the continuum plasticity-based damage model called *concrete damaged plasticity* in Abaqus, which was developed by Lubliner et al 1998, [5]. The non-linear behavior of the reinforcement was defined as elasto-plastic with a Von Mises yield criteria with the yield strength of 500 MPa.

4. RESULTS

4.1. EFFECT OF MECHANICAL LOADS

The total induced stresses considering all mechanical loads specified in section 2.3 are shown in Fig. 9. In this first study, the forces due to thermal effects such as the temperature gradient and the frictional forces due to thermal expansion of the stator and rotor spider beams are omitted. The simulation with the mechanical loads shows that the tensile stresses are moderate within the structure and at a few locations tensile stresses above approximately 1 MPa can be found. These regions correspond to the location of the rotor spider support shown previously in Fig. 3 and the highest tensile stresses are found at the supports that are located above the three large openings.

Small compressive stresses occur in the whole concrete foundation and the largest compressive stresses are only about 3 MPa at the bottom of the structure. Based on the simulation of the mechanical loads, no indication of cracking or crushing of the concrete can be observed and the structure behaves linear elastic for all the mechanical loads.

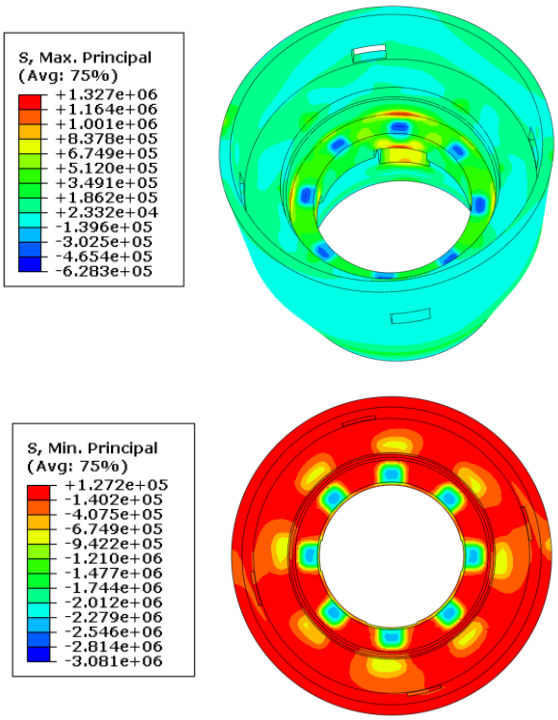

Fig. 9
Maximum tensile (upper figure) and compressive (lower figure) stresses in the concrete from mechanical loads.
Contraintes maximales de tension (figure haut) et de compression (figure bas) du béton dues aux charges mécaniques

4.2. EFFECT OF THERMAL LOADS

During operation, the temperature on the inner surface of the foundation increases due to the heat developed by the generator. Based on measurements shown in Fig. 4 the temperature difference between the inner and outer surfaces of the foundation is normally about 10 ºC. A finite element simulation was therefore performed to calculate a steady state thermal distribution based on the assumed temperature difference, as shown in Fig. 10.

In the first study of the thermal effects, the calculated temperature distribution was applied to the structure and the structural response was calculated. In this analysis, the frictional forces at the stator support and the thermal force at the rotor spider supports were applied.

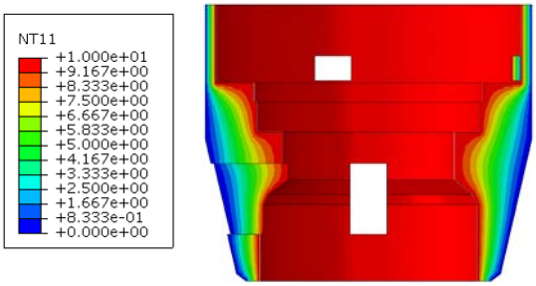

Fig. 10
Temperature difference between the inner and outer surfaces of the concrete foundation.
Différences de température entre les surfaces intérieures et extérieures de la fondation en

The influence of friction was studied in the analyses through a parametric study, where different values of the frictional forces at the stator support were studied. The worst-case scenario is if the frictional supports loose their ability to slide, i.e. becomes a fixed boundary. In this case the full load from the thermal expansion of the stator would be applied to the stator supports. The results from the worst-case scenario, i.e. with a fixed support of the stator beams are presented in the following.

It could be seen that based on this thermal effect, significant amount of cracking was obtained. The concrete foundation cracked mainly on its outside, i.e. on the cold side, and the cracking initiated from the corners of each opening and at the transition to the thin section above the stator supports.

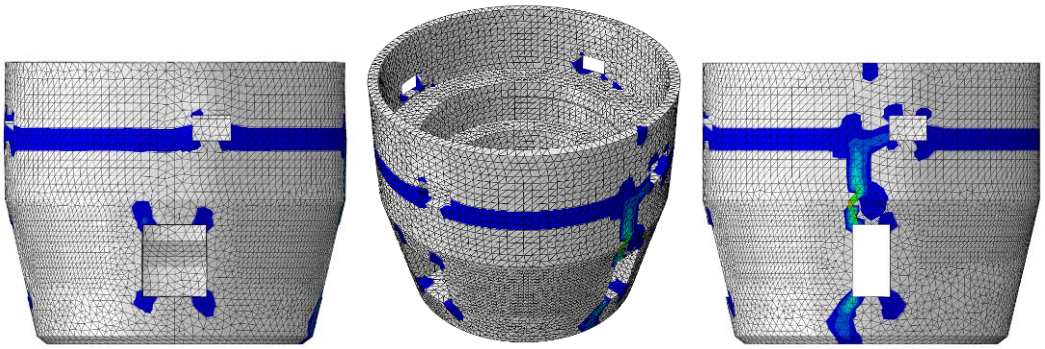

Fig. 11
Areas subjected to cracking due to a temperature gradient.
Zones soumises aux fissures en raison d'un gradient de température

To further study the effect of the temperature, the measuring period shown in Fig. 4 was simulated as a transient thermal calculation. The simulation started with the initial temperature difference between inner and outer surface of 10 ºC and continued to simulate the two-month period that the measurements were performed. The measured temperature of the rotor spider was introduced as an amplitude function and the forces were applied to the concrete foundation at the stator and rotor spider supports. The forces were calculated based on the ther-

mal expansion of the steel beams, i.e. assuming that the stator supports are fixed supports just as the rotor spider supports.

In Fig.12 the crack propagation due to the transient temperature variation is shown. It can be seen that cracking in the foundation is initiated as a result when the temperature decrease due an operational stop.

It is mainly the outside of the concrete foundation that is subjected to cracking due to the transient temperature variation and the variation of the forces from the thermal expansion of the stator and rotor spider beams. In Fig.12 it can be seen that there are some cracks that has occurred near the stator supports, that are similar to the cracks found in-situ. However, the analysis shows no indication of cracking at the supports of the rotor spider. The transient temperature variation due to operational stops is according to this, not likely the main reason for the cracks that are found near the supports of the rotor spider. However, it can be seen that the starts and stops of the generator causes crack initiation in the foundation both on the outside of the foundation and also at the stator supports. The cracking of the concrete foundation reduces its stiffness and it is therefore of importance to be taken it into consideration, since a reduced stiffness of the structure can result in larger loads acting on the structure.

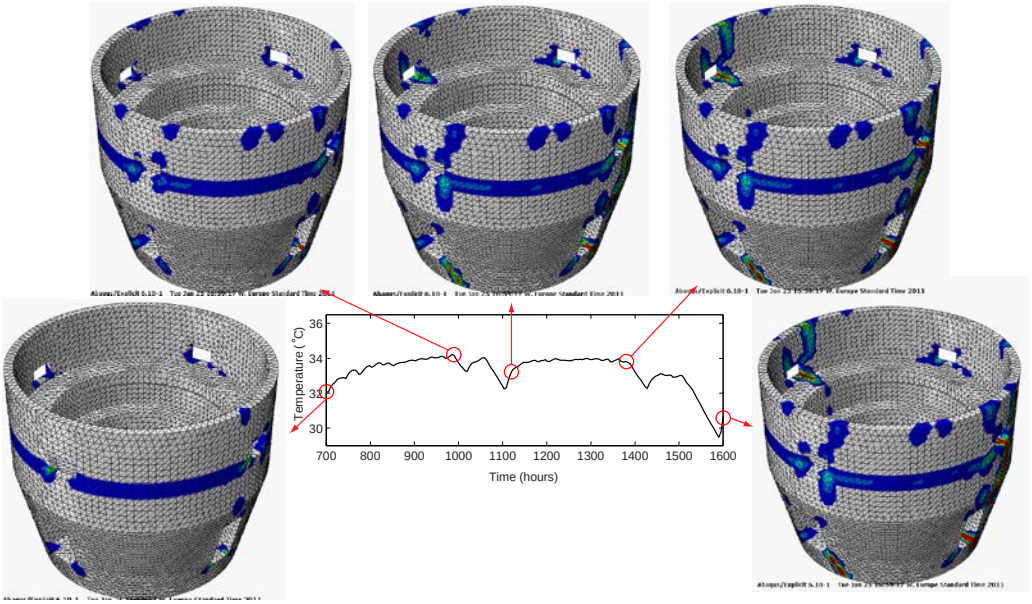

Fig.12
Crack propagation due to transient temperature variation
Propagation de fissures en raison d'une variation transitoire de température

In Fig. 13, the variation in tensile plastic strain, i.e. indicating when the crack width starts to propagate, at one of the elements at the corner of one of the large openings is shown. It can be seen in the figure that crack initiation starts quite rapidly at the time when the temperature has decreased. This stop that initiated the propagation in crack width is about 50 hours long and results in a decreasing ambient air temperature of approximately 3 ºC. It can also be seen that after this, the subsequent stops that cause a decreasing temperature will cause the crack to propagate further. In the simulation, the reinforcement stresses are

at maximum 200 MPa and thereby never reach the yield strength and can therefore be considered as elastic. The stop that occurred before the initiation of this crack was about 30 hours long and resulted in an ambient temperature decrease of approximately 2 ºC. As it seems, this decrease in temperature was too small to cause an initiation of the crack.

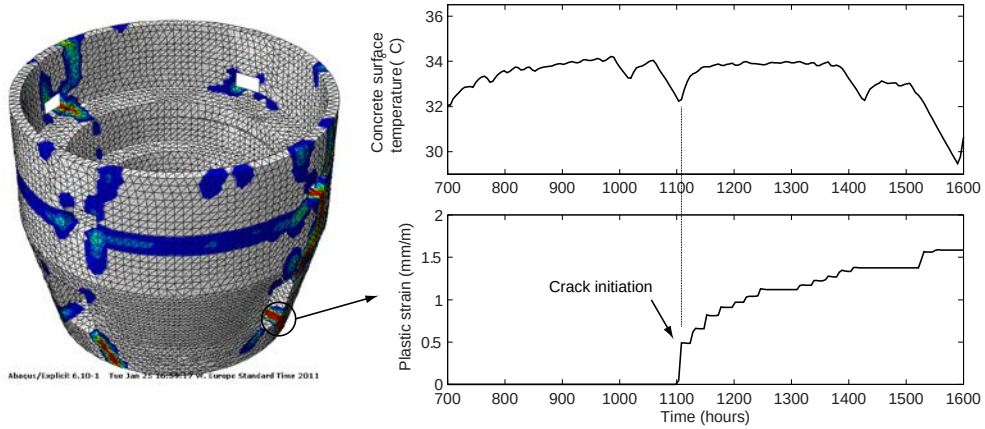

Fig. 13

Development of plastic strain due to transient temperature variation.

Développement d'une déformation plastique en raison d'une variation transitoire de température

In Fig. 14, the measured difference between the ambient air temperature inside the concrete foundation and the temperature measured at the rotor spider is shown. It can be seen from this figure, that the time when the crack was initiated corresponds to the time when there is a significant drop in the relative temperature between the measured temperature in the ambient air and the rotor spider.

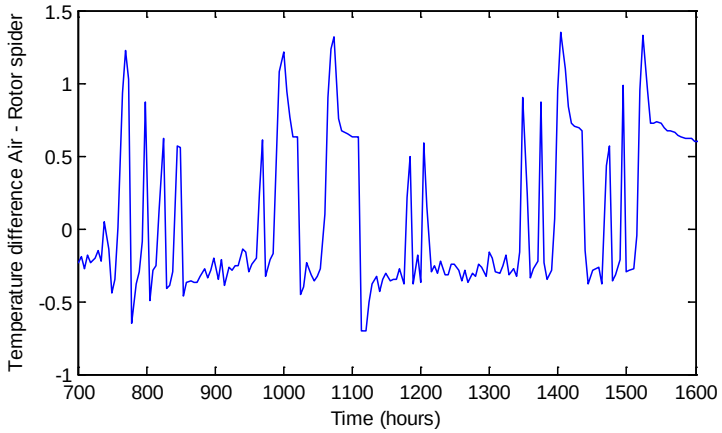

Fig. 14

Difference between temperatures measured in the ambient air and at the rotor spider.

Différences entre les températures mesurées dans l'air ambiant et au niveau de la commande de rotor

4.3. STATISTICS REGARDING OPERATIONAL STOPS

Statistics for operational stops of several different hydropower units have also been studied in this project. Generally, about 250 – 300 start and stops occur on average for a typical aggregate. Several different factors influence the number of starts and stops for the different aggregates, time of year, i.e. the water supply, the number of aggregates in the facility, type of blade wheel etc.

The massive concrete structure that constitutes the foundation has a high heat storage capacity and for stops that are relatively shorts the temperature thereby only decreases slightly. Based on the measurements presented in Fig. 4, the longest stop during that period was about 80 hours and during that time the temperature decreased from about 33.5 ºC to 28.5 ºC, which corresponds to an average temperature decrease of 0.06 ºC/hour.

Initially in the project different extremes were studied, i.e. one type that had a large amount of starts and stops and one that rarely are subjected to stops. For one of the studied generators that had a large amount of stops, the average time when power production was off was about 13 hours based on all the stops during one year, as seen in Fig. 15. One of the power units that have a high availability had only 13 stops in total during one year, with the average stop time being about 28 hours.

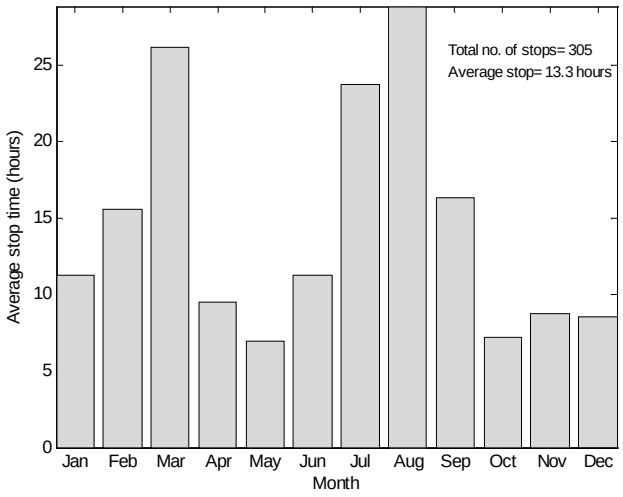

Fig. 15
Average stop time for one of the studied hydropower units.
Temps d'arrêt moyen pour l'une des centrales hydroélectriques étudiées

The simulations based on the measurements presented in section 4.2 showed that cracking is mainly initiated in the structure as a result of the cooling down of the concrete foundation and relatively short stops only result in a small decrease in temperature and due to this effect the cases with stops that last for longer time periods are more important to study in case of thermal cracking.

5. CONCLUSIONS

The analyses performed in this paper shows that reinforced concrete structure that constitute a support to the generator is subjected to cracking due to the combination of mechanical loads and thermal effects. Due to the thermal gradient of the concrete foundation cracking occur on the outside. Nowadays, there are many starts and stops of the generator and these stops results in cooling of the inside of the concrete foundation. It was shown in the paper that these stops result in initiation and propagation of cracks in the concrete foundation. However, the studied loads cannot explain all of the types of damages that can be found in-situ. It is likely that especially the drying shrinkage may be the main reason for the cracks that has been found near the stator supports and especially the rotor spider supports.

It is important from a dam safety perspective to determine the causes of the structural cracks that have been found in-situ and also to evaluate the effect of the reduced stiffness due to cracking, since a reduced structural stiffness can result in larger loads imposed on the structure from the magnetic eccentricity and turbine imperfections or alternatively lead to a fatigue failure of for instance the reinforcement.

In the next step of this project, the focus will be on calculating the uneven drying shrinkage of the concrete structure and evaluate its structural effect. Furthermore, this project will also continue to study the oscillating forces that can occur due to magnetic eccentricity caused if the rotor is not centred in relation to the turbine axle. In the next phase the dynamic effect of this load will be evaluated as well as its influence on a cracked foundation.

ACKNOWLEDGEMENT

The presented work was financially supported by ELFORSK AB, the Swedish Power Companies R&D association. The authors wish to thank Mattias Näsellqvist, Mats Rehn, Lamis Ahmed, Daniel Eriksson and Tobias Gasch for their valuable participation throughout this project.

REFERENCES

[1] Björnström, J., Ekström T., Hassanzadeh M., Cracked concrete dams – overview and calculation methods, R 06:29, Elforsk AB, Stockholm, 2006.

[2] Rhen, M., Proposal for design load cases for the supports of the generator and rotor spider – Rotor and thermal dynamic loads, R 07:54, Elforsk AB, Stockholm, 2007.

[3] Johansson, P., Nilsson, L-O. Climatic conditions at the surfaces of concrete containments – examples for two BWR and PWR reactors, Proceedings of SMiRt 19, Toronto, August 2007, Paper # DH01/2.

[4] Petersson P.-E. - Crack growth and formation of fracture zones in plain concrete and similar materials.. Lund Inst. of Tech., R TVB-1006, 1981.

[5] Lubliner, J., Oliver, J., Oller, S., Onate, E. A plastic-damage model for concrete. International Journal of Solids and Structures Vol. 25, No. 3, 299–326, 1989.

SUMMARY

A rather extensive program for improvement of the Swedish hydropower plants is ongoing. The aims are to secure future production and to maintain and further develop an already high dam safety. In connection with earlier work, which dealt with assessment of an existing buttress dam where a non-linear finite element model was applied to determine the cause of the observed cracks. The results showed that the non-linear finite element method is a powerful tool to determine the structural behaviour of large concrete structures. The study in this paper is a continuation of the previous project, aiming at applying the method to other parts of dam structure such as foundation supporting the generator (stator and rotor), rotor spider, turbine shaft, spiral casing, turbine and draft tube.

The hydropower plant, which is studied, was constructed in the early forties. During the inspection, structural damages (cracks) were discovered around some of the stator and rotor spider supports. The cracks were believed to be related to the function of the stator supports and to new patterns of generator operation. In earlier times, the generators ran continuously, while nowadays there are many stops and starts, some times even several times during one day. The purpose of this study is to illuminate the complex stress conditions in the generator foundations of a hydropower plant and to reveal the causes of the stresses and to verify their role in formation of the cracks.

The structural behaviour of a foundation has been analysed taking into account the transient thermal gradients in combination with dead loads and some of the operational loads imposed to the foundation. A three dimensional non-linear finite element model has been applied in order to analyse formation and propagation of the cracks. The analyses showed that based on the assumption made, the concrete foundation cracks mainly on the outside but also near some of the stator supports due to the combination of mechanical and thermal loads. However, the studied loads cannot explain all of the types of damages that can be found in-situ. It is likely that especially the drying shrinkage may be the one of the reasons for the cracks that has been found near the stator supports and especially the rotor spider supports.

It is important from a dam safety perspective to determine the causes of the structural cracks that have been found in-situ and also to evaluate the effect of the reduced stiffness due to cracking, since a reduced structural stiffness can

result in larger loads imposed on the structure from the magnetic eccentricity and turbine imperfections or alternatively lead to a fatigue failure of for instance the reinforcement.

RÉSUMÉ

Un vaste programme d'optimisation des centrales hydroélectriques suédoises est en cours. Les objectifs sont de préserver la production à venir, de maintenir et de développer le niveau de sécurité déjà élevé des barrages. Le tout est réalisé en lien avec une précédente étude, qui consistait à évaluer un barrage à contreforts auquel un modèle d'éléments finis non linéaires avait été appliqué afin de déterminer la cause des fissures observées. Les résultats ont montré que la méthode des éléments finis non linéaires est un outil puissant pour déterminer le comportement structural de structures massives en béton. La présente étude est le prolongement du projet précédent et vise à appliquer la méthode à d'autres parties de la structure du barrage telles que les fondations qui soutiennent le générateur (stator et rotor), la commande de rotor, l'arbre de turbine, la bâche spirale, la turbine et le tube d'aspiration.

La centrale hydroélectrique étudiée ici a été construite au début des années quarante. L'inspection a révélé des dommages structurels (fissures) autour de certains supports du stator et de la commande de rotor. L'origine des fissures semble liée au fonctionnement des supports du stator et aux nouveaux schémas de fonctionnement du générateur. Autrefois, les générateurs fonctionnaient en continu, alors qu'aujourd'hui ils connaissent plusieurs arrêts et redémarrages, parfois plusieurs fois par jour. Cette étude vise à faire le point sur les contraintes complexes que subissent les fondations du générateur d'une centrale hydroélectrique et sur leurs causes et à vérifier leur rôle dans la formation des fissures.

Le comportement structurel d'une fondation a été analysé en tenant compte des gradients thermiques transitoires combinés aux charges permanentes et à certaines charges opérationnelles imposées à la fondation. Un modèle d'éléments finis non linéaires tridimensionnel a été appliqué de façon à analyser la formation et la propagation des fissures. Cela étant posé, les analyses ont montré que la fondation en béton fissurait essentiellement à l'extérieur, mais également près des supports de stator en raison de la combinaison des charges mécaniques et thermiques. Cependant, les charges étudiées ne permettent pas d'expliquer tous les types de dommages trouvés sur place. Le retrait au séchage semble être l'une des principales causes des fissures trouvées près des supports de stator, notamment près des supports de la commande de rotor.

Dans le cadre de la sécurité des barrages, il est important de connaître les causes des fissures structurelles trouvées sur place et d'évaluer l'impact d'une réduction de la rigidité provoquée par la fissuration. En effet, une rigidité structurelle amoindrie peut aboutir à l'application de charges plus importantes à

la structure à cause de l’excentricité magnétique et des imperfections de la turbine ou encore à une rupture par fatigue de l’armature, par exemple.

Keywords:

Analysis, concrete, computer calculation, cracking, damage, finite element method, foundation, stress, thermal expansion

Mots-clés:

Calcul, béton, calcul par ordinateur, fissuration, dégâts, méthode des éléments finis, fondation, contrainte, dilatation thermique

ELFORSK

SVENSKA ELFÖRETAGENS FORSKNINGS- OCH UTVECKLINGS - ELFORSK - AB

Elforsk AB, 101 53 Stockholm. Besöksadress: Olof Palmes Gata 31
Telefon: 08-677 25 30, Telefax: 08-677 25 35
www.elforsk.se